Chem

CellPress

Review

Sigma Hole Interactions in Anion Recognition

Jason Y. C. Lim[1] and Paul D. Beer[1]*
[1]Chemistry Research Laboratory, Department of Chemistry, University of Oxford
Mansfield Road, Oxford, OX1 3TA (UK)
*Correspondence: paul.beer@chem.ox.ac.uk

SUMMARY

Sigma (σ)-holes are electron-deficient regions which arise from the anisotropic distribution of electron density on the atom of Group 14 (tetrels), 15 (pnictogens), 16 (chalcogens) and 17 (halogens) elements when covalently bonded to electron withdrawing groups. Named after the donor atom's Group, the σ-hole interactions, halogen bonding and chalcogen bonding, with anionic species have found ground-breaking applications in anion supramolecular chemistry within the last decade. In this review, we feature key recent discoveries and advances across the whole range of σ-hole interactions for anion recognition, from the familiar halogen bonding to the almost-unknown pnictogen and tetrel bonding. In particular, the novel anion recognition properties and applications that result from the unique aspects of each σ-hole interaction, together with detailed design considerations of anion binding receptor motifs are highlighted.

Keywords: sigma holes; anion; halogen bonding; chalcogen bonding; pnictogen bonding; tetrel bonding

The Bigger Picture

In the last decade, supramolecular interactions such as halogen bonding have endowed synthetic host systems with contrasting and often superior anion binding strength and selectivities not achieved using analogous hydrogen bonding (HB) host systems. Only very recently has the wider family of sister σ-hole interactions such as chalcogen bonding begun to be explored for anion binding applications. Through the integration of a range of σ-hole-donor motifs into various acyclic, macrocyclic and mechanically bonded interlocked molecular structural frameworks, their stringent directionality has enabled the resulting host systems to exhibit unprecedented novel anion recognition behaviours which have been applied to fields such as anion sensing, transport, catalysis, materials science and nanotechnology. While still in its infancy, the exploitation and study of σ-hole interactions in anion supramolecular chemistry promises to reveal new innovations in functional materials design and many areas of chemical research in general.

UN Sustainable Global Goals: SGD3- good health and well-being

1. INTRODUCTION

The important fundamental roles played by anions in biological, chemical, industrial and environmental processes has driven tremendous advances in the field of anion supramolecular chemistry within the last two decades.[1] However, despite the vast range of synthetic anion receptors reported, few have attained the impressive selectivities of natural anion-binding proteins. Part of the difficulty stems from the intrinsic properties of anions, which possess lower charge densities and weaker coordination preferences than cations. In addition, their often high solvation enthalpies, protonation equilibria arising from their pH sensitivity and wide range of geometries also thwart attempts towards selective binding. Although hydrogen

bonding (HB) is the most prevalent non-covalent interaction found amongst anion receptors to date, recent years have also seen increasing exploitation of less common interactions to expand the repertoire of anion recognition and selectivity. Anion receptors utilising solvophobic effects, anion-π interactions, coordinate bond formation with Lewis acidic metals and main group elements, as well as halogen bonding (XB), are gradually gaining prominence.[2] As an attractive non-covalent interaction between an electron-deficient halogen (Group 17) atom and a Lewis base,[3] the comparable strength of XB to HB and notably its greatly enhanced linear directionality (at least 175 ° in the gas phase) engendered the extensive exploitation of XB in solid-state crystal engineering and materials design.[4] Importantly, in solution, XB often augments the anion binding affinities and selectivities compared to HB analogues arising from complementary electronic, steric, geometric and solvent influences.[5]

It has since become apparent, through a multitude of experimental and computational studies,[6,7] that atoms in the neighbouring Groups 14-16 of the Periodic Table can also participate in attractive interactions with Lewis bases in an analogous manner as XB. In fact, attractions between electrophilic sulfur and selenium atoms with oxygen or nitrogen atoms can stabilise protein structure and even assist in biological host-guest recognition.[6] Hence, it is now widely accepted that XB is only one member of a wider family of non-covalent interactions known collectively as sigma (σ)-hole interactions. Like XB, these interactions are named according to the Groups the donor atoms belong to, such that chalcogen bonding (ChB), pnictogen bonding (PnB) and tetrel bonding (TrB) arise from Groups 16, 15 and 14 elements respectively. Encouraged by the success of XB in anion recognition, the potential of these sister σ-hole interactions, in particular ChB, are just beginning to be explored in earnest within the last three years. Compared to the halogens, Group 14-16 elements are more electropositive, and possess contrasting steric, geometric and electronic requirements owing to their intrinsic polyvalent character. Accordingly, incorporating these σ-hole donor groups into synthetic receptor design offers ample opportunities to attain varying anion binding strengths and selectivities.

Amongst the σ-hole interactions, XB is currently the most widely studied and best understood, which is reflected in a number of excellent reviews focusing on various fundamental studies and applications.[4,8–10] On the other hand, the sister interactions have received much less attention.[11–13] In this review, we focus on recent advances in the theoretical and experimental study of σ-hole interactions for anion recognition. Although it has been recently suggested that nanostructured metals (Au, Pt)[14] and noble gas compounds (e.g. XeF_2O) can participate in σ-hole interactions (termed aerogen bonding for the latter),[15] we will limit our discussion to those originating from Group 14-17 donor atoms. After summarising the fundamental properties of σ-holes, we first describe recent computational findings on the anion binding preferences of the different σ-hole interactions. Thereafter, the host design considerations of key synthetic receptors that function utilising σ-hole interactions (XB, ChB, PnB and TrB) for anion recognition are highlighted. The huge impact of σ-hole interactions on various applications of anion binding, and their contrasts with existing HB systems, are featured in the final section of this review.

1.1 Characteristics of Sigma-hole Interactions

When a Group 14-17 atom (X) is covalently bonded to chemical functionalities (R) more electronegative than itself, anisotropic distribution of electron density on the atom forms regions which are more electron-deficient than their surroundings. These are termed 'σ-holes' in a seminal 2007 paper[16] by Clark,* as they occur on the elongation of the R-X σ bond. In the computed molecular electrostatic potential (MEP) surface of iodine monofluoride (Figure 1), the σ-hole on the iodine atom (the less electronegative of the two halogens) appears as a distinct

* It should be clarified that although σ-holes were initially considered to have only positive electrostatic potentials (ESPs),[16] subsequent work has amply demonstrated that even σ-holes with negative ESPs exist. Consequently, it has been proposed that a σ-hole should be considered as a 'region of lower electronic density on the extension of a covalent bond'.[17]

region of positive electrostatic potential in blue, surrounded by an electron-rich equatorial belt. The same phenomenon also occurs for the other atoms (Te, Sb, Sn) bonded to fluorine across the Period. Due to the highly-localised electrophilic σ-holes on these donor atoms, their attractive interactions with Lewis base acceptors (A) are consequently highly-directional, leading to more restricted R-X···A angular distributions compared with HB.[6]

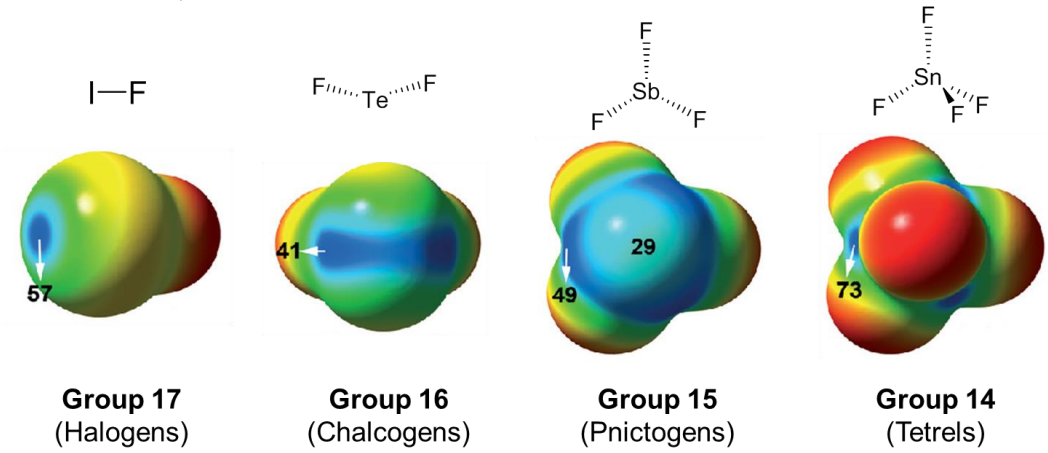

Figure 1. Computed molecular electrostatic potential (MEP) surface (computed at the MP2/aug-cc-pVTZ level) showing the locations of the σ-holes on Group 14-17 elements of the same Period bonded to fluorine. MEP values of the σ-holes are indicated in kJ mol^{-1}. Adapted from ref 15 by permission of John Wiley & Sons, Inc.

Figure 1 also reveals several important differences in the nature of each σ-hole interaction. Firstly, while only one σ-hole can be formed on a monovalent halogen atom, more can be found on progressively lighter donor atoms of the Period which reflects increasing multivalency. Consequently, the geometry of interaction between each σ-hole and a Lewis base differs across the Period. For instance, a CSD search revealed that XB interactions from donor iodine atoms have R-X···A bond angles > 170 °, while ChB interactions show angles centred around 80° and 170°.[18] In addition, the magnitude of the calculated MEPs on each σ-hole also varies, which is a cumulative effect of the enhanced tendency to form σ-holes due to increasing electropositivity of the donor atoms from Group 17 to 14, different numbers of electron-withdrawing fluorine atoms, as well as the abundance and spread of σ-holes across the atom. At the same time, increased donor atom multivalency results in progressively less sterically-accessible σ-holes, leading to those on tetrel bonding SnF_4 being confined to narrow troughs (in dark blue) between the fluorine atoms. Furthermore, the nature of the donor atom's covalent bonding can also determine the distribution of σ-holes on it, as exemplified by $F_2C{=}Se$[19] and TeF_2 containing one and two σ-holes on their chalcogen atoms respectively (more details in Section 2.3). All these factors act in concert to determine the strength and direction of each σ-hole interaction.

The strength of σ-hole interactions can be tuned by varying the nature of the donor atom and covalently-bonded electron-withdrawing group. Larger donor atoms down a Group are more polarizable and less electronegative, facilitating σ-hole formation with more positive ESPs. Amongst the halogens, the size and magnitudes of the σ-holes increases in the order of F < Cl < Br < I,[16] and it is of no surprise that only the heavier halogens (Br, I) are effective σ-hole donors in solution-phase anion recognition.[5] The situation is more complicated for ChB, PnB and TrB donor atoms, as the heavier members of each group have greater metallic character and tendency towards hypervalency. Thus the heaviest members of the pnictogen (Sb, Bi) and tetrel (Sn, Pb) families, for which the strongest σ-hole interactions can be expected, may not be suitable for σ-hole-anion binding as they tend to participate in more traditional metallic coordination chemistry. Regarding the nature of the neighbouring group attached to the σ-hole donor atom, electron-withdrawing groups (e.g. CN, F, perfluoroarenes) can form larger σ-holes than electron-donating

ones (e.g. CH_3). Similarly, directly attaching σ-hole donor atoms to cationic organic motifs (e.g. pyridinium/ triazolium) or Lewis acidic metal centres can strengthen the resulting σ-hole interactions considerably. Finally, while it should be emphasised that the presence of σ-holes is intrinsic to the molecule itself, their magnitude and size can also be influenced by external factors such as Lewis bases, including anions (see Section 2.3), in close proximity.[20]

The nature of σ-hole interactions has always been a topic of considerable debate. It has been argued that all non-covalent interactions are fundamentally electrostatic in nature, which also encompasses the effects ascribed to polarisation.[21] While electrostatics are generally recognised as an important contribution to these interactions, the observation that even a σ-hole with negative ESP on CH_3Cl can form attractive XB interactions with formaldehyde (stabilisation energy of 1.17 kcal mol^{-1})[22] suggests that attractive dispersion forces may also play significant roles.[20] Recent work also further suggests the importance of covalency/ charge transfer in σ-hole interactions as well. In a combined experimental and computational study, Beer, Kennepohl and co-workers used Cl and Br K-edge X-ray Absorption Spectroscopy (XAS) to demonstrate the significant charge transfer character of XB interactions with halide anions. In fact, the degree of covalency was found to be comparable to those of transition metal complexes.[23] In a separate study, Cockroft *et. al.* very recently used a series of neutral molecular balances to delineate the contributions of electrostatics, solvophobic effects, dispersion forces and charge-transfer interactions in ChB, revealing the dominance of n (amide/ thioamide) → π^* (thiophene/ selenophene) charge-transfer contributions.[24] Indeed, σ-hole interactions can result in elongation of the pertinent covalent bond containing the donor atom as observed for XB complexes,[25] which can be interpreted as originating from donation of electron density from the Lewis base into the σ^* orbital. The significant charge-transfer character of σ-hole interactions may help explain some of the anion binding behaviour and preferences described later in the review.

Traditionally, a σ-hole interaction is identified experimentally in the solid state by short contacts, defined to occur when the interatomic distance between two interacting atoms is less than the sum of their respective van der Waals (VdW) radii. A shorter contact is often interpreted to arise from stronger interactions. However, as pointed out by Politzer,[17] the use of VdW radii as a yardstick is problematic due to difficulties in their determination, most notably arising from the assumptions that covalently-bonded atoms remain spherical and that the interatomic distance between two atoms are always invariant regardless of their solid state packing. Unsurprisingly, this approach inevitably omits many actual σ-hole interactions. In addition, intermolecular contacts in crystal structures involve interactions between regions with the most positive and negative ESPs on neighbouring molecules, which may in some cases lie between atoms. Using tetrafluoro-1,3-dithietane as an example, Politzer demonstrated that the most positive and negative ESPs have been found to occur approximately midway along each C-S bond and on the fluorine atoms respectively, whose attraction defines the molecular packing arrangement in the crystal lattice (Figure 2).[26] However, traditional short contact identification manifests this interaction as spurious chalcogen and tetrel bonds between the fluorine atom on one molecule with sulfur and carbon atoms respectively on the adjacent molecule (shown by dashed blue lines in Figure 2), which are not representative of the actual intermolecular interactions. These important points should be kept in mind when identifying σ-hole interactions with anions in the solid state, which will become more pertinent with heavier PnB and TrB donor atoms due to the complexities of their bonding environment and geometries (see Section 2.4).

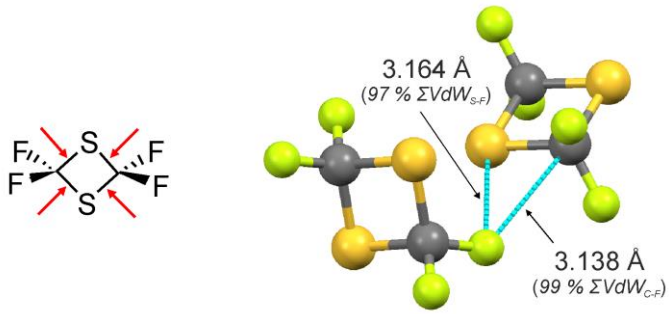

Figure 2. (Left) Structure of tetrafluoro-1,3-dithietane (red arrows indicate the approximate locations of the most positive ESP values); and (right) the spurious TrB (F···C) and ChB (F···S) short contacts between adjacent molecules in the solid state crystal structure.[26] Atom labels: green = F, grey = C and yellow = S; short contacts are shown as blue dashed lines.

2. SIGMA HOLE ANION BINDING MOTIFS AND RECEPTORS

2.1 Fundamental Computational Studies

The fundamental contrasting electronic properties of Group 14-17 elements suggest that variations in the anion binding preferences of each σ-hole interaction may be expected. Although there is still considerable debate regarding the use of appropriate computational models to describe σ-hole interactions,[20] recent comparisons between the behaviour of σ-hole donors for halide (F^-, Cl^-, Br^-, I^-) binding have been made *in silico*, most notably by Scheiner and coworkers. Performed using DFT in both the gas phase and in a dielectric continuum designed to model water using a range of host molecule designs, we highlight the most important findings of these comparative studies.

Halide binding by ChB, PnB and TrB was first compared with neutral dithienothiophene-based receptors **1** containing various σ-hole donor atoms (X) in the gas phase (Figure 3A).[27] Halide binding invariably occurred between both donor atoms, equidistant between each C-X bond other than F^- binding with PnB and TrB donors which was skewed towards one donor atom. In all cases the σ-hole interactions show good directionality with the C-X···A^- angles within 16 ° of linearity, along the extensions of each C-X bond. A strong preference for F^- is consistently demonstrated by all receptors, with affinities decreasing in the order $Cl^- > Br^- > I^-$. More strikingly, sharp increases in halide binding energies and greater F^- selectivity resulted when the donor atom was changed from chalcogen to pnictogen to tetrel. In fact, larger binding energy enhancements were observed on moving across the Period (e.g. S to P; As to Ge) than using heavier atoms of the same Group (e.g. P to As). Electron withdrawing oxygen atoms added to the bridging sulfur atom remote to the anion binding site (Y in Figure 3A) augmented all halide binding energies, underscoring the tunability of the σ-hole interaction strength.

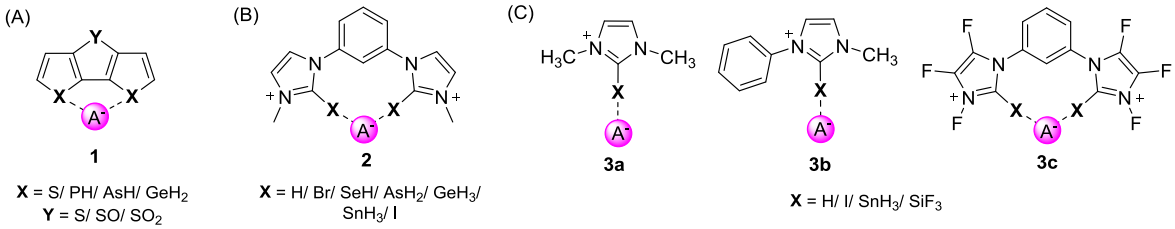

Figure 3. Structures of receptors bearing different σ-hole donor groups used in comparative studies by Scheiner, with the main halide anion (A^-) binding locations indicated: (A) neutral thienothiophenes 1;[27] (B) dicationic substituted imidazoliums 2[28] and (C) various substituted imidazolium-based host designs 3a - 3c.[29] σ-hole interactions are represented by dashed lines.

Varying the receptor framework, anion binding geometry and the addition of charge modified the halide binding trends amongst the σ-hole-donor hosts.

Dicationic receptors **2,** containing imidazolium groups substituted at the 2-position with XB, ChB, PnB and TrB σ-hole donor groups (Figure 3B), bound all halides between the donor atoms in an aqueous medium.[28] The free energies of F^- binding was found to be highly sensitive to the nature of the σ-hole donor group, even within the same Period (Br, Se, As, Ge), which decreased following the order of TrB > PnB > XB > ChB. Much smaller variations between the different σ-hole interactions were seen for the binding free energies of Cl^- and Br^-, with XB appearing to be the preferred interaction (XB > ChB > PnB > TrB). Nonetheless, F^- was once again found to be the strongest bound halide (F^- > Cl^- > Br^-) amongst all the σ-hole receptors studied, and selectivity could be enhanced with heavier donor atoms (X = I/ SnH_3). Compared to the HB receptor analogue (X = H), only Ge, Sn and I-based receptors showed superior binding of F^-, while almost all σ-hole donors (except Ge) bound Br^- more strongly.

The influence of receptor design on TrB and XB interactions was then studied using the receptors **3a**-**c** shown in Figure 3C,[29] which invariably bound F^- preferentially over Cl^- in both gas phase and using an aqueous solvent model. While the binding energies were insensitive to the receptor end-group (*N*-methyl in **3a** and phenyl in **3b**), having a ditopic receptor design (receptor **2** in Figure 3B, with X = H/ I/ SnH_3/ SiF_3) augmented F^- and Cl^- binding, which could be further enhanced by receptor fluorination (design **3c**). Although the binding energy of Cl^- was increased by more than two-fold, suggesting cooperative involvement of both substituted imidazolium groups, that of F^- was enhanced by less than two times (anti-cooperative). Changing the donor atom increased the halide binding strength in the order of H < I < SnH_3 < SiF_3. It is especially notable that despite Sn being found two Periods lower than Si, enhanced halide binding and F^- selectivity by the SiF_3-containing analogue over SnH_3 was seen, possibly due to the presence of the fluorine atoms directly bonded to the Si donor atom. Nonetheless, in a majority of the F^- complexes, the donor atoms (I, Sn and Si) appear to lie closer to F than to C, suggesting a transfer of the donor atoms to the halide. These atom transfer reactions were not seen for Cl^-.

These comparative studies *in silico* demonstrated that significant variations in halide binding affinities can result by simply changing the nature of the σ-hole donor groups. This suggests that anion selectivity may be modulated and tuned using such an approach. Furthermore, a strong case is made for predicting PnB and TrB host molecules to be highly potent anion receptors.

2.2 Halogen Bonding Anion Recognition

Halogen bonding interactions, characterised by their prominent linearity and strength arising from the highly-localised σ-hole on the donor halogen atom, have been increasingly applied for anion recognition and sensing during the last decade. Amongst the halogens, only the heaviest members (Br, I) are utilised for anion coordination due to their polarizability and ability to form highly electrophilic σ-holes, while the lighter members (F, Cl) form σ-holes which are either insignificant or not of sufficient Lewis acidity for appreciable anion interactions in solution. XB anion receptors span a diverse range of structural complexity, ranging from simple acyclic molecules to elaborate mechanically bonded higher-order interlocked structures. Compared to HB receptors however, XB receptor design needs to take into account several unique geometric and structural considerations for effective anion binding to be achieved. These include the strict angular-dependence of XB strength which falls off more sharply with increasing deviations from linearity,[20] the steric bulk of XB donor groups containing the heavier halogens (with large VdW radii) and consequently, the much longer XB-anion supramolecular contacts compared with HB analogues. In this section, a survey of neutral and cationic XB-donor motifs is followed by a consideration of special receptor design features that are required for optimising XB anion binding strength. The anion recognition properties of XB anion receptors of varying structural complexities are discussed and optimisation of XB anion binding geometries highlighted. Importantly, in many of these examples, XB receptors exhibit considerably augmented anion affinities compared to HB receptor analogues. The most prominent differences in anion binding properties between XB and HB receptors are underlined in a concluding discussion section.

2.2.1 Design of Halogen Bonding Host Molecules

XB host molecules for anion recognition contain XB-donor motifs which invariably comprise of a heavy halogen donor atom covalently bonded to a highly electron-deficient group. Ideally, these motifs should be synthetically accessible, as well as be stable and robust enough to be incorporated into different host structural molecular frameworks. These factors account for the preponderance of aromatic XB-donor groups for anion binding over aliphatic motifs, as the latter is often susceptible to nucleophilic substitution in the presence of anions. The most common neutral and cationic XB motifs which fulfill these criteria in general are collected in Table 1, together with representative examples of host molecules.

Haloperfluoroarenes are some of the earliest XB motifs shown to bind anions effectively.[5] Other than being highly electron-deficient, the possibility of varying the XB donor-atom's substitution position on the perfluoroarene ring allows convenient tuning of directionality, as exemplified by the convergent halide (Cl^-, Br^- and I^-) coordination by Taylor's tripodal XB receptor **4** (Table 1, entry 1).[30] Despite their anion binding potency, their popularity was eventually overtaken by halotriazoles, whose ready accessibility via copper(I)-catalysed azide-alkyne cycloaddition (CuAAC) reactions enabled them to be conveniently incorporated into a multitude of diverse host architectures, such as Beer's XB foldameric receptor **5** (Table 1, entry 2A).[31] Furthermore, the possibility of metal coordination (host **6**, Table 1 entry 2B)[32] or methylation of the Lewis basic triazole nitrogen atoms allow further enhancement of their XB donor strength. The latter reaction forms the halotriazoliums, which are highly potent anion binding XB motifs and allow strong anion coordination even in highly-competitive solvents such as DMSO as demonstrated by Schubert's dicationic receptor **7** (Table 1 entry 3).[33] Compared to the halotriazoliums, haloimidazoliums show similar Lewis acidic behaviour[34,35] and thus constitute another highly-effective and synthetically-versatile class of charge-assisted XB-donor motifs (e.g. receptor **8**, Table 1 entry 4), which have been extensively applied in areas such as anion binding catalysis (see Section 3.2).[36] Finally, pyridinium-based XB motifs can take the form of either covalent appendage of XB-donor motifs (e.g. iodotriazoles in Beer's receptor **9**, Table 1 entry 5A)[23] or direct attachment of halogen atoms to the pyridinium aromatic ring. The effectiveness of the latter motif was impressively demonstrated by Berryman using acyclic host **10**, whose linear XB interactions between the para-iodopyridinium motifs and iodide drives the formation of a unique triple helix comprising of three intertwined host molecules encapsulating two iodide anions within its central channel (Table 1 entry 5B).[37]

It should be noted that cationic XB motifs such as haloimidazoliums also potentially allow anions to interact via side-on anion-π interactions as well as by HB to the Lewis acidic hydrogen atoms on the back face of the imidazolium group, in addition to XB (Figure 4A). This possibility was first recognised by Resnati and Metrangolo using XB receptor **11**, which showed a weak hydrogen bond between chloride and backbone proton H_β in the solid state (Figure 4B).[38] This interaction, however, did not contribute significantly to the solution-phase anion recognition properties of **11**, which was dominated by XB interactions as evident from ^{1}H NMR studies. Huber *et. al.* subsequently further addressed the possibilities of these alternative anion interactions in a combined experimental and computational study with a range of substituted iodoimidazoliums including compounds **12a** (Figure 4C), **12b** (Figure 4D) and **8** (Table 1, entry 4).[36] Although solid-state, computational and calorimetric studies ruled out anion-π contributions, HB anion coordination was shown to be present with **12a** and triflate in its solid state structure (Figure 4C) and in solution by the downfield ^{1}H NMR shifts of the backbone imidazolum protons with increasing concentration of the **12a**-OTf salt. This could however be mitigated by replacing these hydrogen atoms with chlorine (**12b**) or methyl groups (**8**), which interact negligibly with anions. Notably, the greater electron-deficiency of **12b**'s imidazolium ring resulted in stronger bromide binding (K_a = 7.0 x 10^4 M^{-1}) compared with **12a** (K_a = 1.2 x 10^4 M^{-1}) in acetonitrile, as determined by isothermal calorimetry (ITC).

Table 1. Common neutral (entries 1-2) and cationic (entries 3-5) XB motifs for anion binding and representative examples of host molecules.

	XB-donor Motif [a]	Representative Examples [b]	Ref
1	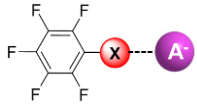 Haloperfluoroarene	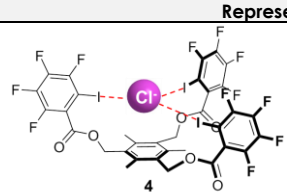 **4** K_a (Cl^-) = 1.9 x 10^4 M^{-1} in d_6-acetone	30
2	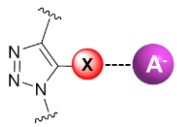 halotriazole	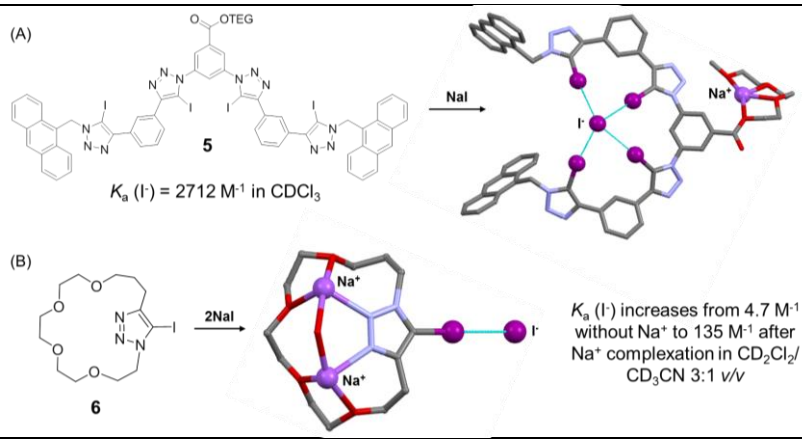 (A) **5** K_a (I^-) = 2712 M^{-1} in $CDCl_3$; NaI; Na^+; I^- (B) **6**; 2NaI; Na^+; Na^+; I^- K_a (I^-) increases from 4.7 M^{-1} without Na^+ to 135 M^{-1} after Na^+ complexation in CD_2Cl_2/CD_3CN 3:1 *v/v*	31 32
3	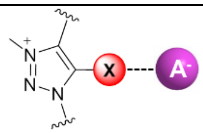 Halotriazolium	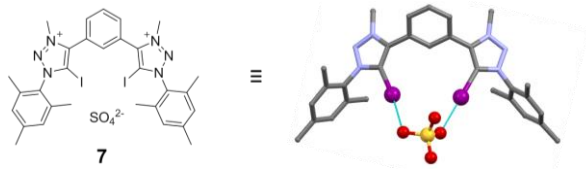 **7** SO_4^{2-} ≡ K_1 (SO_4^{2-}) = 3400 M^{-1}; K_2 (SO_4^{2-}) < 15 M^{-1} in d_6-DMSO	33
4	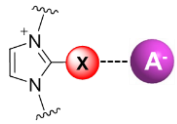 Haloimidazolium	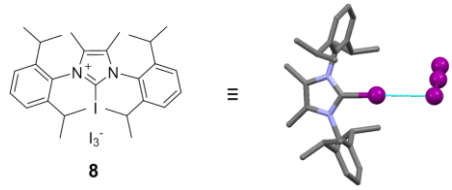 **8** I_3^- ≡	36
5	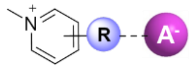 Substituted pyridiniums (R = halogen atom/ XB donor group)	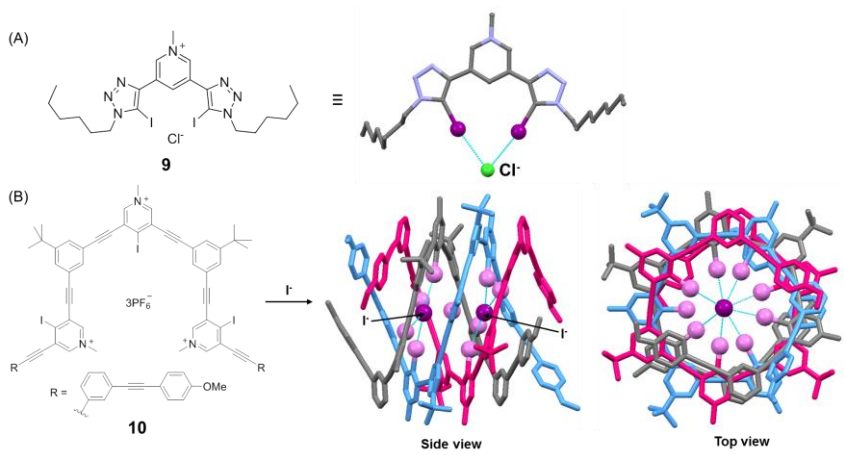 (A) **9** Cl^- ≡ Cl^- (B) **10** $3PF_6^-$ R = OMe I^- Side view Top view	23 37

[a] X = Br/I; [b] XB interactions shown as dashed lines. Hydrogen atoms omitted from the crystal structures for clarity.

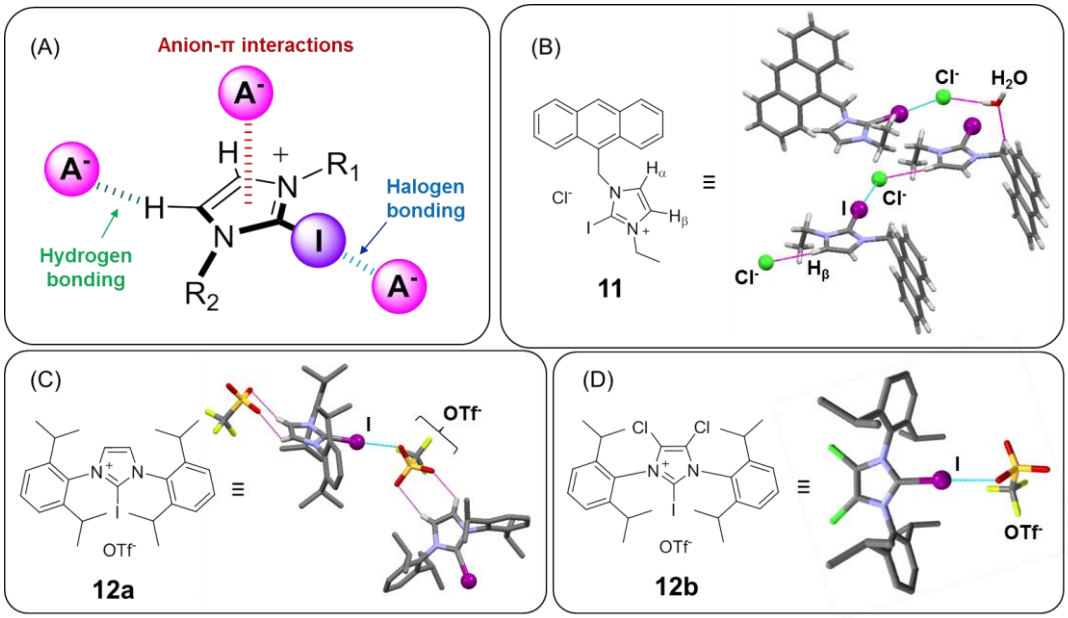

Figure 4. (A) Possible anion-π, HB and XB anion binding interactions with haloimidazoliums; (B) Resnati and Metrangolo's XB receptor 11 and its solid state Cl^- adduct, showing the involvement of both HB and XB interactions in Cl^- binding;[38] Huber's iodoimidazolium anion hosts (C) 12a and (D) 12b as well as the crystal structures of their triflate complexes.[36] HB and XB interactions are shown as pink and blue dashed lines respectively.

Having considered the various XB donor motifs, we now discuss how these motifs can be integrated into XB receptor design to maximise anion binding strength by optimising the aforementioned geometric and steric properties of XB-anion interactions. Firstly, like all host-guest complexes, the concept of receptor structural preorganisation, where host molecules possessing the most favourable conformations before guest binding give the most stable host-guest complexes, features prominently in XB host design. This can be achieved by a combination of rigid spacer groups (e.g. aromatic rings) separating XB-donor moieties and attractive intramolecular donor-acceptor interactions rigidifying the receptor framework. For instance, Schubert's neutral cleft-type XB receptor (**13a**) (Figure 5A) preorganised by intramolecular HB interactions between phenol groups installed on the central carbazole spacer and the triazole N^3 atoms is able to bind Cl^- and Br^- much more strongly than its rotationally-flexible analogue (**13b**) in THF.[39] Strikingly, isothermal titration calorimetry (ITC) experiments revealed that halide binding by **13b** is disfavoured entropically while with preorganised **13a** it is entropically favourable, showing that restriction of rotational freedom in **13a** can significantly reduce the entropic penalty of anion complexation. Other methods of conferring structural rigidity include metal chelation, exemplified by Re(I) complexation between ligating N atoms of iodotriazoles and the pyrimidine spacer of Beer's XB receptor **14** (Figure 5B),[40] and by introducing bulky groups to hinder bond rotations such as in Huber's receptor **15** (Figure 5C). For the latter, the *syn*- and *anti*-atropisomers resulting from steric hindrance of the central benzene ring's trifluoromethyl substituent show very different anion affinities and coordination modes. A larger affinity for Br^- in CH_3CN (K_a = 3.5 X 10^6 M^{-1}) was found for **15·*syn*** compared to **15·*anti*** (K_a = 4.4 x 10^4 M^{-1}), as the latter receptor is only able to coordinate the anion in a monodentate fashion due to the linearity of the XB interactions.[35]

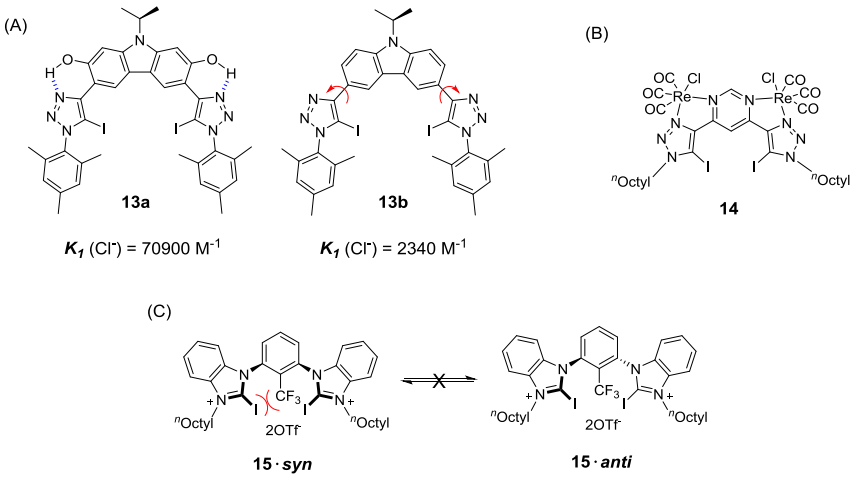

Figure 5. (A) Schubert's cleft-type XB receptors (13a and 13b) containing carbazole spacers, with their host-guest 1:1 stoichiometric association constants for Cl^- in THF;[39] (B) Beer's Re(I)-complexed XB receptor 14;[40] (C) Huber's iodo-benzimidazolium XB receptor 15 showing both *syn*- and *anti*- conformations.[35]

Macrocycles and mechanically-interlocked structures such as rotaxanes and catenanes have conformationally restricted and preorganised anion binding cavities shielded from the bulk solvent environment, and XB donor groups have been incorporated into their frameworks to take advantage of these benefits to enhance anion binding selectivity and strength. The power of this approach is demonstrated in Kubik's cyclic pseudopeptide macrocycle **16** containing three iodotriazole units designed to coordinate halide anions convergently within the restricted macrocycle cavity (Figure 6).[41] In the competitive solvent mixture of 2.5 % D_2O in d_6-DMSO *v/v*, the halides showed anti-Hofmeister binding selectivity (affinities of $Cl^- > Br^- > I^-$), with Cl^- exhibiting an impressively strong binding affinity ($\log_{10}K_a = 3.28$) in spite of the lack of charge assistance. This rare selectivity for more strongly-hydrated halides in wet solvent media (see Section 2.2.2) was attributed to an optimal host-guest size match arising from the bulky XB-donor iodine atoms pointing into the macrocycle cavity. It is notable that the analogous HB receptor containing (proto)triazoles instead of iodotriazoles displayed no appreciable halide binding under identical conditions.

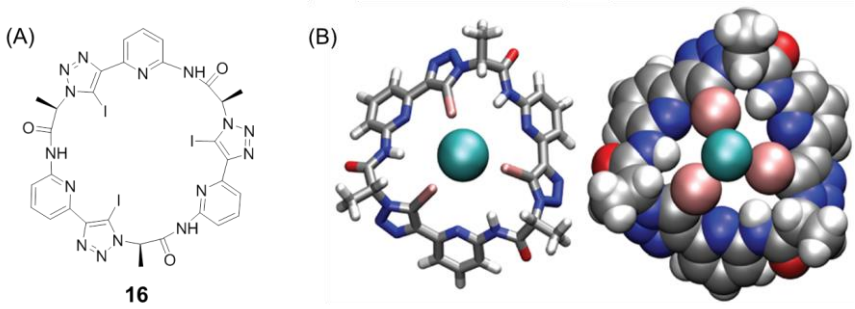

Figure 6. (A) Structure of Kubik's neutral XB cyclic pseudopeptide 16 and (B) the DFT-optimised structure of its Cl^--complex showing the participation of three convergent XB interactions (ball and stick model) and the optimal host-guest size match of the resulting macrocycle cavity with Cl^- (spacefill model). DFT structures are reproduced from ref. 41 with permission from The Royal Society of Chemistry.

Inspired by the buried anion binding domains of enzymes and proteins capable of highly-selective anion binding with exquisite shape and size complementarity, rotaxane and catenane host systems possessing interlocked cavities capable of three-dimensional encapsulation of anionic guests have been developed.[42] These binding sites are often preorganised by numerous secondary non-covalent interactions from the rest of the molecular framework (e.g. donor-

acceptor π-π stacking and HB interactions), and their non-covalent mechanically bonded nature allows some degree of flexibility to accommodate guest species. Decorating these cavities with XB donor groups can enhance their hydrophobic character which facilitates anion dehydration in aqueous media. However, the need to maintain geometric and spatial integrity for anion binding results in considerable design and synthetic challenges. Nonetheless, the stringent directionality and strength of XB-anion interactions allow their exploitation in the synthesis of XB interlocked molecules via anion templation, as demonstrated by the Beer group. For example, XB interactions between Br^- and a bromoimidazolium bis-vinyl-appended macrocycle precursor (as its PF_6^-) salt facilitated the synthesis of homocatenane **17** (Figure 7A).[43] The diametrically-opposite XB donor groups enabled strong selective coordination of halides (K_a for Cl^- = 3.7 x 10^6 M^{-1}; K_a for Br^- = 1.5 x 10^5 M^{-1}) between them in CH_3CN, whilst showing no detectable binding for a range of oxoanions ($CH_3CO_2^-$, $H_2PO_4^-$, NO_3^-, HCO_3^-) by fluorescence spectroscopy. Using a similar principle, a [2]rotaxane (**18**) containing four iodotriazole/lium groups around its binding cavity was constructed by Cl^- anion templation,[44] where the significant spatial separation between the XB donor groups allowed halides to be bound convergently by linear XB-anion interactions (Figure 7B). In the highly-competitive aqueous solvent mixture of H_2O/ CH_3CN 1:1 *v/v*, luminescence spectroscopy titrations revealed Hofmeister binding bias for I^- (K_a = 2.4 x 10^4 M^{-1}) over the other more strongly-hydrated halides Cl^- and Br^-. It is noteworthy that in these two examples, the presence of a non-coordinating anion (e.g. PF_6^-) resulted in no interlocked structure formation, highlighting the important influence of XB-anion template interactions in governing precursor assembly in solution. Other XB motifs capable of strong bidentate anion coordination, such as 3,5-bis(iodotriazole)-pyridinium (shown in compound **9** of Table 1) have also enabled rotaxane[45] and catenane[23] structures to be prepared for strong anion binding (*vide infra*).

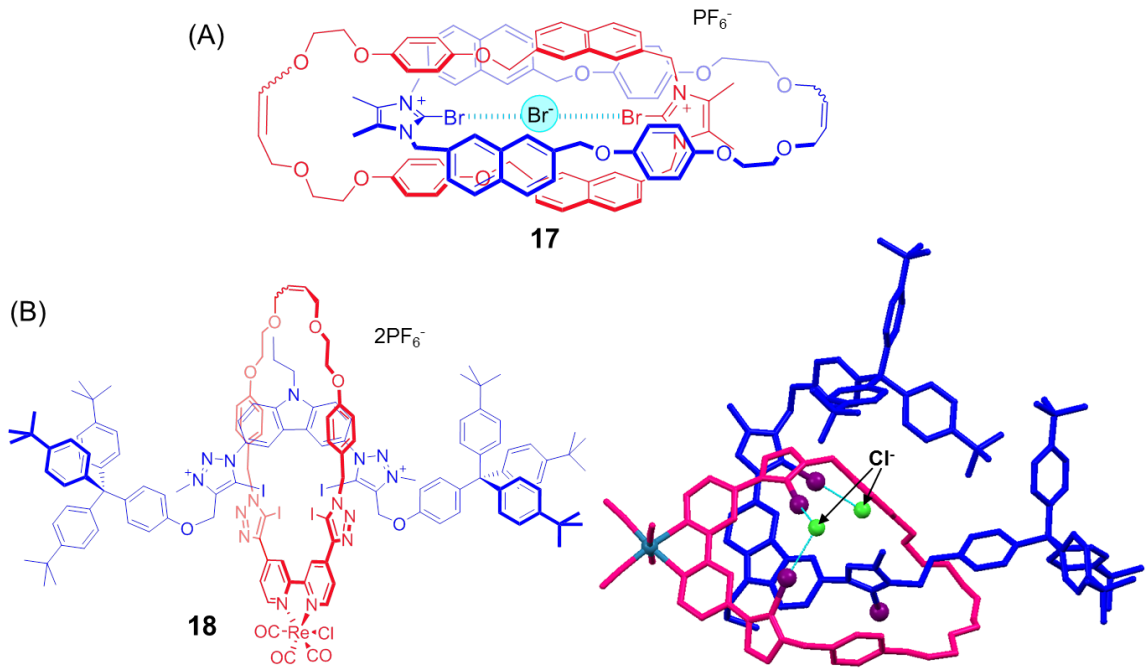

Figure 7. Interlocked host molecules for anion binding containing all-XB cavities formed by XB-mediated halide anion templation: (A) [2]catenane 17 containing two diametrically-opposite bromo-imidazolium groups for halide binding;[43] (B) [2]rotaxane 18 with four iodotriazole/lium anion binding groups and its crystal structure showing XB interactions (blue dashed lines) within the binding cavity for Cl^- coordination. XB donor iodine atoms are shown in purple.[44]

To complement anion templation, the active metal template strategy (AMT)[46] has recently emerged as a versatile and effective method to synthesise XB rotaxane host structures. This method relies on a catalytically-active metal cation

(e.g. Cu^{+}) coordinated endotopically within the cavity of a macrocycle catalysing a covalent bond-forming reaction (e.g. CuAAC) through the cavity itself from appropriately-functionalised axle precursors. Although cation and anion coordination involve fundamentally antagonistic interactions, Beer *et. al.* circumvented the problem by designing a macrocycle containing two adjacent covalently-linked iodotriazole groups which is able to *N*-ligate Cu^{+} between them (Figure 8). By capitalising on the endo/exo conformational flexibility of this motif on the macrocycle, the bound Cu(I) can form a rotaxane by catalysing iodotriazole formation from iodoalkyne and azide-containing axle precursors.[47] Subsequent replacement of the ligated Cu(I) with a bulky Re(I) complex forced the macrocycle iodotriazole groups to be now endotopically oriented into the rotaxane cavity for anion binding. The resulting Re(I)-containing neutral rotaxane **19** bound Cl^{-} selectively (K_a = 560 M^{-1}) over the other halides and $CH_3CO_2^{-}$ by UV-Vis spectroscopy titrations in $CHCl_3$, while the metal-free analogue showed no evidence of binding under identical conditions, showing the critical role played by the Re(I) complex in preorganising and polarising the iodotriazole units for anion coordination.

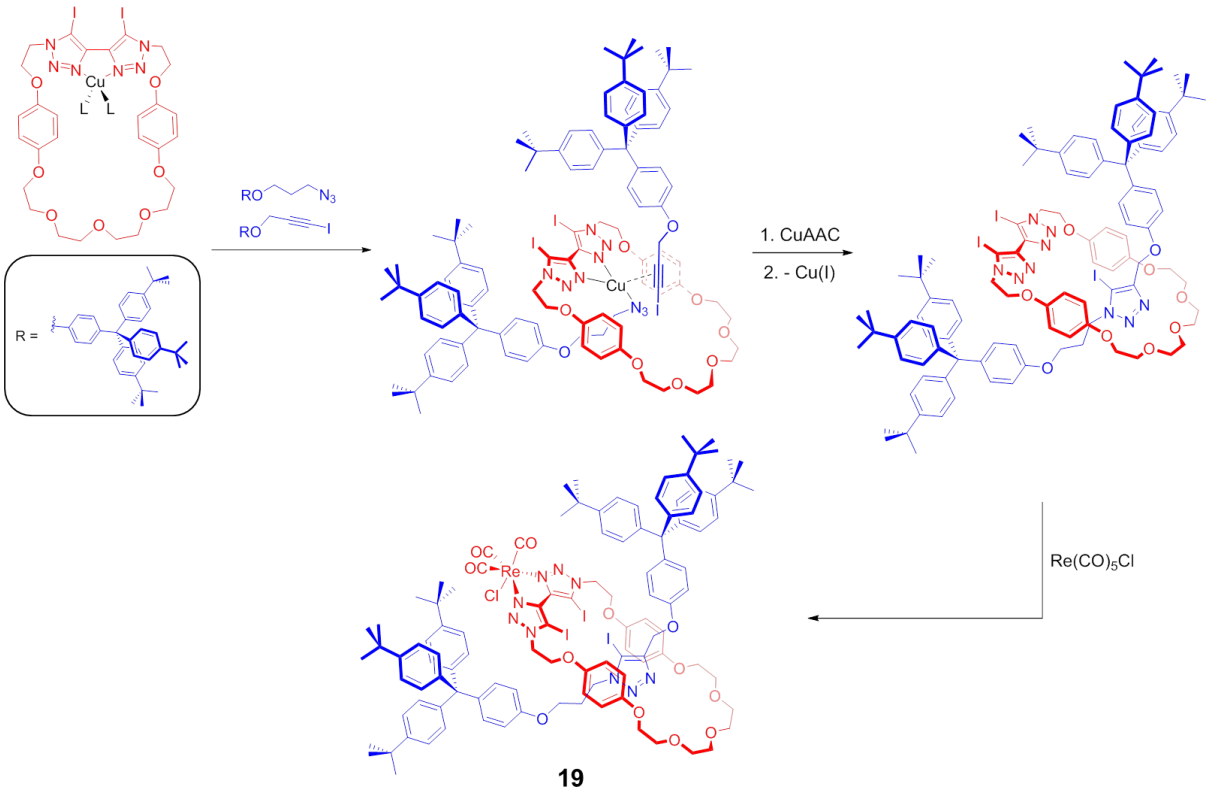

Figure 8. CuAAC-AMT synthesis of neutral Re(I)-complexed [2]rotaxane 19 with an all-XB binding cavity for anion binding and sensing.

The CuAAC-AMT methodology was subsequently exploited to prepare another family of metal-free neutral [2]rotaxanes (**20**-**22**) which possess different numbers and geometries of XB-donor iodotriazoles within their interlocked binding cavities (Figure 9),[48] which highlight the critical role of optimal multidentate XB bite angles for anion binding. Rotaxane **20a** possesses a macrocycle component with *meta*-substituted iodotriazoles on a central benzene spacer, and is capable of binding halides strongly (K_a for Cl^{-} = 4384 M^{-1}) in d_6-acetone by a mixture of XB interactions from the macrocycle and HB from the axle's prototriazole unit. However when the macrocycle unit was replaced with one containing *ortho*-substituted iodotriazoles (**20b**), dramatic loss of halide binding affinity was observed (K_a for Cl^{-} = 89 M^{-1}) under identical conditions (Table 2). This likely arises from the XB-donor

iodine atoms of **20b** being twisted out-of-the-plane relative to each other due to their steric clash, preventing bidentate halide coordination by convergent XB interactions. Interestingly, **20a** was able to bind SO_4^{2-} ($K_a > 10^4$ M^{-1}) more strongly than Cl^- despite its larger size, likely due to the mechanically bonded axle and macrocycle components being able to adjust their relative positions to accommodate the oxoanion guest. Despite the constrained rotaxane binding site, the number of iodotriazoles can exert an additive effect on anion affinities if judiciously designed. In this case, substituting the axle prototriazole of **20a** with an iodotriazole unit (rotaxane **21**) allowed tridentate Cl^- coordination by three convergent XB interactions, noticeably enhancing its Cl^- binding affinity ($K_a > 10^4$ M^{-1}) in d_6-acetone, Even without the preorganisation or iodotriazole polarisation arising from metal complexation, rotaxane **21** was able to bind Cl^- more strongly than rotaxane **19** (Figure 8) in a more competitive solvent, showing the importance of XB bite angle and geometry for strong anion coordination. Subsequently, binding studies performed in the more competitive solvent mixture of d_6-acetone/ D_2O 98:2 *v/v* reduced the halide binding affinities of rotaxanes **20a** and **21** (Table 2), underscoring the important role of the solvent in XB-anion binding. Nonetheless, increasing numbers of iodotriazole groups flanking each interlocked cavity between rotaxanes **20a**, **21** and **22** (with four iodotriazole groups) gave stronger halide binding. It is noteworthy that doubling the number of iodotriazole units from two (**20a**) to four (**22**) increased the magnitudes of the halide binding association constants by more than twice, likely due to cooperative tetradentate halide coordination in the vicinity of rotaxane **22**'s binding cavity achieved by the flexible axle alkyl linkers. Rotaxane **22** was able to bind spherical halides exclusively over anions with alternative geometries such as azide, perrhenate and nitrate in d_6-acetone/ D_2O 98:2 *v/v*.

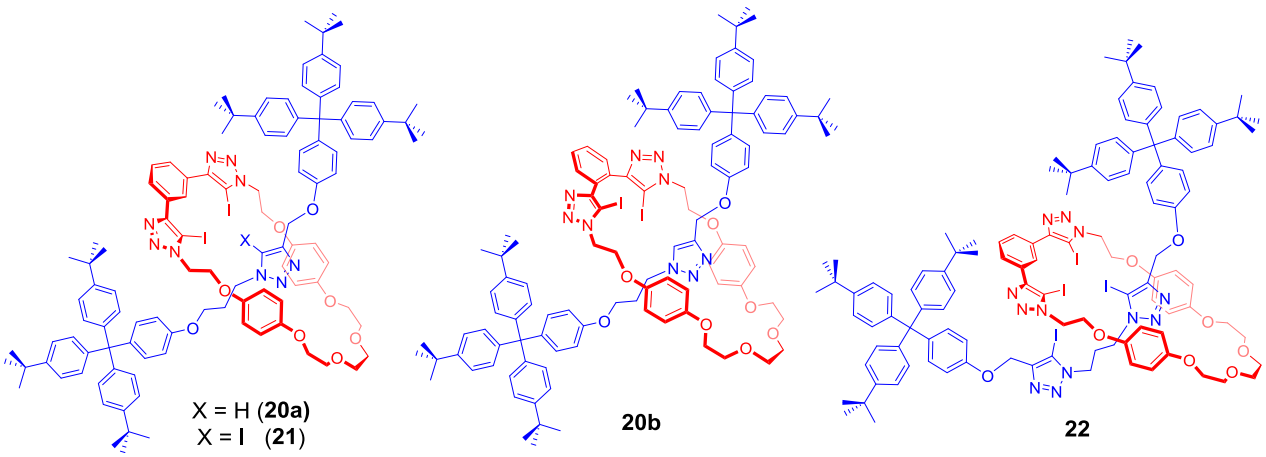

Figure 9. Structures of neutral XB [2]rotaxanes 20a, 20b, 21 and 22 possessing different numbers and geometries of XB-donor iodotriazole units flanking their interlocked cavities.[48]

Table 2. Host-guest 1:1 stoichiometric association constants of rotaxanes 20a, 20b, 21 and 22 in d_6-acetone-containing solvent mixtures[a].[48]

Solvent	d_6-acetone		2 % D_2O in d_6-acetone		
Rotaxane	**20a**	**20b**	**20a**	**21**	**22**
Cl^-	4384	89	114	280	496
Br^-	2139	64	371	461	1200
I^-	902	34	533	617	1100
SO_4^{2-}	> 10^4	$K_{2:1}$ = 211 [b] $K_{1:1}$ = 425	38	19	-[c]

[a] Errors (±) < 10 %; [b] Host-guest 2:1 binding was found which became 1:1 with excess anion; [c] No binding. Data reproduced with permission from reference 48.

2.2.2 How does Anion Binding by XB and HB Hosts Differ?

Other than their more stringent binding angles, XB-anion interactions also possess greater degrees of covalent character than HB,[23] and the XB donor atoms are fundamentally more hydrophobic, sterically-bulky and insensitive to pH. These differences act in tandem to elicit often dramatically contrasting binding behaviour which allow XB host molecules to complement HB analogues in many ways. Commonly, XB hosts display augmented anion binding affinities compared to their HB analogues, which has been observed in receptors of all degrees of structural complexity. Indeed, many preceding examples, including bidentate receptor **9** (Table 1), foldamer **5** (Table 1) and macrocycle **16** (Figure 6) are capable of significantly stronger anion binding than their HB analogues, sometimes with more than an order-of-magnitude enhancement in association constants, in both wet and dry organic solvents. Consequently, this also results in an often heightened response and sensitivity towards anion sensing by optical or electrochemical means (see Section 3.1).

The solvent dependency of XB-anion interactions, especially to HB-donor solvents such as methanol and water,[49] has been critical in determining the anion selectivity displayed by many XB host systems. This property is exemplified by the anion binding affinities and trends of neutral rotaxane **20a** in the absence and presence of water (Table 2). In dry d_6-acetone, the affinity of **20a** for anions decreases with less charge dense guests (SO_4^{2-} > Cl^- > Br^- > I^-). However, a complete reversal of binding trend was observed in d_6-acetone/ D_2O 98:2 *v/v* (K_a of I^- > Br^- > Cl^- > SO_4^{2-}), with the most strongly-hydrated anions showing the greatest diminution. This binding preference for the least-solvated anion in protic solvents by XB receptors often contrasts with the behaviour of their HB counterparts, with many examples of HB macrocycles and interlocked molecules showing preference for Cl^-.[42] For instance, XB rotaxane **23a** (Figure 10A) shows Hofmeister halide binding bias (K_a of I^- > Br^- > Cl^-) in $CDCl_3$/ CD_3OD/ D_2O 45:45:10 *v/v/v*, while its HB counterpart (**23b**) shows a preference for the lighter halides (K_a of Cl^- ≈ Br^- > I^-) in the protic solvent mixture $CDCl_3$/ CD_3OD 1:1 *v/v*. Dramatically, a water-soluble XB rotaxane (**24a**) stoppered by hydrophilic β-cyclodextrin groups (Figure 10B) showed selective and impressively strong I^- binding (K_a = 2200 M^{-1}) over the lighter halides in D_2O. On the other hand, its HB analogue (**26b**) showed dramatically weaker iodide association (K_a = 20 M^{-1}) in water.[45]

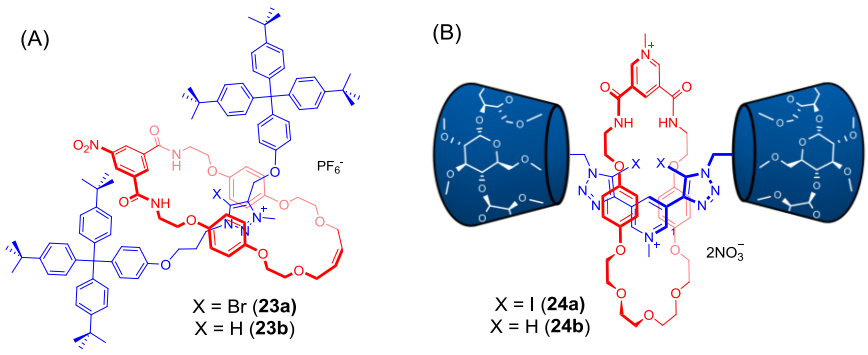

Figure 10. Chemical structures of (A) a XB-rotaxane host (23a) and its HB analogue (23b); (B) XB (24a) and HB (24b)-analogues of ß-cyclodextrin-stoppered water-soluble rotaxanes.[45]

The greater steric bulk of XB donor groups compared with HB can be exploited to modulate the available space in an anion binding cavity which can change its anion selectivity. This effect is most pronounced in spatially-constrained binding sites, such as those of rotaxanes **25a** and **25b**, which differ only by the presence of an iodine atom on the axle's triazole unit (Figure 11).[50] In the protic solvent mixture $CDCl_3$/ CD_3OD 1:1 *v/v*, HB rotaxane **25a** binds $H_2PO_4^-$ selectively over the halides and acetate (K_a ($H_2PO_4^-$) = 2399 M^{-1} > K_a (Cl^-) = 1831 M^{-1} > K_a (Br^-) = 1299 M^{-1} > K_a ($CH_3CO_2^-$) = 543 M^{-1} > K_a (I^-) = 449 M^{-1}). Contrastingly, selective Br^- binding was observed for the XB analogue **25b** concomitant with a decrease in the

affinities of all anions (K_a (Br^-) = 532 M^{-1} > K_a (I^-) = 466 M^{-1} > K_a (Cl^-) = 381 M^{-1} > K_a ($H_2PO_4^-$) = 211 M^{-1}; $CH_3CO_2^-$ no binding). This interesting change in anion selectivity was ascribed to the interlocked cavity of **25a** having more space to accommodate the tetrahedral $H_2PO_4^-$ guest, whereas the spatially more constrained cavity of **25b** is of complementary shape and size to Br^- whilst simultaneously sterically hindering anion access.

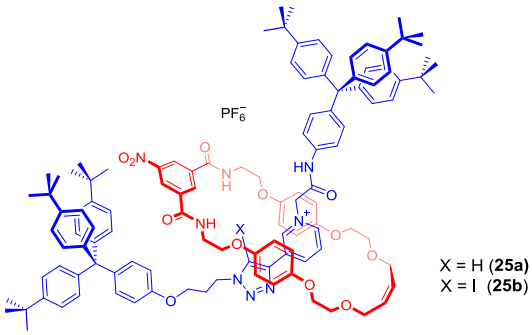

Figure 11. Structures of $H_2PO_4^-$-selective HB rotaxane 25a and its XB analogue 25b which shows preferential Br^- binding.[50]

In highly-competitive polar protic solvent media such as water, anion binding by XB receptors often show contrasting thermodynamic signatures with their HB counterparts - the latter is often largely driven by entropy increase resulting from dehydration of the interacting species, with small or unfavourable enthalpic (ΔH) contributions to the overall free energies of binding (ΔG).[51] In a striking example of this difference, the binding of I^- to rotaxane **24a** (Figure 10B) is driven exclusively by enthalpy and disfavoured entropically, indicating that binding was not merely driven by host/guest dehydration in the classical hydrophobic effect.[45] Conversely, the HB analogue **24b** shows the opposite contribution, with iodide binding being entropically-driven with an unfavourable endothermic enthalpy component. The favourable enthalpic contribution to XB-mediated anion binding in water was also observed during perrhenate (ReO_4^-) binding to dicationic receptors **26**[52] and **27**[53] (Figure 12A and B respectively), where in both cases entropy was disfavoured. These prominent enthalpic contributions which drive the strong binding may be attributed in part to a significant charge transfer/covalent contribution to the XB-anion interactions. In less competitive polar aprotic solvent media such as acetonitrile, anion binding to XB receptors still retains their favourable enthalpic signatures, while now also displaying significant positive entropic contributions as well. This was demonstrated by Huber using ITC to probe halide (Cl^-, Br^- and I^-) binding to a large range of XB receptors which show varying extents of enthalpic/ entropic dominance, as seen from receptors **2.I** and **2.Br** (Figure 12C and Table 3).[49]

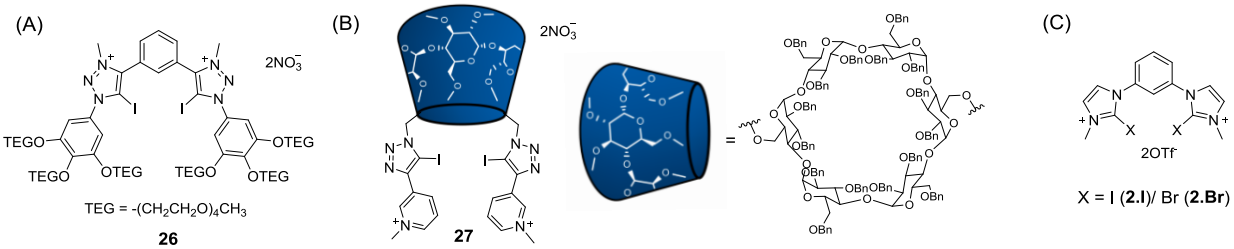

Figure 12. Beer's dicationic XB receptors capable of perrhenate binding in water, solubilised by (A) tetra(ethylene-glycol) units for 26 and (B) α-cyclodextrin for 27; (C) Huber's haloimidazolium XB receptors 2.I and 2.Br.

Table 3. Thermodynamic contributions (ΔH and $T\Delta S$/ kJ mol^{-1}) to the overall free energy of halide binding (ΔG/ kJ mol^{-1}) by Huber's XB receptors 2.I and 2.Br.[a]

Receptor	Halide	ΔG/ kJ mol^{-1}	ΔH/ kJ mol^{-1}	$T\Delta S$/ kJ mol^{-1}	Percentage contribution of ΔH to ΔG/ %
2.I	Cl^-	-33.2	-13.5	19.7	40.7
	Br^-	-32.8	-16.2	16.6	49.4
	I^-	-31.4	-16.8	14.6	53.5
2.Br	Cl^-	-18.0	-10.2	7.8	56.7
	Br^-	-17.5	-14.5	3.0	82.9
	I^-	-15.6	-12.4	3.2	79.5

[a] Values obtained from ITC measurements in CH_3CN (T = 303 K). Adapted with permission from reference 49. Copyright (2012) American Chemical Society.

2.3 Chalcogen Bonding Anion Recognition

Like XB, the heavier and more polarisable chalcogen atoms (Se, Te) are stronger ChB donors than their lighter counterparts, giving interactions with Lewis bases of comparable strength to HB.[6] However, the study and applications of Te-containing ChB donor molecules are often hampered by their proclivity towards hypervalency, and the inherent weakness of the C-Te bond (bond strength c.a. 200 kJ mol^{-1})[54] which renders them sensitive to moisture, air and susceptible to metal insertion reactions. As a result, the vast majority of ChB donor molecules employed for applications such as chemical synthesis, catalysis and materials design are limited to acyclic structures incorporating the lighter chalcogens (e.g. S, Se).[11] Regarding anion binding, the inherent nucleophilicity and basicity of many anions require that feasible ChB motifs are stable to their presence without undergoing decomposition or further reactions. Thus, the search for ChB motifs striking a balance between these contrasting criteria of stability and σ-hole Lewis acidity are critical for the full potential of ChB-mediated anion binding and sensing to be realised.

In contrast to XB, the number of σ-holes available for anion binding on the donor chalcogen atom depends on its bonding character. Three main scenarios are known amongst the range of ChB-donor molecules studied (Figure 13): doubly-coordinated chalcogen atoms as (i) part of an electron-deficient aromatic ring or (ii) divalent exocyclic substituent on (usually aromatic) electron-withdrawing groups, as well as (iii) singly-coordinated chalcogen atoms in chalcogeno-carbonyls (e.g. F_2C=Se). In scenarios (i) and (ii), up to two distinct σ-holes can be present on the chalcogen atoms, while only one is present for (iii) on the terminus of the chalcogen atom along the extension of the C=Ch bond akin to XB. Accordingly, the geometries of anion binding differ considerably, and hence ChB anion receptors have to be designed to take these contrasting directionalities into account. Presently, (i) accounts for a large fraction of all doubly-coordinated ChB-donor systems known to interact with anions in solution and in the solid-state, while (iii) has only been studied *in silico* with neutral Lewis bases.[19] Divalent exocyclic ChB donor molecules (ii), while once scarce due to their synthetic inaccessibility and inherently greater instability compared to their aromatic endocyclic counterparts (i), are beginning to gain popularity. It should be noted that these contrasting anion coordination scenarios provide a much wider repertoire of geometric possibilities for anion binding compared to XB, offering potentially interesting variants in selectivity when exploited in receptor design.

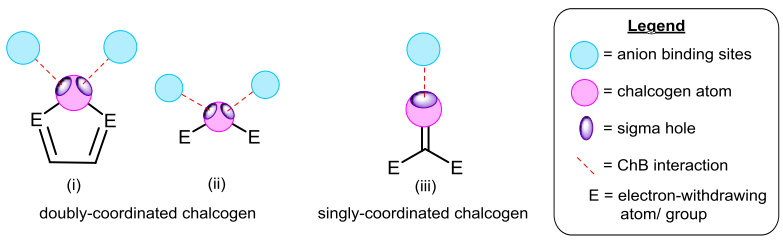

Figure 13. Distribution of σ-holes on ChB donor atoms of different coordination character with the resulting geometries of ChB-anion interactions.

Representative of (i), chalcogeno-diazoles are five-membered aromatic heterocycles comprising of a central chalcogen atom symmetrically bonded directly to two nitrogen atoms (Figure 14). Other than possessing highly electron-deficient chalcogen atoms, the narrow N-Ch-N bond angles (c.a. 90° for Ch = Se;[55] c.a. 84 ° for Ch = Te[56]) also allow the resulting σ-holes to be highly exposed for anion interactions. Capitalising on this, Taylor and co-workers studied the solution-phase ChB anion binding properties of a series of benzo-fused chalcogenodiazoles (**28a-e**) (Figure 14A),[57] bearing different substituents on the benzene ring, via UV-Vis spectroscopy in THF. By changing the number and electron-withdrawing nature of the substituents attached to the fused benzene ring, dramatic modulation of anion binding affinities could be achieved (association constant values for Cl^- shown in Figure 18A below the structures), highlighting the tunability of ChB-anion interaction strength with more electron-deficient substituents. In dry THF, preferential binding for more charge dense halides ($Cl^- > Br^- > I^-$) was observed for all Te-containing receptors (**28a-d**), whilst no appreciable binding for Cl^- could be discerned for the benzo-selenodiazole analogue **28e**. More competitive solvents elicited dramatic weakening of ChB-anion binding, with the K_a for receptor **28a** with Cl^- decreasing from 970 M^{-1} in THF to 74 M^{-1} in CH_3CN. Unfortunately, the benzo-tellurodiazoles were unstable to moisture under ambient conditions, which hampered their study in more competitive aqueous solvent media. Decomposition of the hosts were also observed in the presence of F^-, $CF_3SO_3^-$, $CH_3CO_2^-$, $H_2PO_4^-$ and HSO_4^-. Contrastingly, the structurally-related 3,4-dicyano-tellurodiazoles **29** (Figure 14B) were found to be sufficiently stable for crystal structure determination of their adducts with Cl^- and Br^-.[56] Notably, the Te-A$^-$ (A = Cl/ Br) contacts were up to 1 Å shorter than the sum of their respective VdW radii (c.a. 75 % of $\Sigma VdW_{Te\text{-}Cl/Br}$), which the authors proposed to be more appropriately described as hypercoordinate halide complexes on account of their strength.

The greater chemical stability of selenodiazoles compared to their tellurium analogues is compensated for by their reduced Lewis acidity and tendency to form ChB interactions with anions. To enhance the electron deficiency of the Se atoms, Vargas-Baca *et. al.* prepared cationic benzo-selenodiazolium compounds *N*-alkylated with substituents of varying steric bulk (**30a** = methyl, **30b** = isopropyl, **30c** = tert-butyl), which crystallised as either iodide or triiodide salts.[55] In all solid-state structures, short ChB contacts were observed between the Se atoms and iodide/ triiodide (Figure 14C) along the elongation of each selenodiazolium Se-N bond, clearly showing the influence of both Se σ-holes on the anion binding geometry. The size of the N-alkyl substituent was found to exert significant steric influence on the Se···I^- interactions, where **30a** forms dimers bridged by I^-, while **30c** forms infinite $[Se\ I]_\infty$ supramolecular chains (the longer out-of-plane Se···I^- contacts labelled (*) are likely electrostatically-driven). Interestingly, the crystal structure of the **30b**-I_3^- adduct shows a rare example of both σ-holes from the same donor atom interacting with the same anion: the shortest ChB contact occurs with the terminal iodine atom on I_3^- (Se···I(1) 84 % of ΣVdW radii), while the other is notably longer (Se···I(2) 93 % of ΣVdW radii). However, replacing one of the nitrogen atoms of the chalcogenodiazoles heterocycle with a carbon appears to somewhat restrict the geometry of anion interaction. In the crystal structures of compounds **31a/b** as a series of halide salts, interactions with halides occurred solely along the extension of the N-chalcogen bond of the heterocycle.[58] While the Cl^- interaction with Se in **31a** is more appropriately described as a single Se-Cl bond, a significant S···Cl^- short (S···Cl 80 % of ΣVdW radii) contact was seen for **31b** (Figure 14D).

Chalcogenophenes are fundamentally electron-rich aromatic heterocycles which are more stable than chalcogeno-diazoles. Nonetheless, the chalcogen atoms can be rendered sufficiently electrophilic for anion interaction by covalently attaching electron-withdrawing groups to the heterocycle. This was demonstrated by Taylor *et. al.* with ChB receptors **32a-c**, each bearing a tellurophene unit substituted symmetrically with electron-deficient arenes (Figure 15A).[59] UV-Vis spectroscopic anion binding studies in THF revealed that of the three receptors, only perfluoroarene-containing **32c** showed appreciable interaction with halides and oxoanions, with affinities decreasing in the order Cl^- (K_a = 310 M^{-1}) > Br^- > NO_3^- ≈ toluenesulfonate (TsO^-), and receptor decomposition occuring during I^- and benzoate titrations. Interestingly, MEP calculations showed that the σ-holes on **32a** and **32c**

were of similar magnitudes, suggesting that anion binding was aided by anion-π interactions with the more π-acidic perfluoroarene substituents of **32c**. Nonetheless, replacing the Te atom on **32c** with S resulted in no detectable Cl^- binding, which suggested that ChB interactions were important contributors to the overall anion association. To further enhance the anion affinities, another ChB receptor **33** (Figure 15B) was designed such that the ethynylene spacer between both perfluoroarene-substituted tellurophenes allowed sufficient space for ditopic ChB-anion binding. While receptors **33** and **32c** displayed the same anion binding trend under the same conditions, dramatic enhancements in anion affinities (K_a for Cl^- = 2290 M^{-1}) resulted for **33** accompanied by large optical changes. DFT calculations revealed that Cl^- is bound by two highly-linear $Cl^-\cdots$Te-C ChB interactions (bond angle = 170 °) without anion-π contributions from the distant perfluoroarenes, resulting in close to an order-of-magnitude increase in the K_a value for Cl^- binding compared with **32c**. Other chalcogenophenes such as thiophenes have also found applications in anion transport (see Section 3.3)[60] and their ChB-anion interactions have also been studied computationally (Figure 3A).[27]

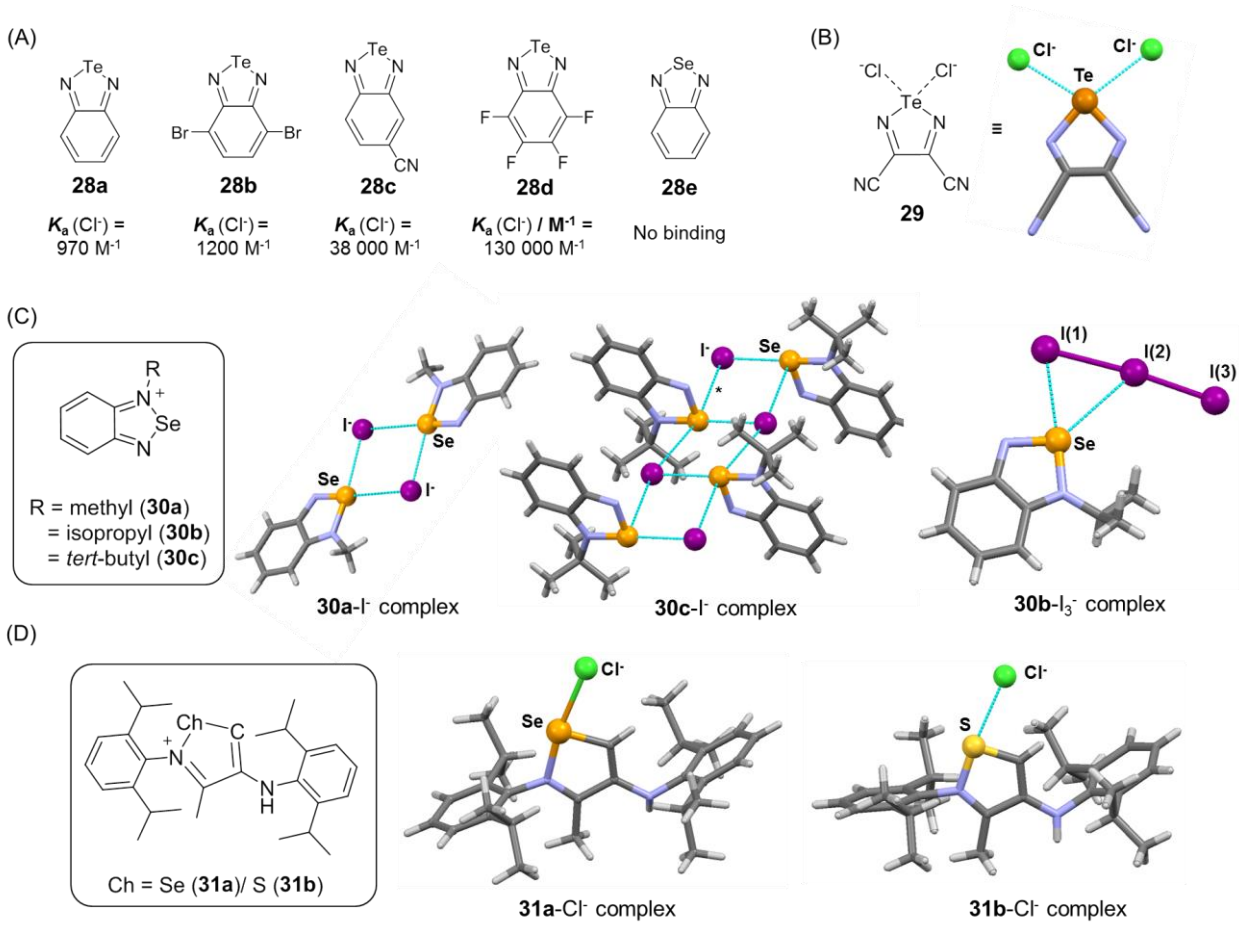

Figure 14. Chalcogeno-diazole-based ChB donor molecules: (A) Taylor's substituted benzo-chalcogenodiazoles **28a-e**;[57] (B) 3,4-dicyano-tellurodiazole **29** and the crystal structure of its Cl^- adduct;[56] (C) N-alkyl-substituted cationic benzo-selenodiazolium **30a-c** and their solid state structures with either I^- or I_3^-;[55] (D) Crystal structures of Cl^- complexes between asymmetric chalcogen-containing heterocycle **31a/b**.[58]

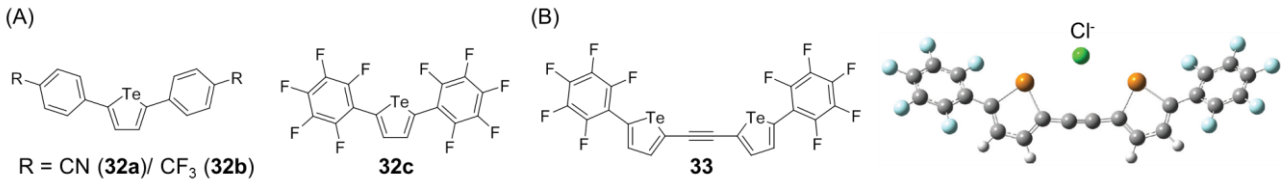

Figure 15. Tellurophene-based ChB receptors by Taylor: (A) monotopic ChB receptors **32a-c** and (B) ditopic ChB host **33** with its DFT-optimised Cl^--binding geometry obtained with permission from reference 59 - published by The Royal Society of Chemistry.

Non-aromatic ChB donor groups are invariably more sterically bulky and hindered than the aforementioned examples due to the presence of additional substituents on the chalcogen atoms to satisfy their valency. Even so, their anion-binding properties have been observed in a variety of host molecules. In an intruiging example, Chandrasekhar *et. al.* prepared a dicationic organotelluroxane macrocycle (**34**) containing four tetra-substituted Te(IV) chalcogen centres, with either chloride or iodide counteranions.[61] Despite the steric bulk around each Te centre, the solid-state halide adducts adopt an interesting inverse sandwich binding geometry, where two halide counteranions reside on the top and bottom face of the almost-planar 12-membered macrocycle ring (Figure 16A). Each halide anion is held convergently by four short ChB interactions (84 % to 94 % of ΣVdW radii for the Cl^- salt and 90 % to 95 % for the I^- salt), which are approximately linear with the C-Te bond (average bond angle c.a. 170 °) of each aryl ligand. Bromide coordination could also occur using a $Te_{12}O_{16}$ telluroxane ring (**35**) which was able to spherically encapsulate the halide via eight convergent ChB interactions (Figure 16B).[62] While these studies demonstrate the potential of electron-deficient non-aromatic tellurium atoms for anion coordination, usage of the first and so-far-only formally-cationic telluronium motif for anion recognition was demonstrated by Gabbai in 2010 using a borane-based anion sensor (**36**) (Figure 16C).[63] In methanol, F^- was the only anion (amongst Cl^-, Br^-, I^-, $CH_3CO_2^-$, NO_3^-, $H_2PO_4^-$ and HSO_4^-) able to coordinate to the Lewis acidic boron centre and interact strongly with the adjacent telluronium moiety via $n^2(F) \rightarrow \sigma^*(Te\text{-}C)$ interactions to give marked changes in the UV-Vis spectrum of **37**. The resulting $F^-\cdots Te\text{-}C$ interaction is highly linear (174 °), with a F-Te bond distance just slightly longer than the sum of the individual elements' covalent radii. The resulting association constant of 750 M^{-1} for fluoride is especially impressive, considering the strong HB solvation of fluoride in protic solvents. Notably, replacement of the telluronium motif with sulfonium analogue completely attenuated the receptor's fluoride affinity under identical conditions, underscoring the importance of the greater polarizability and electropositivity of the Te centre in governing anion binding.

Given the effectiveness of XB motifs such as haloimidazoliums and halotriazole/halotriazoliums for anion binding, analogous ChB motifs have very recently been studied where the halogen donor atoms of the former are replaced with divalent chalcogen atoms. Methylseleno-imidazoliums were incorporated into a family of bidentate receptors **37** very recently by Huber (Figure 17A),[64] which like their XB receptor analogue **15** (Figure 5), exist as both *syn*- and *anti*-conformers. A crystal structure of receptor **37a•*anti*** with triflate counteranions showed unequivocal evidence of ChB interactions to the oxygen atoms of triflate, occurring along the extension of the $C_{benzimidazolium}$-Se bonds (Figure 17B). Unfortunately, the receptors bearing Se-CH_3 (**37b**) and Se-octyl (**37c**) were found to be susceptible to S_N2 dealkylation reactions with Br^- to liberate methyl- and octyl bromide respectively. However, replacing the alkyl substituent on Se with an isopropyl group reduced the propensity of S_N2 substitution, rendering receptor **37d** stable enough to be studied as a Br^- anion abstraction catalyst (see Section 3.2).

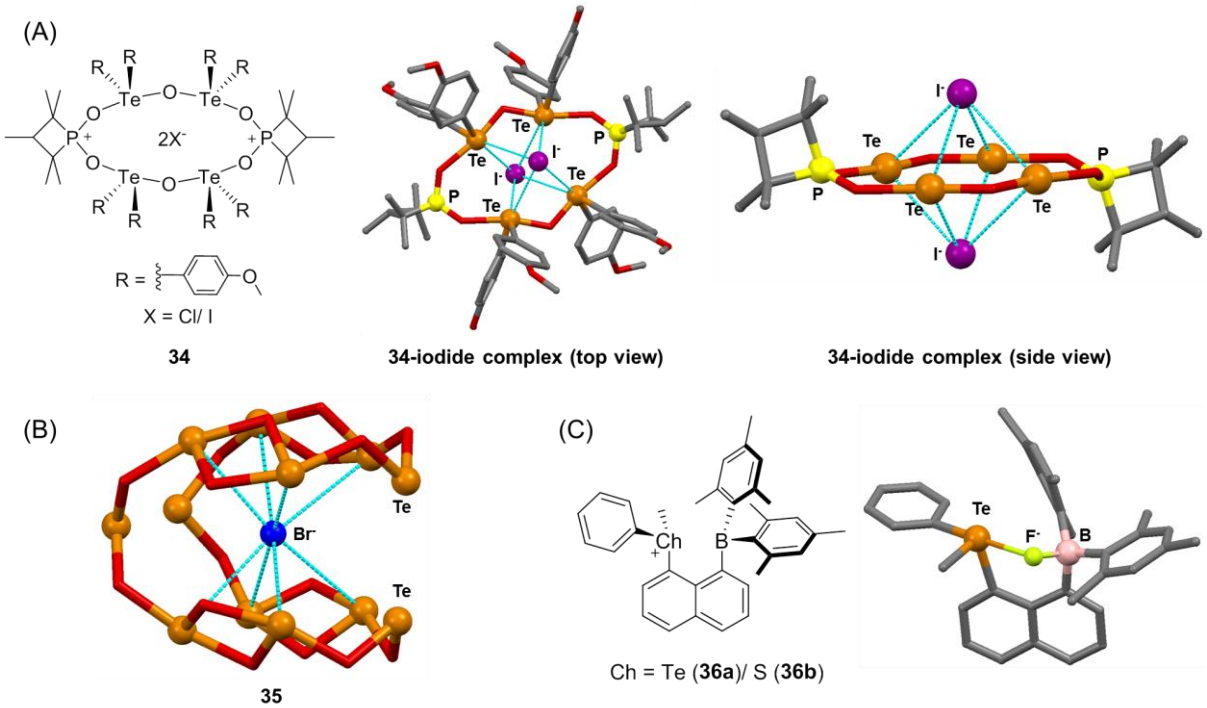

Figure 16. (A) A dicationic organotelluroxane macrocycle (**34**) and crystal structures of its adduct with I^-, showing the formation of an inverse sandwich complex (aryl ligands of Te removed from the side view for greater clarity);[61] (B) Crystal structure of a $Te_{12}O_{16}$ telluroxane ring **35** with the encapsulated Br^- (Li^+, propyl groups and THF solvent removed for clarity);[62] (C) Gabbaï's telluronium-borane ditopic receptor **36** and solid state structure of its F^- adduct. Hydrogen atoms are not shown in the crystal structures.[63]

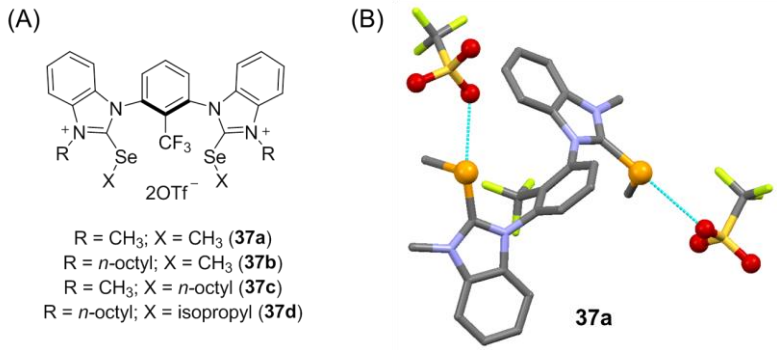

Figure 17. (A) Huber's benzimidazolium-based ChB host molecules **37a-d**; (B) Crystal structure of **37a** with its triflate counteranion, with ChB interactions shown as blue dashed lines.[64] Hydrogen atoms removed for clarity.

The appendage of $SeCH_3$/ $TeCH_3$ groups onto the 5-position of a 1,2,3-triazole unit afforded surprisingly robust ChB-donor motifs for anion binding. Using the potent 1,3-bis(iodotriazole) benzene motif which was capable of strong bidentate anion coordination, Beer et. al. incorporated these methylchalcogeno-triazoles into macrocycles to enhance the host structural preorganisation.[65] Interestingly, despite being attached to electron-withdrawing triazole units, the chalcogen atoms were found to be Lewis basic enough to also coordinate to cationic Cu(I), which enabled the first and only examples of CuAAC-AMT rotaxane synthesis to be performed by Cu(I) ligated by atoms other than nitrogen in a macrocycle (Figure 18A). Notably, the HB rotaxane analogue could also be synthesised by the

same strategy, albeit with a different Cu(I) coordination mode involving (proto)triazole *N*-ligation. In dry d_6-acetone, the first and only example of a neutral Te-containing ChB-donor [2]rotaxane **38a** was found to bind a range of oxoanions and halides in roughly decreasing order of anion charge density (SO_4^{2-} > F^- > Cl^- > Br^- > $CH_3CO_2^-$ > I^-). Notable affinity enhancements were seen for Cl^- and Br^- compared to the HB rotaxane analogue **38b**, which decomposed in the presence of F^- and SO_4^{2-} (Table 4). The Se-containing rotaxane analogue (**38c**), on the other hand, did not bind to any anions in the same solvent, showing that the anion binding by **38a** mainly resulted from Te-mediated ChB interactions. Compared to the neutral XB rotaxane analogue **20a** (Table 2) however, **38a** displayed weaker anion binding under identical conditions.

The ChB macrocycles and [2]rotaxanes were methylated to enhance the strength of anion binding via charge-assistance. Although the Te analogues could not be isolated due to instability of the resulting methyltelluro-triazolium motifs, a crystal structure of the dicationic Se-containing macrocycle (**39a**) was obtained as its iodide adduct (Figure 18B). Interestingly, Se···I^- short contacts were the predominant interaction in the crystal structure despite the potential of HB with Lewis acidic sites, and the influence of both σ-holes were evident from the highly linear chalcogen bonds formed along the extensions of the both C-Se bonds. However, compared to structurally-similar XB motifs (compounds **5** and **9** in Table 1), the methylseleno-triazoliums of **39a** were binding I^- in an *anti*-conformation in the solid state, possibly to minimise steric clash between the bulky ChB-donor groups.

Using cationic macrocycle **39a** and rotaxane **40a**, the unprecedented behaviour of charge-assisted ChB interactions for anion binding in the presence of water could be elucidated. Both ChB hosts showed distinct Hofmeister halide binding bias (K_a of I^- > Br^- > Cl^-), which contrasted with the HB host analogues **39b** (K_a of Br^- > I^-) and **40b** (K_a of Br^- > I^- > Cl^-). Interestingly, DFT studies of the charge-assisted ChB-anion binding revealed that the presence of anions induced additional polarisation of the ChB-donor Se atoms to further enhance their electron deficiency. MD simulations (Figure 18C) also revealed the origin of the iodide-selectivity: binding of the smaller and more hydrated halides brought about greater competition between the halide and water molecules in the anion's hydration shell for ChB interaction with Se, reducing the anion affinities. Furthermore, owing to the steric bulk of the $SeCH_3$ groups, halide binding occurred not within the interlocked rotaxane cavity of **40a**, but above the plane of the macrocycle component by two convergent ChB interactions and a single hydrogen bond from the axle prototriazolium unit.

Table 4. Host-guest 1:1 stoichiometric association constants of rotaxanes **38a and 38b** in d_6-acetone. [a]

	Rotaxane 38a	Rotaxane 38b
F^-	360 (35)	-[b]
Cl^-	127 (2)	81 (3)
Br^-	110 (2)	65 (5)
I^-	34 (3)	43 (1)
$CH_3CO_2^-$	98 (2)	-[c]
SO_4^{2-}	1130 (63)	-[b]

[a] Data reprinted with permission from reference 65; Copyright (2017) American Chemical Society; [b] decomposition of rotaxane; [c] not performed.

The examples discussed above showcase numerous similarities between XB and ChB interactions, namely their linearity, preference for more charge dense anions in dry solvents and Hofmeister binding bias for less solvated anions in protic media (e.g. presence of water). However, the contrasting directionalities of ChB interactions from divalent donor atoms compared to XB necessitates different receptor design considerations to maximise the strength of anion binding. Although recent efforts have considerably expanded the repertoire of ChB motifs for anion recognition, stable cationic Te-based motifs which are capable of the strongest ChB-anion interactions, are thus far very rare (Gabbaï's receptor **36a** being the only example). The search for such Te-bearing motifs is likely to feature prominently in ChB research in the coming years.

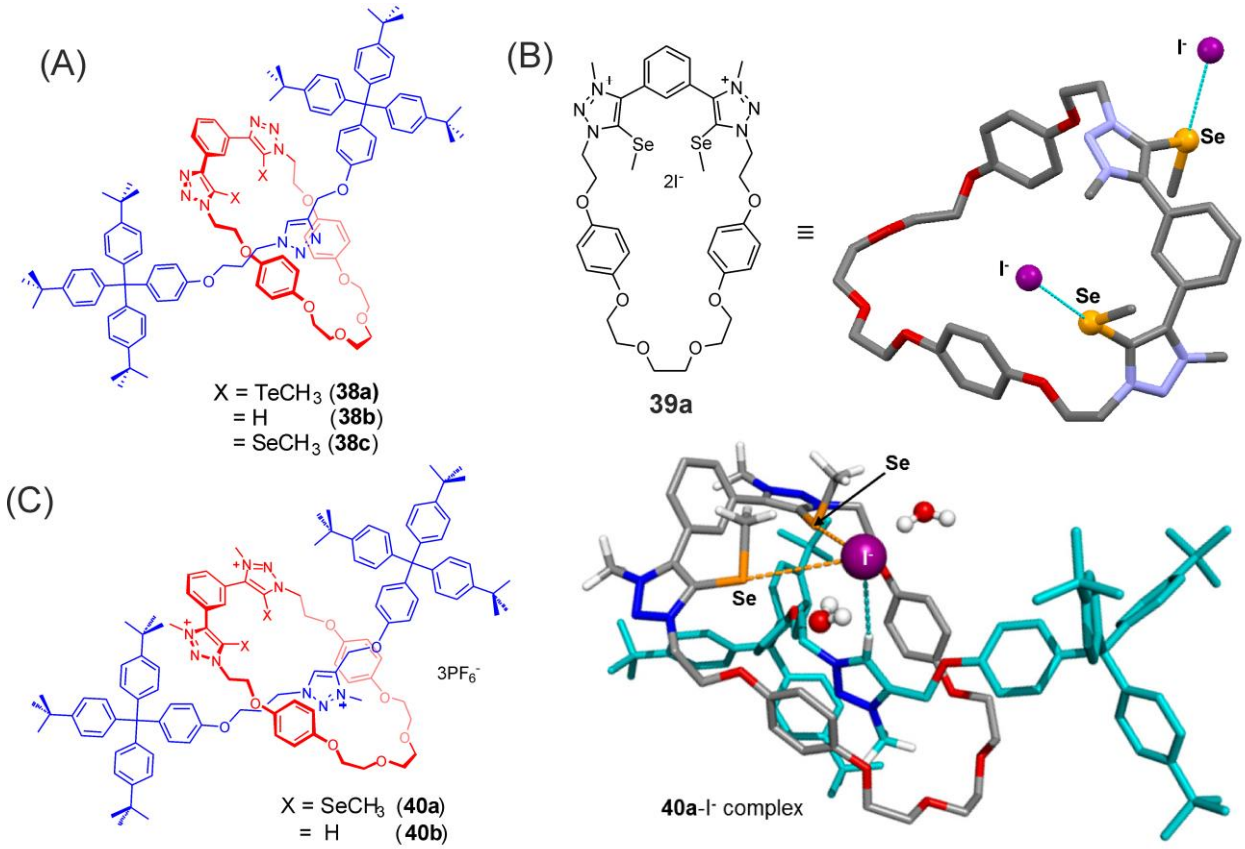

Figure 18. (A) Structures of neutral ChB [2]rotaxanes (**38a** and **38c**) and their HB analogue (**38b**) prepared by CuAAC-AMT; (B) Crystal structure of the iodide adduct of dicationic ChB macrocycle **39a**; (C) Structures of tricationic ChB [2]rotaxane **40a**, its HB analogue **40b**, and the MD simulation of iodide binding by **40a** by a combination of ChB (orange dashed lines) and HB (blue dashed lines) interactions. Hydrogen atoms omitted for clarity. Adapted with permission from reference 65. Copyright (2017) American Chemical Society.

2.4 The Potential of Pnictogen and Tetrel Bonding for Anion Recognition

Compared with XB and ChB anion hosts, receptors containing PnB and TrB-donor motifs are very rare. Other than the very recent realisation that Group 14 and 15 elements can participate in analogous σ-hole interactions, this dearth also partly arises from a number of additional factors that need to be considered in PnB and TrB host design:

(1) Lighter elements (e.g. Si, P), while non-metallic and less likely to participate in hypervalent bonding, have σ-holes sterically crowded by substituents necessary to satisfy the valency of the donor atoms (e.g. SiR_4 and PR_3, where R = EWG). This hinders access to anions, which are more likely to participate in other non-covalent interactions (e.g. HB, anion-π interactions) with functionalities on the electron-deficient substituents themselves.

(2) Although heavier elements are more electropositive and are often strong Lewis acids in high oxidation states, they can expand their valencies and tend to participate in metal coordination chemistry with anions. While Gabbaï and coworkers have exploited the Lewis acidity of some of these elements, most notably Sb(V) atoms for anion sensing,[66] the resulting Sb--X^- contacts are often of comparable dimensions or indistinguishable from Sb-X covalent bonds, and hence are generally considered more as covalent (dative) bonds than actual supramolecular/ secondary bonding interactions.

(3) The generally larger numbers of σ-holes on Group 14 and 15 elements, if sterically accessible, can allow multiple sites of anion interactions. It is thus more difficult to control the geometry of anion binding necessary to achieve shape/size complementarity for selective anion recognition.

Nonetheless, the strength of TrB and PnB interactions can be comparable to those of other σ-hole interactions, or even exceed those of XB/ ChB, as shown earlier by Scheiner's computational studies.[6] While the vast majority of these TrB[13] and PnB[12] interactions have been studied computationally with neutral Lewis bases (e.g. NH_3) in the gas phase, more recent work has extended them towards the recognition of anions. We highlight several notable studies and solid-state examples showing (sometimes unexpected) TrB or PnB interactions with anions, which serve as a guide for further exploration.

2.4.1 Pnictogen Bonding with Anions

As early as 2001, Müller and co-workers isolated a crystal structure showing intriguing PnB-anion short contacts when investigating the donor-acceptor complexation reactions between *N,N,N′,N′*-tetramethylethylenediamine (TMEDA) and phosphorus tribromide.[67] As shown in Figure 19A, two P···Br^- short contacts (77 % and 84 % of $\Sigma VdW_{P\text{-}Br}$ radii) roughly collinear with each P-N covalent bond constituting the heterocycle **41** were evident. However, it was not till 2014 when Lin and co-workers performed the first computational study to assess the possibility of PnB with a variety of anions (F^-, Cl^-, Br^-, I^-, NO_3^-, SO_4^{2-}) using the model compounds FH_2X (X = P/ As) in the gas phase.[68] In these simple host molecules containing only one strongly electron-withdrawing fluorine atom, ESP calculations revealed the presence of only one dominant σ-hole on the pnictogen atom, and thus each non-covalent P/As···anion interaction could occur almost collinear with the P/As-F covalent bond (angles ranging from 162 ° to 172 °). Each PnB···anion interaction comprises significant charge-transfer character from the anions' lone pair into the energetically-accessible σ*(P/As-F) orbital, resulting in lengthening of the pertinent covalent bond. In addition, the anions were able to bind to the PnB-donor molecules with different stoichiometries (host-guest 1:1, 2:1, 3:1 and 4:1 complexes with Cl^-, Figure 19B). Unsurprisingly, FH_2As was a stronger PnB-donor than FH_2P, with the interaction energies with anions decreasing in the approximate order of their charge densities: SO_4^{2-} > F^- > Cl^- > NO_3^- > Br^- > I^-.

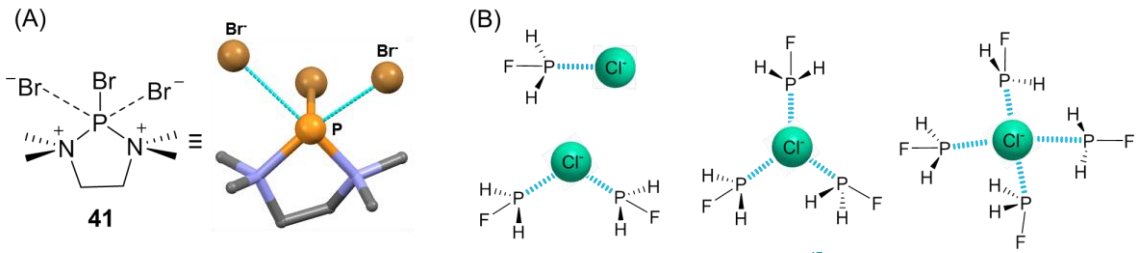

Figure 19. (A) Solid state structure showing P···Br^- short contacts in a TMEDA-PBr_3 complex **41**;[67] (B) Schematic representation of the different binding stoichiometries of FH_2P with Cl^-.[68] In all cases, Pn···X^- interactions are shown in light blue.

Amongst the heavier pnictogens, Sb(III) centres appear to be more susceptible to supramolecular interactions with anions than forming full (dative) covalent bonds. For instance, the crystal structure of Gabbaï's bis-stilbonium host **42** bearing formally cationic Sb(III) centres shows distinct short contacts with the oxygen atoms of one of its triflate counteranions (81 % and 85 % of the $\Sigma VdW_{Sb\text{-}O}$ radii) (Figure 20A).[69] In a recent (2016) survey of the Cambridge Structural Database (CSD), Cozzolino *et. al.* identified a bidentate PnB anion binding motif containing two Sb(III) centres bridged by either an oxygen or sulfur atom with the general formula $X_2Sb\text{-}E\text{-}SbX_2$ (E = O/S, X = F/ Cl/ Br).[70] Computational simulations reveal the presence of σ-holes and low-lying σ*(Sb-X) orbitals in the space flanked by both Sb(III) centres, allowing halide binding to occur within that space in the solid state. Interestingly, host-guest 1:2 halide complexes are much more prevalent than the

1:1 stoichiometric complexes (Figure 20B). In all cases, the bridging Sb-X^- (X = Cl/ Br) bonds are considerably longer than their terminal counterparts, and occur approximately collinear with a Sb-$X_{terminal}$ covalent bond (c.a. 170°), which was interpreted as supramolecular PnB···halide interactions rather than true dative bond formation. On account of the short Sb···halide contact lengths, which are typically around 75 % of the sum of $\Sigma VdW_{Sb\text{-}X}$ radii, the PnB interactions are very strong and contain a significant degree of covalency.

Building on these findings, a PnB host molecule (**43**) was then computationally designed with the same $X_2Sb\text{-}E\text{-}SbX_2$ structure but having the terminal halides replaced by catecholates, and their halide (F^-, Cl^-, Br^-, I^-) binding behaviour modelled by DFT calculations.[70] The presence of carbon-based peripheral groups allow the possibility of tuning the electronics of the Sb(III) centres by functionalisation of the catechol aromatic rings, while the restricted 5-membered catecholate complex provides a more exposed area on the Sb atom for anion access. In the gas phase, energy-minimised halide complexes with host-guest binding stoichiometries of 1:1, 2:1 and 1:2 were observed (Figure 20C), with terminal halide coordination appearing to be energetically more favoured than the bridging mode for the 1:1 and 1:2 complexes. This was attributed to the energetic cost of host structural reorganisation which disrupts favourable intramolecular Sb···O interactions for the bridging halide complexes to be achieved. Generally, the Sb···halide contacts were of similar length as those in the $X_2Sb\text{-}E\text{-}SbX_2$ crystal structures, suggesting strong interactions. Binding energies were found to decrease with larger halides (F^- > Cl^- > Br^- > I^-), and also generally with decreasing halide coordination number (host-guest complex stability: 2:1 > 1:1 > 1:2). Notably, the target Sb(III) host molecules could be successfully synthesised experimentally and while solid-state structures of halide complexes were not obtained, crystal structures of 1:2 stoichiometric host-pyridine adducts show clear evidence of Sb···$N_{pyridine}$ PnB interactions with terminally-bound pyridine guests.

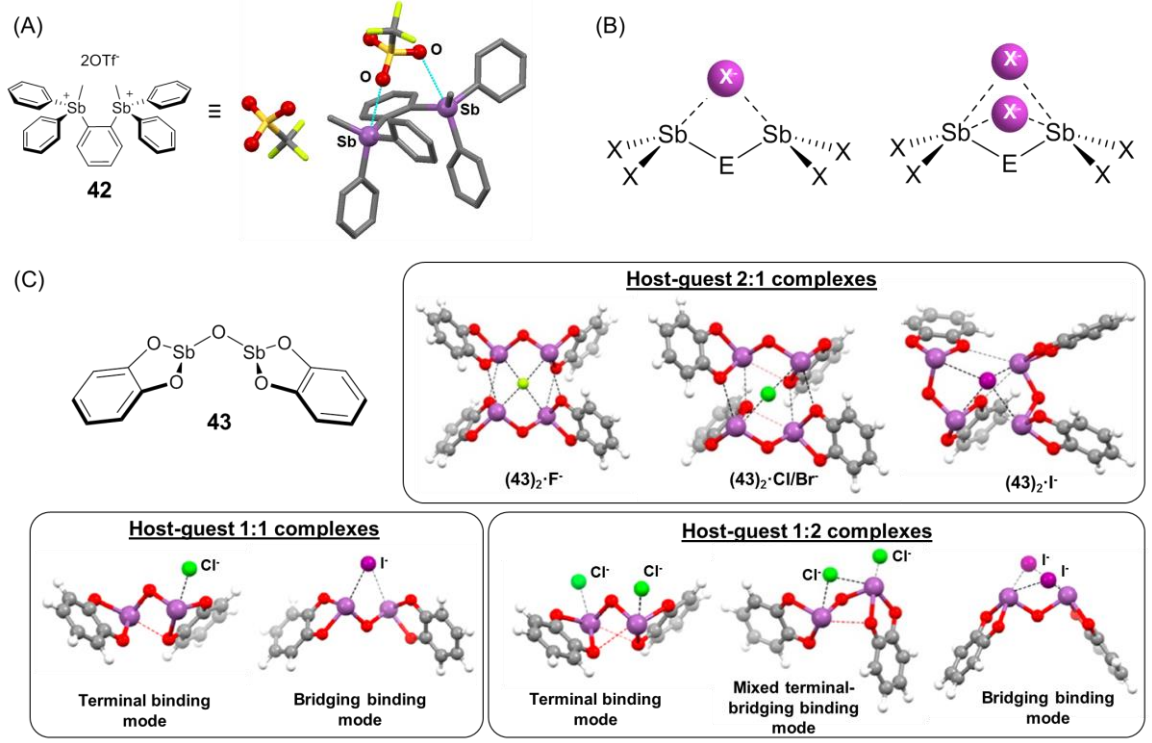

Figure 20. (A) Gabbaï's dicationic Sb(III) compound 42 and crystal structure which shows PnB interactions with a triflate counteranion;[69] (B) $X_2Sb\text{-}E\text{-}SbX_2$ (X = F/ Cl/ Br; E = O/ S) anion binding motif and their host-guest stoichiometric 1:1 and 1:2 anion coordination modes; (C) Cozzolino's bis-Sb(III)-catecholate complex 43 and its DFT energy minimised structures with halide anions, with PnB interactions shown as dashed lines. DFT structures reproduced with permission from reference 70. Copyright (2016) American Chemical Society.

2.4.2 Tetrel Bonding with Anions

The experimental possibility of designing TrB host molecules for anion binding is supported by several intriguing experimental studies, with all solid state structures showing contacts between electron-deficient Group 14 atoms and anions which are shorter than the sum of their respective vdW radii. For instance in 2002, Lightfoot and Morris reported a germanium-based cuboidal double four ring (D4R) structure (**44**) which was found to encapsulate a F^- anion within its cavity by powder X-ray diffraction and ^{19}F NMR experiments (Figure 21A).[71] In the averaged model of all possible F^- conformations within the cage, the anion is held concurrently by eight TrB interactions from the Ge atoms (c.a. 80 % $\Sigma VdW_{Ge\text{-}F}$ radii), each occurring approximately linearly along the extension of a Ge-$O_{external}$ bond. Structurally-analogous spherosilicate cages with either phenyl (**45a**) or vinyl (**45b**) peripheral substituents have also been prepared with the aid of F^--templation, with the resulting products isolated containing encapsulated 'naked' F^- anions held by eight symmetrical Si···F^- TrB interactions within the cage (Figure 21B).[72] Interestingly, the addition of one equivalent of triflic acid could remove the encapsulated F^- from within the cage in a CH_2Cl_2/ THF mixture while retaining its integrity, proposed to occur via proton complexation/ strong HB formation with the acid outside the cage structure. Notably, usage of Cl^-, Br^- and I^- as templates failed to form any halide-encapsulated spherosilicates, suggesting that the strong Si···F^- interactions were instrumental in their formation.

Another notable example of the structure-influencing ability of TrB···halide interactions was seen when the presence of halides (Cl^-, Br^-, I^-) cause six-membered perhalocyclohexasilanes Si_6X_{12} (X = Cl/ Br) rings (**46**), which originally adopt chair-conformations, to planarise (Figure 21C).[73] Most interestingly, the driving force for this structural rearrangement appears to be the formation of 'inverse sandwich' complexes, comprising of one halide anion coordinated above and below the resulting hexagonal ring structure by six symmetrical TrB interactions, each occurring on the extension of a Si-X covalent bond. Computation of the MEP surfaces of the Si_6X_{12} hosts in both chair and planar conformations revealed that the latter allowed a highly electron-deficient region to form in the middle of the D_{6h} hexagon on both top and bottom faces due to superposition of six Si-based σ-holes, thus dictating the loci of halide coordination.[13] Contrastingly, the σ-holes are sterically inaccessible in the chair-conformation for halide interaction.

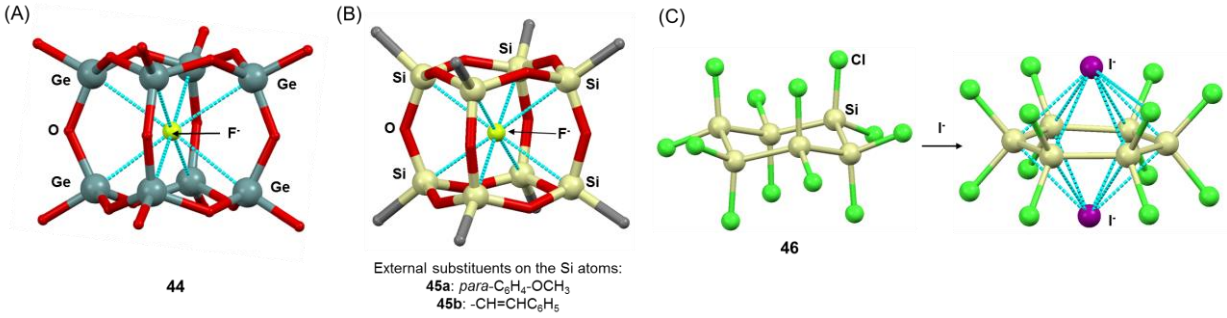

Figure 21. Solid-state structures showing F^- encapsulation within (A) Ge-based (44)[71] and (B) Si-based cages (45a, 45b)[72] by eight TrB interactions (external substituents on Si bonded to the carbon atoms are not shown for clarity); (C) Crystal structures showing induction of planarity on Si_6Cl_{12} perhalocyclohexasilane ring 46 by the coordination of iodide.[73] Red = O; grey = C; TrB interactions indicated by light blue dashes. Hydrogen atoms omitted from crystal structures for clarity.

Host molecules capable of TrB interactions with anions are not restricted to macrocyclic or caged structures. In a study of S_N2 reactions on silicon complexes of diketopiperazine substituted with different leaving groups (F, Cl, OTf, Br and I) on the Si centres, the presence of a good leaving group (e.g. iodine) was found to promote the formation of a Si-O covalent bond in compound **47** (Figure 22A).[74] The resulting electrophilic Si atom was found to engage in strong TrB interactions with

the displaced iodide anion (77 % $\Sigma VdW_{Si\text{-}I}$ radii) which is almost collinear with the Si-O bond. Separately, a disiloxane compound containing highly electron-deficient Si atoms covalently bonded to several electron-withdrawing groups (**48**) was found to bind a Cl^- bridged between both Si centres via two convergent TrB interactions in the solid state (Figure 22B).[75] Other than short Si···Cl^- contacts (71 % and 75 % of $\Sigma VdW_{Si\text{-}Cl}$ radii), two notable short contacts with carbon centres directly bonded to a formally cationic tetra-coordinated amine unit are seen (89 % and 91 % of $\Sigma VdW_{C\text{-}Cl}$ radii). Although the use of sp^3 carbon centres as TrB donors are encumbered by steric crowding and the atom's low polarisability, a survey of the CSD and computational studies by Frontera and co-workers have suggested the possibility of such interactions with anions and neutral Lewis bases.[13] In constrained ring structures such as cubanes, cyclobutanes and cyclopropanes substituted with electron-withdrawing groups (e.g. F, CN), the distorted tetrahedral arrangement around the carbon centres may allow σ-holes to be sufficiently exposed. While smaller rings allow greater σ-hole accessibility, they also enhance the magnitude of the electrostatic potentials on the σ-holes, with the consequence of facilitating stronger anion interactions in the gas phase with cyclopropanes than cyclobutanes bearing the $X_2C\text{-}CX_2$ (X = F/ CN) motif (Figure 22C). Notably, cyclopentanes and cyclohexanes containing the $F_2C\text{-}CF_2$ unit were found to be unsuitable for carbon-based TrB interactions due to σ-hole steric inaccessibility.

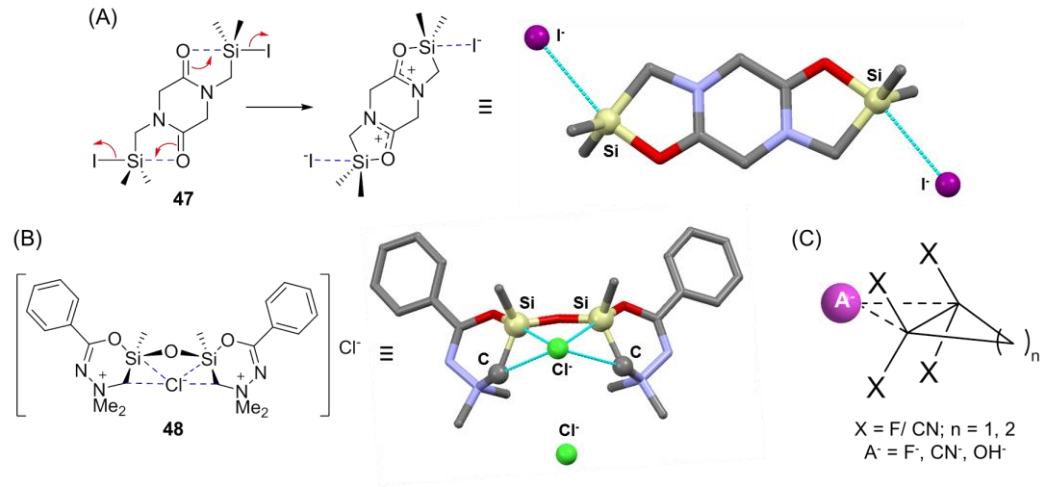

Figure 22. (A) Si···I^- TrB interactions in the solid-state structures of silicon-containing diketopiperazine 47;[74] (B) convergent TrB interactions with a bridging Cl^- anion between electron-deficient Si and C-based donor atoms in the crystal structure of disiloxane 48;[75] (C) Cyclic aliphatic structures possessing the $X_2C\text{-}CX_2$ (X = F/ CN) motif shown computationally to allow carbon-based TrB interactions.[13] Hydrogen atoms omitted from crystal structures for clarity.

The possibility of Si···halide TrB interactions demonstrated in the solid state prompted Frontera and co-workers to design a TrB anion receptor (**49a**) containing a calix[4]pyrrole core with four pendant SiF_3 arms and evaluate their anion binding properties *in silico* (Figure 23A).[76] The σ-holes on the electrophilic Si centres were designed to be orientated into the receptor cavity for anion interaction in conjunction with HB interactions from the calix[4]pyrrole unit (Figure 23B). Analyses using the non-covalent interaction (NCI) plot, which enables effective visualisation and identification of supramolecular interactions, demonstrated the contributions of TrB and HB towards the strong binding of Cl^- and N_3^- by **49a**. With Br^- and I^-, the larger N-H···halide distances which primarily governed the location of halide anion binding within the cavity resulted in unfavourable directionality with the σ-holes on Si, reducing the contribution of TrB for anion coordination. In comparison, receptor analogues bearing octamethyl (**49b**) and tetramethyl (**49c**) substituents were found to bind all anions, in particular Cl^- and N_3^-, significantly more weakly.

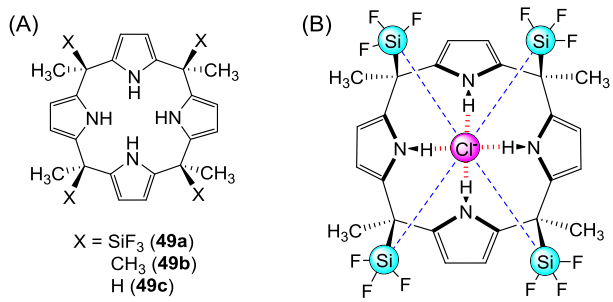

Figure 23. (A) Structure of Frontera's receptors 49a-c; Top view of the computed Cl^- binding mode of receptor 49a, showing the TrB (blue dashed lines) and HB (red dashed lines) interactions.[88]

The potential of lead as a TrB donor has been investigated in the solid state as it is the heaviest, most polarisable and electropositive member of the Group 14 elements. Although lead has a tendency towards hypervalency, it is known to adopt two distinct coordination environments. As shown in Figure 24A, a holodirected geometry allows coordination of ligands around the entire sphere of lead, while a hemidirected geometry shows only partial occupancy, rendering a distinct void on the atom which provides steric access to any σ-holes arising from electron-withdrawing ligands on the opposite face. All Pb(IV) compounds adopt holodirected coordination geometries, contrasting with Pb(II) which can adopt both.[77] Nonetheless, the usage of Pb(II)-based centres for TrB-mediated anion binding is complicated by the possibility of covalent anion coordination, and hence experimental methods of distinguishing between these and supramolecular TrB interactions need to be developed. Towards this end, Bryce and co-workers recently suggested the possibility of using solid-state ^{207}Pb NMR to study TrB interactions in a series of Pb(II)-complexes **50a-e** (Figure 24B).[78] ^{207}Pb (I = ½) has a natural abundance of 22 % and a chemical shift range of approximately 17 000 ppm, suggesting an exquisite chemical shift sensitivity to its local electronic environment such that even weak TrB interactions can be probed. Solid-state NMR also allows determination of the ^{207}Pb anisotropic chemical shift tensors which offer insights on the local Pb electronic and coordination environment. Notably although all complexes are expected to possess a hemidirected Pb(II) centre, this technique showed that complexes **50a** and **50b** adopt holodirected geometries, consistent with crystallographic data showing strong supramolecular interactions with pyridine N atoms opposite the ligand coordination sphere. On the other hand, solid-state ^{207}Pb NMR data suggested that **50c** and **50e** show predominantly hemidirected Pb(II) geometries, indicating weaker TrB interactions; while **50d** displayed intermediate spectroscopic properties between holo- and hemidirected Pb(II) centres possibly due to TrB interactions inducing partial holodirected character to the atom. In an analogous manner, solid-state ^{207}Pb NMR may provide a means to probe Pb-based TrB···anion interactions as well.

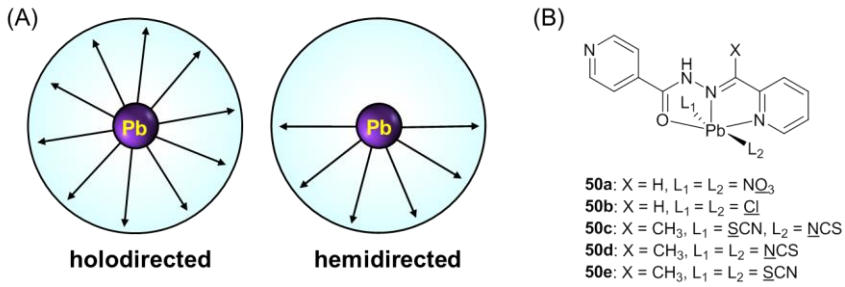

Figure 24. (A) Cartoon representation of holo- and hemidirected coordination geometries around Pb centres; (B) Bryce's Pb(II) complexes (50a-e) used to probe TrB interactions with solid-state ^{207}Pb NMR spectroscopy. Atoms underlined in (B) indicate the site of coordination to the Pb(II) centre in each complex.[78]

3. APPLICATIONS OF ANION BINDING WITH SIGMA-HOLE INTERACTIONS

3.1 Anion Sensing

Anion sensing occurs when the presence of an anion causes a detectable change in the macroscopic properties of a host molecule (optical, electrochemical, rheological) functionalised with suitable reporter groups. While considerable advances in this highly-active area of supramolecular research has been made using HB receptors in recent years,[2] σ-hole interactions, in particular XB, have shown tremendous promise in this regard, often providing augmented sensory responses compared to HB analogues owing to their enhanced anion binding affinities and covalent character of the anion interaction- the latter property providing a conduit to facilitate electronic communication with the reporter group. This has been demonstrated in a number of XB host molecules designed for fluorescence/ luminescence anion sensing. For instance, Ghosh's XB Ru(II)-containing anion sensor containing an iodotriazole *N*-coordinated to the metal centre **51** (Figure 25A) was found to exhibit significantly larger luminescence turn-on responses in the presence of $HP_2O_7^{3-}$ and $H_2PO_4^-$ in CH_3CN/ H_2O 4:1 *v/v* compared to its HB analogue.[79] Similarly, Beer's XB receptor **26** (Figure 12) showed significant fluorescence enhancement on ReO_4^- addition in HEPES buffered water (pH 7.4), while the HB receptor analogue exhibited no response under identical conditions.[52] Indeed in the majority of cases, XB receptors appear to favour turn-on responses, which may be due to a combination of factors including increased receptor structural rigidity upon anion binding and perhaps to some extent, attenuation of the 'intramolecular heavy atom effect' on anion binding arising from the presence of heavy XB-donor atoms on the receptor molecule itself. As an illustration of the latter effect, Molina and co-workers have found that the incorporation of increasing numbers of bromine and iodine atoms in a bis-pyrene-functionalised host **52** (Figure 25B) resulted in a progressive decrease of the receptors' quantum yields (Φ of **52a** > **52d** > **52b** > **52c**) in the absence of anion.[80] However, all XB receptors (**52b-d**) gave larger fluorescence enhancements than **52a**. A less common example of luminescence quenching on anion binding was demonstrated by Beer's [2]rotaxane host **18** containing an all-XB anion binding cavity (Figure 7B), which sensed iodide selectively in 1:1 CH_3CN/ H_2O *v/v*.[44] At the time of writing, ChB/ PnB/ TrB-mediated fluorescence/ luminescence anion sensing has yet to be demonstrated.

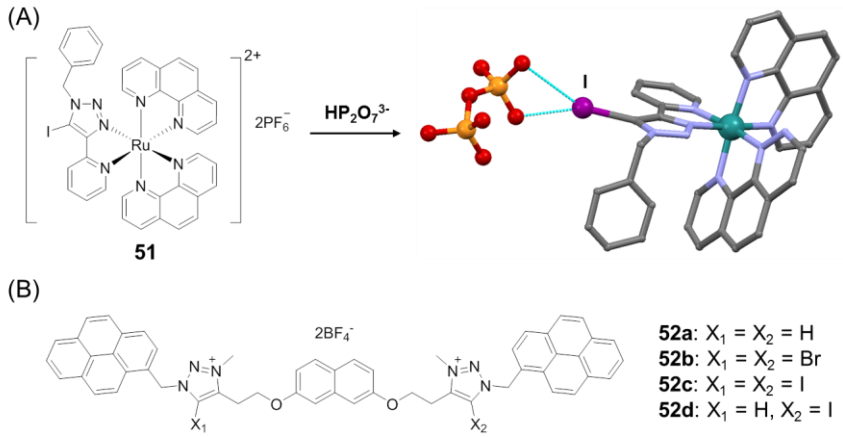

Figure 25. (A) Ghosh's heteroleptic Ru(II) XB anion receptor 51 for sensing of phosphates and the solid-state structure of its $HP_2O_7^{3-}$ adduct (H atoms and solvents omitted for clarity);[79] (B) Molina's ditopic pyrene-functionalised receptors XB receptors (52b-d) and their HB analogue (52a).[80]

Colorimetric anion sensing is highly desirable from an end-user's perspective due to the possibility of 'naked-eye' visible colour change in the presence of an anion, and can be achieved via two main approaches. Firstly, σ-

hole···anion interactions can directly perturb the frontier molecular orbital energy levels of a chromophore due to electronic conjugation or direct coordination to a metal centre. This has been achieved using Beer's Re(I) receptor **14** (Figure 5) where the addition of halides, $H_2PO_4^-$ and SO_4^{2-} resulted in enhancement of its MLCT emission intensity,[40] as well as with Taylor's ChB metal-free hosts **28** (Figure 14A)[57] and **33** (Figure 15B)[59] which showed notable changes in their absorption spectra in the presence of halides in dry THF. A second and much less common approach involves the exploitation of σ-hole···anion interactions to radically change the conformation of the host receptor which brings about a concomitant change in its bulk optical properties. To demonstrate this concept, Beer *et. al.* designed a four-station [3]rotaxane **53a** which binds NO_3^- selectively over Cl^- and oxoanions ($H_2PO_4^-$, HCO_3^-, $CH_3CO_2^-$). This was achieved by the formation of a 1:1 stoichiometric host-guest sandwich complex resulting from concerted shuttling of both macrocycle components from naphthalene diimide (NDI) stations located at the termini of the axle component to the centrally-located iodotriazolium anion binding sites (Figure 26).[81] This dynamic pincer movement is accompanied by a 'naked-eye' visible colour change, where the orange colour of the rotaxane solution (as its non-coordinating $2PF_6^-$ salt) arising from NDI-hydroquinone charge transfer interactions, turns colourless when the macrocycle units move away to occupy the iodotriazolium binding sites. Although the HB [3]rotaxane analogue **54b** also shows a similar colorimetric response, the XB host **54a** was found to bind all anions more strongly with augmented selectivity for NO_3^- in $CDCl_3$/ CD_3OD 1:1 *v/v*.

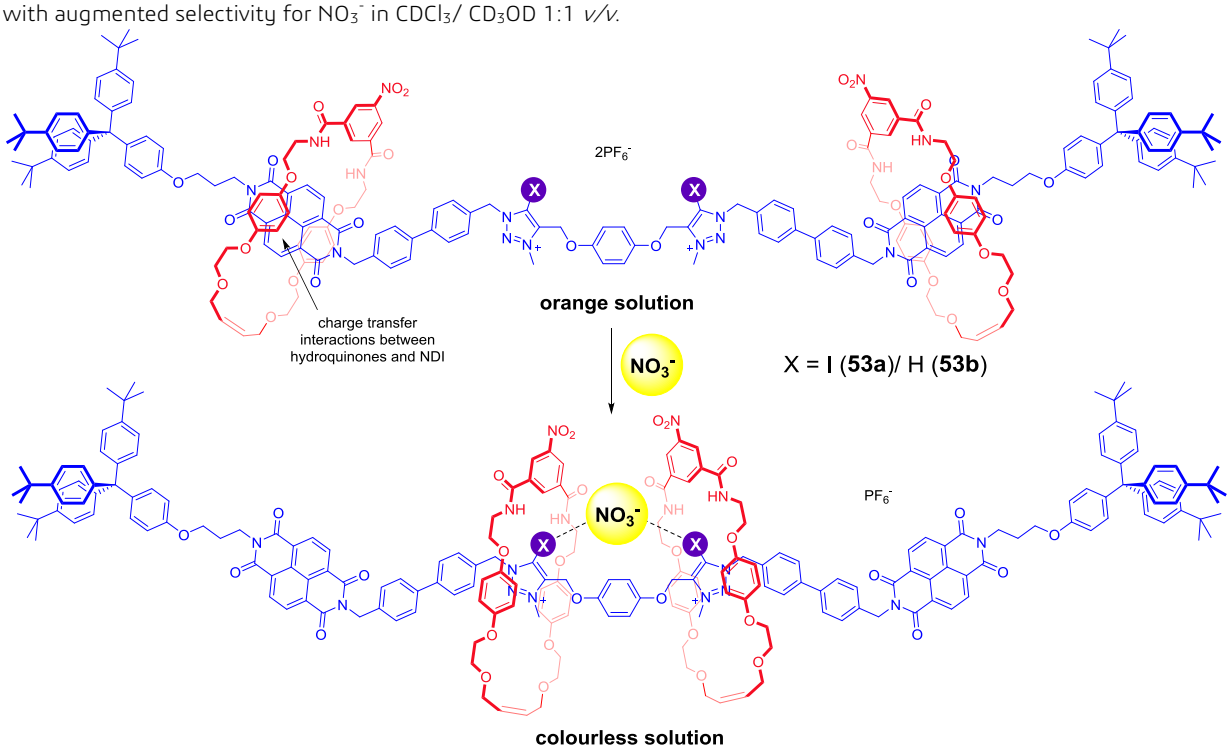

Figure 26. Beer's XB four-station [3]rotaxane 53a and its HB analogue 53b capable of 'naked eye' colorimetric NO_3^- sensing.[81]

Electrochemical anion sensors facilitate not only the highly-sensitive detection of anions, but also the possibility of integration into functional devices. Like optical anion sensors, their electrochemical counterparts often comprise of a redox-active moiety (e.g. ferrocene) covalently appended close to the anion binding site, which allows efficient communication of the anion binding event to bring about a redox response, which is typically a perturbation of the receptor's redox potential detectable via voltammetric techniques. The first application of XB in redox anion sensing was reported by Beer *et. al.* in 2016 using ferrocene (Fc)-containing

receptors functionalised with either iodotriazoles (**54a**) or iodotriazolium groups (**55a**) (Figure 27A).[82] In dry CH_3CN, both XB receptors (**54a** and **55a**), showed significantly larger magnitudes of cathodic pertubations of their respective Fc/Fc^+ redox potentials than their HB analogues towards Cl^- and Br^-, attributed to the enhanced covalent character of the XB-anion interactions which facilitated through-bond electronic communication with the ferrocene reporter groups. Interestingly, both XB receptors **54a** and **55a** gave comparable redox responses to the halides despite possessing different charges, with greater augmentation of redox response over the HB analogues seen for neutral sensor **54a** compared with dicationic **55a**. Subsequently, by appending iodotriazole units on the 1,3-positions of the same cyclopentadienyl ring of ferrocene (**56a**, Figure 27A), Beer demonstrated the unprecedented use of XB in the selective redox sensing of the highly-toxic and environmentally-hazardous azide (N_3^-) anion.[83] Possibly due to greater host-guest size complementarity of the resulting wide XB bite angle and the linear N_3^- anion, sensor **56a** bound N_3^- more strongly than any of the halides in d_6-acetone and d_6-acetone/ D_2O 99:1 *v/v*, with at least an order-of-magnitude enhancement in K_a values compared to its HB analogue **56b**. Impressively, **56a** displayed a larger redox potential cathodic shift of -40 mV with 10 equivalents of N_3^- in CH_3CN/ H_2O 99:1 *v/v*, compared to the -18 mV seen for HB host **56b**, clearly demonstrating the importance of XB interactions for enhancing the sensitivity of redox anion detection even in the presence of water. Nonetheless owing to the redox potential of the Fc/Fc^+ redox couple being more anodic than that of I^- oxidation, these ferrocene-based XB anion sensors were not amenable for I^- sensing, despite their known preference for the halide in protic solvent media.

Other than ferrocene, XB-donor motifs have been incorporated onto other redox-active frameworks. For instance, Schöllhorn and co-workers reported the use of iodo-tetrathiafulvene **57a** (I-TTF) (Figure 27B) as an electrochemical sensor for Cl^- and Br^-, which gave larger magnitudes of cathodic shifts than the halogen-free analogue **57b**.[84] Significantly, the cathodic shift observed for the second oxidation wave, corresponding to the redox couple $I\text{-}TTF^+/ I\text{-}TTF^{2+}$, was larger in magnitude than the first ($I\text{-}TTF^0/ I\text{-}TTF^+$) due to greater extent of charge-assisted Cl^- stabilisation of dicationic $I\text{-}TTF^{2+}$ than monocationic $I\text{-}TTF^+$. Recently, Beer *et. al.* have also studied the redox anion sensing properties of an iodotriazole-substituted diquat (DQ) derivative (**58a**) (Figure 27C) in CH_3CN.[85] Although diquat displays two one-electron reduction processes, corresponding to the $DQ^{2+}/ DQ^{+\bullet}$ and $DQ^{+\bullet}/ DQ$ redox couples, only $DQ^{2+}/ DQ^{+\bullet}$ showed quasi-reversibility for **58a** and thus could be monitored for anion sensing. Due to its redox potential value of $E_{1/2}$ = -0.305 V v.s. Ag/ AgCl reference, **58a** could be used to sense iodide. Interestingly, the HB sensor analogue **58b** showed larger cathodic shifts than XB **58a** in the presence Cl^- and Br^-, whilst I^- elicited an augmented response by the XB sensor analogue.

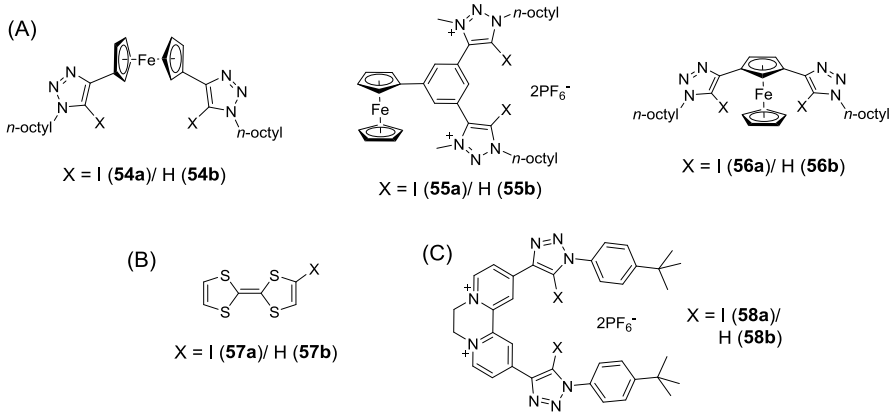

Figure 27. Examples of electrochemical anion sensors utilising XB interactions containing the redox-active groups (A) ferrocene; (B) TTF and (C) diquat, together with their HB sensor analogues.

Rheological sensors detect anions by a 'naked eye' change in the bulk viscosity properties of a sample, often due to breaking down of the cross-linked molecular networks constituting a highly-viscous gel phase by an anionic stimulus to form a free-flowing sol phase. The first XB-mediated rheological sensor selective for chloride was reported by Fan utilising iodoperfluoroaryl-functionalised dendritic organogelators (Figure 28).[86] In the absence of an anion, strong π-π stacking interactions between largely-planar XB monomers (**59**) formed extensive fibrillar networks in acetone-hexane mixtures. Chloride addition triggered gel collapse due to the formation of a non-planar XB-anion complex which disrupts the π-π stacking interactions. In near stoichiometric quantities (0.8 equivalents) of Cl^-, extensive gel-to-sol transition was seen for the XB organogelator, while more than 2.0 and 5.0 equivalents of Br^- and I^- were required for gel collapse respectively. It is noteworthy that this trend mirrors the solution-phase anion binding affinities of monomer **59** in d_6-acetone (K_a of Cl^- > Br^- > I^- >> NO_3^-, HSO_4^-, CN^-), with the oxoanions being ineffective in triggering a bulk rheological change.

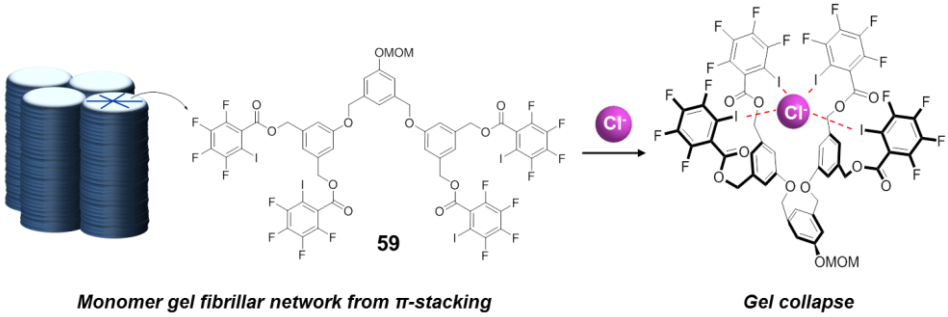

Figure 28. Fan's iodoperfluoroarene XB organogelator monomer 59 capable of Cl^- sensing due to formation of XB···Cl^- complexes which lead to gel collapse.[86]

3.2 Anion Binding Catalysis

The abundance of anions in chemical reactions as reagents, intermediates or counterions offer opportunities to influence the reaction rate or product distribution with appropriate anion interactions. Stimulated by the well-established field of organocatalysis mediated by Lewis acidic HB donors, σ-hole donors have been studied for their potential and activities for halide abstraction catalysis on substrates amenable for stable carbocation formation. Mechanistically, it has been suggested that the σ-hole donors can interact with the R-X bond (X = halide leaving group), thus facilitating a S_N1 cleavage (pathway i in Figure 29A), or bind to halide anions released during breakage of the R-X bond, shifting the equilibrium forward to enhance the rate of carbocation intermediate formation (pathway ii in Figure 29A). While experimental evidence distinguishing both possible pathways is currently lacking, the fact that these σ-hole donors can interact a lot more strongly with halide anions than the neutral pre-dissociated R-X precursor compound appears to suggest that the latter mechanism is more likely.[87] XB-mediated halide abstraction organocatalysis was first demonstrated by Huber *et. al.* with dicationic XB molecule **2.I** using the Ritter reaction, which involves the solvolysis of benzydryl bromide **60** (an S_N1 substrate) by wet acetonitrile to form an *N*-benzyldryl acetamide **61** (Figure 29B).[34] This reaction is a useful benchmark due to the ease of monitoring by ^1H NMR, lack of side reactions, as well as negligible background rates in the absence of catalysts and even in the presence of unintentional trace amounts of acid. Notably, stoichiometric quantities of catalyst **2.I** (1.0 eqv. relative to **60**) as its triflate salt resulted in 85 % substrate conversion after 96 hours at room temperature, whilst the HB bis-(proto)imidazolium analogue resulted in < 10 % conversion under identical conditions. When benzyl bromide (**62**) and α-methylbenzyl bromide (**63**) were used as substrates, catalyst **2.I** resulted in 0 % and 40 % conversions to their corresponding amides respectively, mirroring the stability of the carbocation intermediate formed from halide abstraction. Nonetheless, the strong binding of **2.I** to the liberated Br^- anion in the reaction can result in catalyst deactivation due to

preferential halide coordination over the neutral substrate. This may explain the low conversion observed (28 %) when sub-stoichiometric quantities of catalyst **2.I** was used relative to substrate **60**.

ChB catalysis of the Ritter reaction with substrate **60** was also subsequently explored using for the first time using a Se-containing host molecule (**37d**) (Figures 17 and 29B).[64] After 140 hours at room temperature, a stoichiometric 1.0 equivalent of the **37d•*syn*** resulted in a 64 % substrate conversion. Comparatively, only 45 % conversion was observed with **37d•*anti***, likely due to its weaker binding of the liberated Br^- anion in a monodentate manner. Interestingly, **37d•*syn*** was more active than the *syn*- XB bis-bromobenzimidazolium catalyst analogue (45 % conversion after 140 hours) bearing σ-hole donor atoms belonging to the same Period. However, its activity paled in comparison to its bis-iodobenzimidazolium catalyst analogue **15•*syn*** (Figure 5C), which showed >95 % conversion after just 2 hours, mirroring the catalysts' binding affinities to Br^- in acetonitrile.

The usage of *catalytic* (sub-stoichiometric) quantities of σ-hole organocatalysts necessitated the design of a suitable reaction system that prevented catalyst inactivation upon halide abstraction. For this purpose, the reaction of 1-chloroisochroman (**64**) and ketene silyl acetal (**65**) proved ideal, as the chloride liberated from the reaction is sequestered by the silyl moiety released concomitantly and is thus prevented from forming strong long-lasting halide complexes with the organocatalyst. Furthermore, the reaction is also insensitive to the presence of trace acid, and has negligible background activity. A range of bidentate dicationic XB organocatalysts (Figure 29: **15•syn**, **66**, **67**, **68a**, **68b**, **69**, **70**) have been studied by Huber for this reaction,[35] differing in their XB donor motif (iodoimidazolium/ iodotriazolium) and degree of preorganisation. Under identical conditions of 10 mol% catalyst loading in THF at room temperature, azo-bispyridinium catalyst **66** showed the least activity, giving a 14 % substrate conversion after 6 hours. Comparative monodentate XB catalysts containing iodoimidazolium (**67**) and iodobenzimidazolium (**70**) showed greater activities, giving 25 % and 49 % substrate conversions respectively. Owing to their more effective halide coordination, even more facile reactions were observed with bidentate catalysts **68a/b** and **69**, with no appreciable differences in catalytic activity induced using either the iodoimidazolium or iodotriazolium motifs which reflected their comparable anion affinities. However, having *para*-substituted iodoimidazolium motifs (**68b**) resulted in reduced activity compared with the *meta*-substituted analogue (**68a**). Notably, the more preorganised catalyst **15•syn** (*vide supra*) showed the greatest activity amongst all catalysts screened by giving complete substrate conversion in less than 6 hours. More impressively, a very low catalyst loading of **15•syn** (0.5 mol %) could still give 70 % product formation in 6 hours. Despite the widely differing catalytic activities observed, all XB organocatalysts showed dramatically enhanced activities compared with their HB analogues, affirming the dominant influence of XB interactions on the halide abstraction catalysis observed.

Given the sensitivity of the catalyst activities to their anion binding affinities, the nature of the counteranion of a positively charged catalyst plays an important role in the observed rates. Indeed, the triflate (OTf^-) salt of XB catalyst **2.I** resulted in a lower substrate conversion (85 %) in the Ritter reaction (Figure 29B) compared to the tetrafluoroborate (BF_4^-) salt (97 %) under identical conditions.[34] Strangely, although a more weakly coordinating counteranion is expected to interfere less and hence augment anion binding affinity, the use of the highly non-coordinating tetrakis[3,5-bis(trifluoromethyl)phenyl]borate $(BAr^F{}_4)^-$ counteranion with catalysts **67**, **68a**, **68b** and **70** consistently resulted in *lower* catalytic activities compared with the triflate salts in the reaction of 1-chloroisochroman and ketene silyl acetal (Figure 29C). This counter-intuitive finding has yet to be satisfactorily explained, although the possibility that the greater steric bulk of $(BAr^F{}_4)^-$ blocking the catalytically-active XB donor groups in the solution-phase ion-pairs has been proposed.[35]

The concept of XB organocatalysis was subsequently further expanded by Takagi *et. al.* in the controlled cationic polymerisation of isobutyl vinyl ether (Figure 29D).[88] Mechanistically, XB catalysts **67**, **68a** or **70** facilitates the formation of the

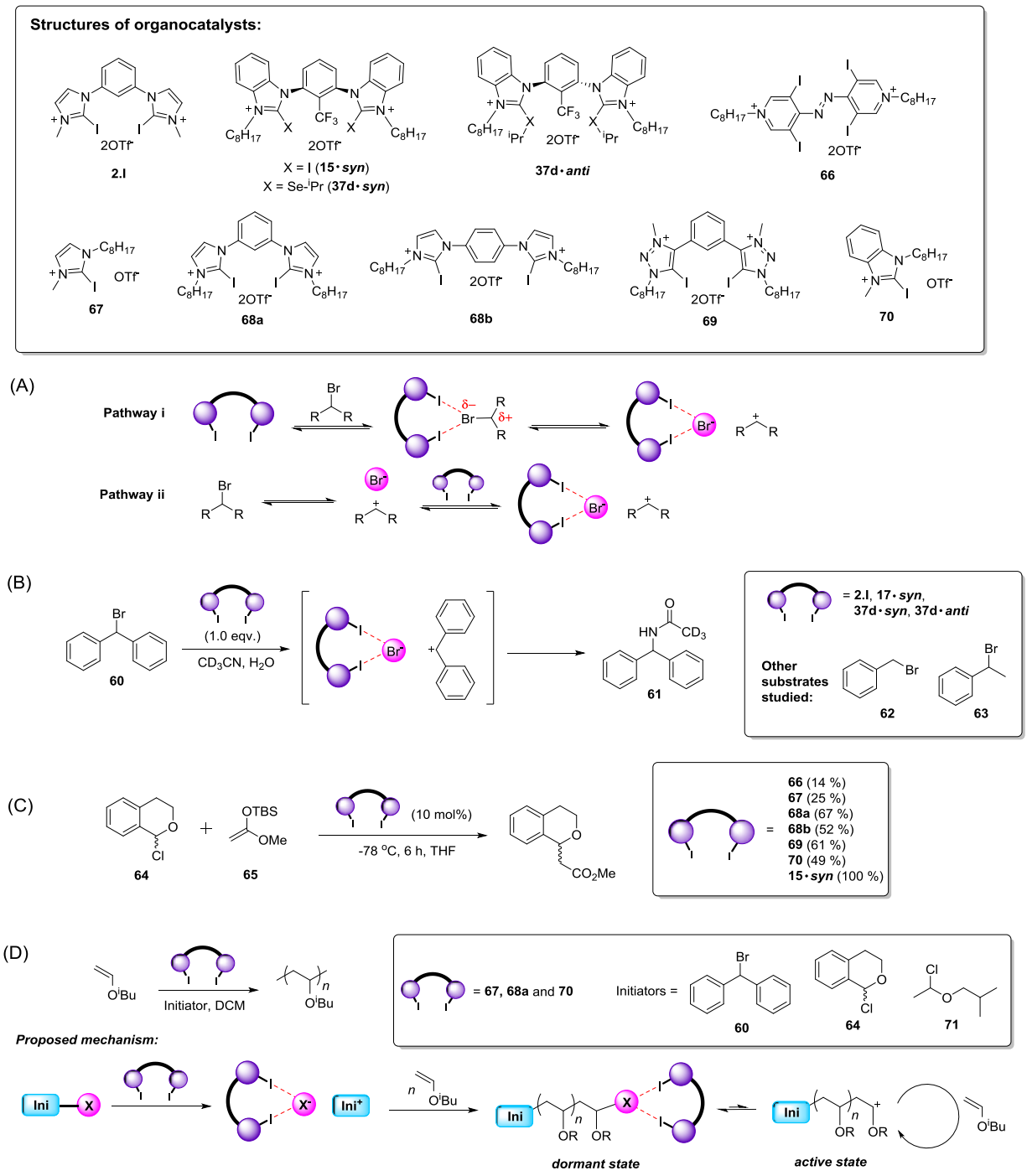

Figure 29. XB and ChB-mediated halide abstraction catalysis using organocatalysts showed in the box: (A) Proposed mechanisms of σ-hole-activation/ catalysis;[87] (B) Ritter reaction promoted by organocatalysts 2.I and 37d respectively[34]; (C) Reaction of 1-chloroisochroman (64) and ketene silyl acetal (65) mediated by XB organocatalysts, values in parentheses next to catalyst labels represent percentage conversions of substrates after 6 hours;[35] (D) XB-organocatalysed cationic polymerisation of isobutyl vinyl ether.[88]

resonant-stabilised carbocation from an initiator (**60**, **64** or **71**) which then propagates the polymerisation reaction. Concurrently, the liberated halide (X^-) from the initiator can recombine with the cationic propagating end of the growing polymer chain, whereupon the resulting C-X bond is then re-activated by the XB catalyst to continue the propagation reaction. As detectable degradation of catalyst **68a** occurred when the reaction was performed at 20 °C, the polymerisations were performed at -10 °C instead. Between initiators **60**, **64** and **71**, **60** gave the widest polyvinyl molecular weight distribution ($M_w/ M_n \approx 3$). Although **64** and **71** both resulted in narrower weight distributions ($M_w/ M_n \approx 2$), the use of initiator **64** proved challenging due to difficulties in purification and ensuring batch-to-batch consistency. Using initiator **71**, catalysts **67** and **68a** showed similar activities per iodoimidazolium group, while the benzimidazolium analogue **70** exhibited improved catalytic activity as described by Huber above. Interestingly, the addition of 0.02 eqv. of TBACl relative to **68a** resulted in a more controlled polymerisation with narrower molecular weight distribution ($M_w/ M_n = 1.3$), attributed to suppression of side reactions such as elimination of isobutyl alcohol during the polymerisations which also acts as a chain-transfer agent. However, a higher loading of TBACl (0.2 eqv.) greatly suppressed catalytic activity due to catalyst poisoning by Cl^- coordination.

Other than halide abstraction, organocatalysis can also involve σ-hole donors interacting with and stabilising the anionic transition states/ intermediates of specific reactions. Transition state stabilisation was recently explored by Matile *et. al.* using a neutral ChB receptor (**72**) containing the benzo-di[1,3]selenazole moiety in the organocatalysis of the transfer hydrogenation reaction of quinoline **73** using the Hantzsch ester **74** (Figure 30A).[89] In this reaction, hydride transfer from **74** to **73** results in negative charge accumulation on the latter's N atom which can be stabilised by the bidentate ChB interactions from catalyst **72**. At a catalyst loading of 1 mol %, 93 % substrate conversion was observed in 24 hours in CD_2Cl_2 at 20 °C with an impressive 150,000 times rate enhancement compared to the absence of the catalyst. Importantly, both the electron-withdrawing sulfone and cyano-groups were essential for the high activity of **72**, as their omission in related catalyst analogues dramatically reduced their catalytic activity. ChB catalyst **72** (1 mol %) was also shown to catalyse imine reduction in N-benzylidene-aniline **75** using Hantzsch ester **74** (Figure 30B) via a similar mechanism in quantitative yields under identical reaction conditions.

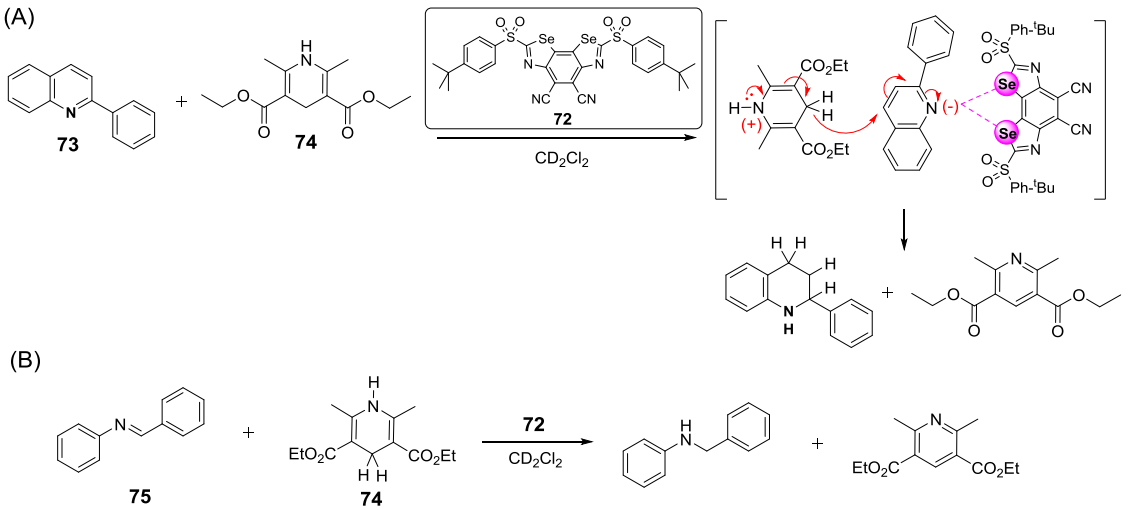

Figure 30. Transfer hydrogenations catalysed by Matile's neutral ChB organocatalyst 72 using (A) quinoline 73 and (B) imine 75 with Hantzsch ester 74.[89]

The potential of PnB-donor molecules for organocatalysis by transition state/ intermediate stabilisation was also studied for the first time using DFT calculations with P(V)-based compounds such as PO_2F.[90] Compared with phosphines

[P(III)], P(V) compounds are much less nucleophilic and more susceptible to forming PnB interactions from the P-centred electrophilic region occurring perpendicular to the P=O bonds, which can be more accurately described as a π-hole. Nonetheless semantics aside, PO_2F was able to interact strongly with the anionic regions of the zwitterionic intermediates in a Diels-Alder (Figure 31A) and a Friedel-Crafts reaction (Figure 31B), drastically reducing the free energies of activation in each case compared to the uncatalysed reaction and thus facilitating product formation. Based on this criteria, the computational results also suggest that the PO_2F PnB-donor can be more active than XB-donor molecular I_2.

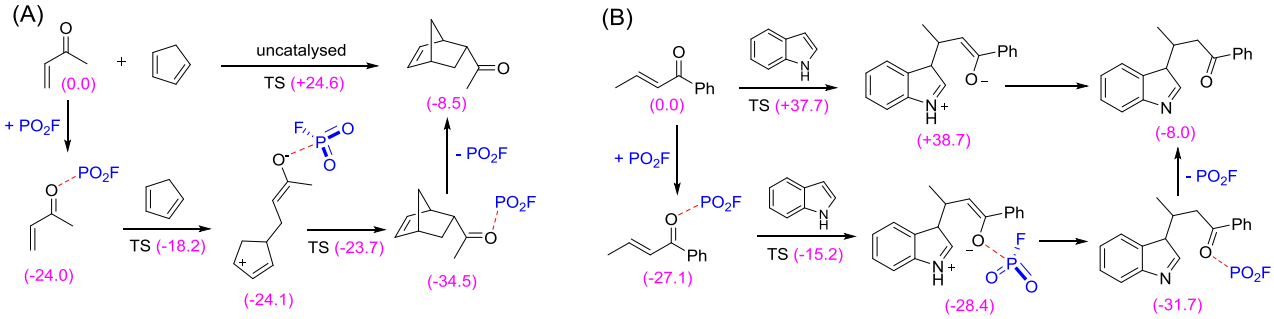

Figure 31. An example of a (A) Diels-Alder and (B) Friedel-Craft reaction which can be potentially catalysed by PnB-donor PO_2F. Values in parentheses indicated calculated free energies in kcal mol^{-1}; TS = transition state (structures not shown).[90]

3.3 Anion Transport

The potential of synthetic anion receptors to directly influence biological activity, and hence combat diseases arising from anion misregulation such as cystic fibrosis, may be realised in their applications as anion transporters. Synthetic anion transport across bilayer membranes can occur via two methods: (1) discrete 'anionophore' molecules which bind to the anion and convey it across the membrane or (2) direct continuous movement across the membrane mediated by membrane-spanning anion channels. Commonly, the need to penetrate the hydrophobic core of a lipid membrane for transmembrane transport conflicts with the intrinsic hydrophilicity of many HB-based or cationic anion binding functionalities. In this respect σ-hole interactions may provide a viable solution to the problem due to their comparatively greater hydrophobic character, while capable of maintaining strong and directional anion interactions.

The incorporation of XB and/or ChB donor groups into anionophores have resulted in great improvements in the atom efficiency of anion transport receptors, allowing molecules of unprecedented and remarkable simplicity and small size to function effectively. In a seminal study, Matile and coworkers studied a series of fluorinated XB aromatic (**76**) and aliphatic compounds (**77**) for their anion transport properties (Figure 32A).[91] Amongst the aromatic receptors, the highest activities were displayed by diiodoarenes **76e** and **76f**. Replacement of one of the iodine atoms with fluorine in **76a** attenuated the transport activity, which was reduced further with the weaker bromo-perfluoroarene XB-donor **76b** and defluorinated iodobenzene **76h**. No activity was seen with controls **76c** and **76i**, showing definitive proof of the crucial roles played by XB in anion transport, while compounds **76d** and **76g** were inactive due to their excessive hydrophilicity.

Aliphatic XB compounds proved to be surprisingly efficient anion transporters as well. Amongst the iodo-perfluoroalkyl homologues **77a**-**77h**, activity increased with longer perfluoroalkyl chains until **77e**, the most active anionophore amongst all compounds studied, due to the greater partition coefficients in the membrane by longer chains. Surprisingly, long-chain homologues **77f**-**77h** displayed negligible activity, attributed to formation of aggregates which prevented transmembrane anion transport. Once again, the inactivity of controls **77i** and **77j** highlighted the critical roles played by XB. Importantly, HB compounds of similar structural simplicity cannot be used for anion transport, as short chain alcohols are

too hydrophilic and longer-chain alcohols are known to disrupt lipid membranes. It is indeed remarkable that the presence of XB-donor groups can allow compounds like iodotrifluoromethane (**77a**), as the structurally-simplest organic anionophore ever reported with a boiling point of -22 °C, to function as anionophores without disrupting membrane structure.

ChB-mediated anion transport was subsequently demonstrated by Matile and coworkers who prepared a series of dithienothiophene-based ChB donors (**78a-e**) (Figure 32B) capable of binding anions in the space between both sulfur atoms by convergent ChB interactions (binding mode shown in Figure 3A).[60] Like the aforementioned XB anionophores, the presence of increasing numbers of electron-withdrawing groups generally enhanced the observed transport activity (smaller EC_{50} values), with sulfone-bearing **78e** being the most active. Despite the proven Cl^- binding ability of **78f** in THF, its inactivity for anion transport was attributed to poor partitioning. Unlike XB anionophores **76** and **77**, the Hill coefficients of all ChB transporters were close to unity, suggesting that anions were transported as discrete host-guest 1:1 stoichiometric complexes due to the well-defined anion binding pocket capable of convergent ChB interactions.

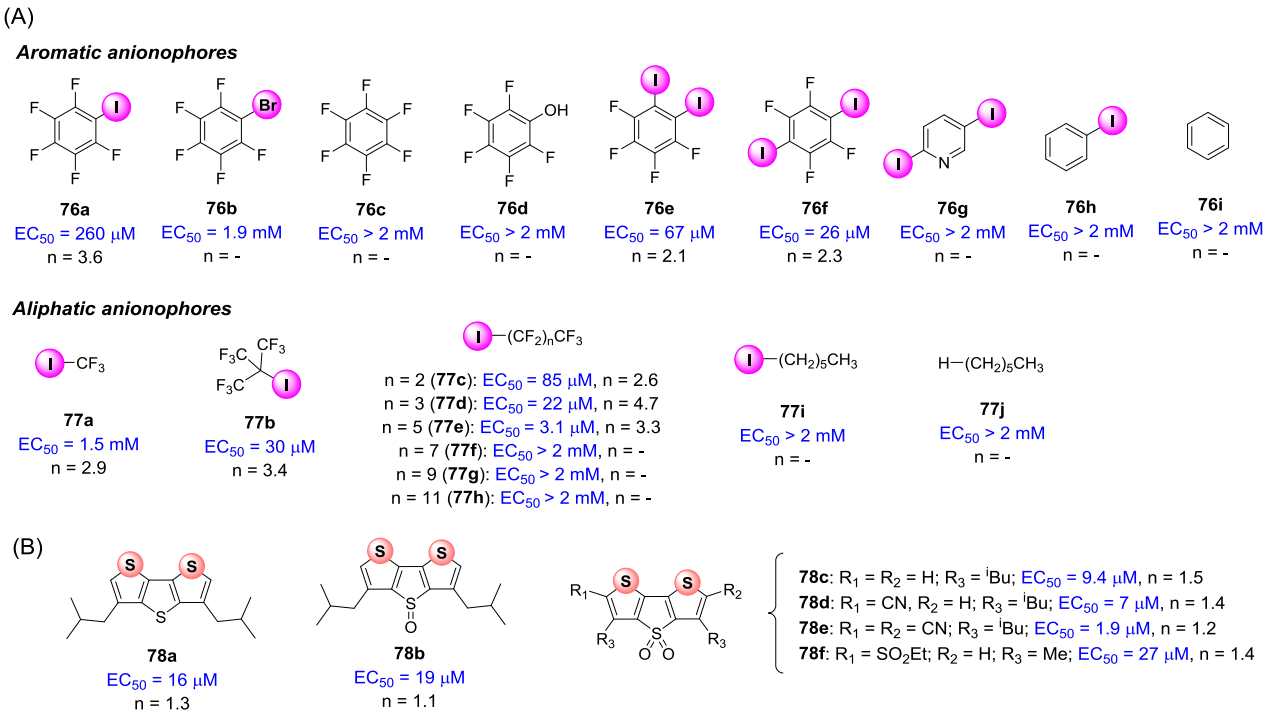

Figure 32. (A) Fluorinated aromatic (76) and aliphatic (77) anionophore candidates studied for XB-mediated anion transport,[91] and (B) Matile's dithienothiophene-based ChB anion transporters (78).[60] Effective concentrations (EC_{50}) represent transport activities of each molecule, while their cooperativity is indicated by the Hill coefficients (n).

An alternative means to achieve transmembrane anion transport involves the construction of artificial channels. Towards this end, a family of linear iodoperfluoroarene XB donor arrays (**79a-d**) studied for their anion transport activities show increased activity with greater scaffold length, with saturation achieved for arrays long enough to span the membrane thickness (Figure 33A).[92] Crucially, the experimental findings suggested that the anions were transported by a 'hopping' mechanism, mediated by the XB interactions within bundles of transmembrane XB scaffolds (Figure 33B).

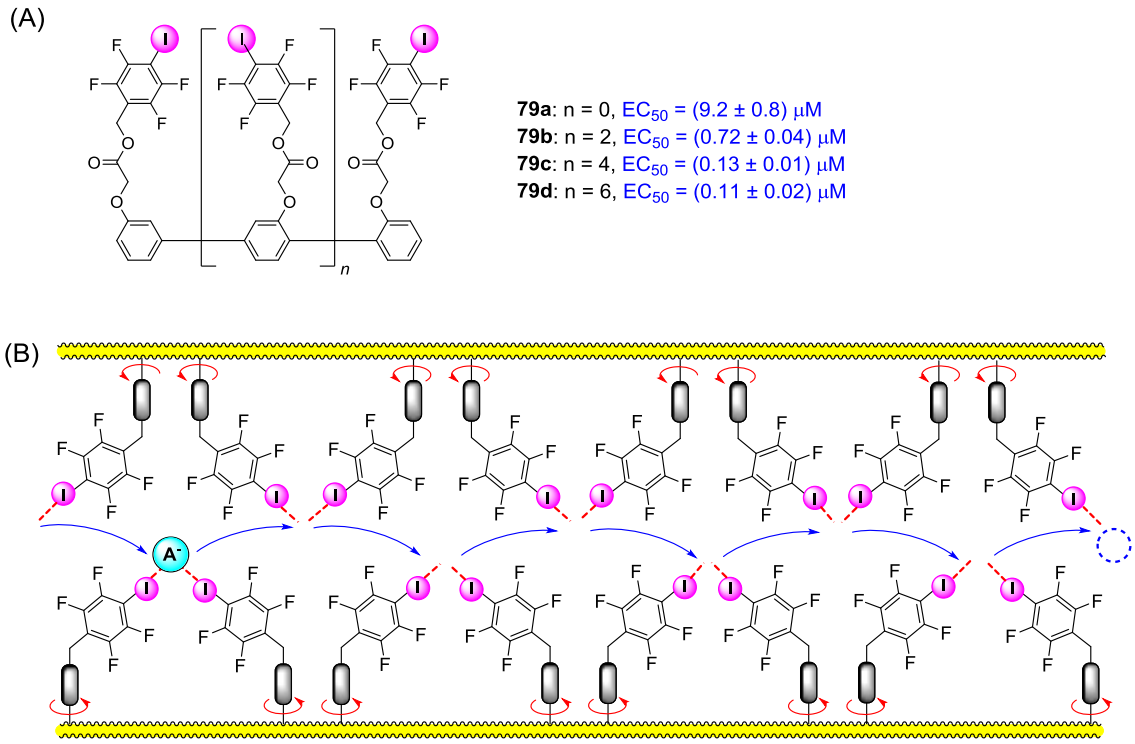

Figure 33. (A) Structures of XB scaffold molecules (79a-d) of varying lengths and their activities indicated by EC_{50} values. (B) Schematic illustration of the XB-mediated 'hopping' mechanism for transmembrane anion transport.[92]

3.4 Chiral Discrimination

Chiral discrimination, the ability of a host molecule to selectively recognise and bind one chiral guest over its enantiomers/ diastereomers, has diverse applications extending from asymmetric catalysis to medicinal chemistry. Nonetheless, this extremely subtle process is still poorly understood, which is reflected in the much poorer enantioselectivities of synthetic chiral receptors compared to natural enzymes. Chiral discrimination depends on attractive and repulsive host-guest supramolecular interactions and solvation of each interacting species, which act in tandem to determine which guest enantiomer is bound energetically the most favourably. Importantly, these factors are heavily influenced by host-guest binding geometry and thus the greater directionality and steric influence of σ-hole donor groups may be exploited to restrict the range of possible guest binding conformations. This could potentially magnify the energetic differences between individual host-guest diastereomeric complexes to augment enantio-discrimination.

The first indication that XB interactions could positively influence chiral discrimination was observed using Beer's XB chiral receptor **80a**, containing the enantiopure axial-chiral (*S*)-1,1'-bi-2-naphthol (BINOL) motif, with a series of chiral anions (Figure 34A).[93] In CD_3CN/ D_2O 99:1 *v/v*, **80a** exhibited a greater degree of enantioselectivity towards amino acid-derived chiral oxoanions containing larger R-groups (Table 4). Appending redox-active ferrocene units to the receptor (**80b**) also enabled XB-mediated electrochemical redox chiral discrimination. Notably, almost negligible enantioselectivity was observed for the HB receptor analogue **80c** under identical conditions for all chiral anion enantiomers regardless of their steric bulk. Other than the much stronger oxoanion binding by **80a** which ensured better host-guest contact for chiral discrimination, DFT calculations also indicated that the greater linearity of the XB interactions (Figure 34B), coupled with the more localised electrophilic XB binding site on **80a** than **80c**, all contributed to the enhanced enantioselectivity of **80a**. In a separate study, a neutral XB chiral foldamer **81** also

exhibited modest chiral discrimination towards amino acid-derived mono-carboxylates in $CDCl_3$/ d_6-acetone 1:1 *v/v*, which also improved with more bulky guests in a similar way as **80a** (Table 5).[31]

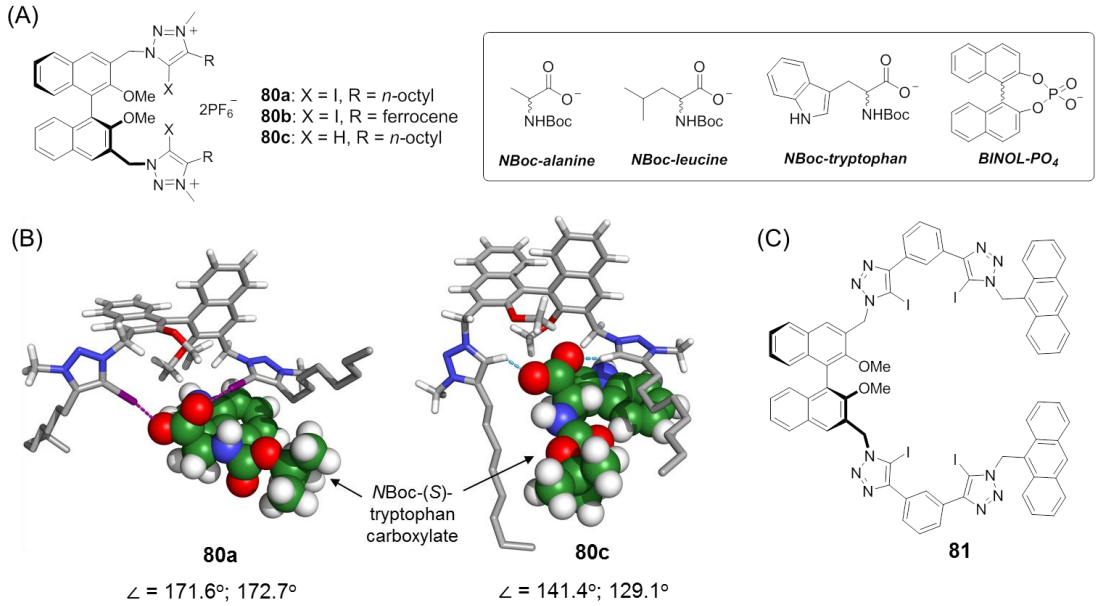

Figure 34. (A) Structures of Beer's XB chiral receptors 80a-c and the oxoanions investigated (shown here as racemates); (B) DFT-optimised structures for host-guest complexes of 80a and 80c with NBoc-(S)-tryptophan, with the C-X···O⁻ (X = I/ H) bond angles indicated below. DFT structures adapted from ref 93 with permission from The Royal Society of Chemistry; (C) Neutral XB foldamer 81 for chiral anion discrimination.[31]

Table 5. Chiral selectivities ($\xi = K_S/K_R$) of chiral XB hosts 80a, c and 81 towards chiral mono-oxoanion guests.[a]

	80a [b]	**80c** [b]	**81** [c]
(NBoc-alanine)⁻	0.85 (0.07)	0.92 (0.03)	0.79 (0.17)
(NBoc-leucine)⁻	0.65 (0.05)	0.92 (0.06)	1.51 (0.21)
(NBoc-tryptophan)⁻	1.67 (0.16)	0.92 (0.11)	1.69 (0.12)
(BINOL-PO_4)⁻	1.51 (0.17)	1.03 (0.03)	-[d]

[a] K_S, K_R = host-guest 1:1 binding constants for the S and R guest enantiomers respectively from ^{1}H NMR titrations; [b] performed in CD_3CN/ D_2O 99:1 *v/v*; [c] performed in $CDCl_3$/ d_6-acetone 1:1 *v/v*; [d] not performed. Data for receptors **80** and **81** reproduced from references 93 and 31 respectively with permission from The Royal Society of Chemistry.

The benefits of XB for chiral anion discrimination were further exploited in a series of XB chiral [2]rotaxanes **82a-c**, designed to distinguish chiral mono-oxoanion guests in the space flanked by their axle and macrocycle components (Figure 35A).[94] Although mechanically-interlocked molecules can be effective chiral discriminators due to the possibility of three dimensional guest encapsulation akin to natural enzymes, this class of receptors has been surprisingly overlooked for chiral recognition. Rotaxanes **82a-c** contain different combinations of chiral and achiral macrocycle and axle to elucidate the relative importance of each component for the overall chiral selectivity. Rotaxanes containing the chiral macrocycle unit (**82a**, **b**) were more effective chiral discriminators than their individual non-interlocked XB axle (**83**) and macrocycle (**84a**) components, giving selectivities of up to 2.93 and 3.45 towards the chiral anions respectively. Surprisingly, the lack of a chiral macrocycle unit in rotaxane **82c**, which contains only a chiral axle, almost completely negated its enantioselective properties. This unexpected behaviour was rationalised using MD simulations, which revealed that the chiral anion binding geometries within each rotaxane binding cavity was dominated by the linear XB interactions. These oriented the chiral oxoanion guests such that their chiral units were brought into close proximity with the macrocycle component's axial-chiral (S)-BINOL unit, accounting for its greater influence over the axle component (Figure

35B). The poorer enantioselectivities of the free macrocycle and axle hosts were consequences of the considerable spatial separation between the bound anions and the hosts' chiral components, each enforced by the linearity of XB interactions and the size of the donor iodine atoms. It is also notable that the hydration shell of each oxoanion played highly important roles in facilitating guest binding by forming numerous but poorly-directional HB bridges with the anion binding motifs in the rotaxane hosts' binding sites.

Other than chiral discrimination, the directionality of XB interactions could also be exploited to distinguish between *E*/*Z* geometric isomers. This possibility was demonstrated with Beer's XB [3]rotaxane **85** as a novel class of receptors for dicarboxylate anions, which are highly-challenging targets due to their hydrophilicity, similarities in structure and physicochemical properties. [3]Rotaxane **85** contain two HB macrocycle components sitting over separate XB-donor sites on the axle, flanking a ditopic binding cavity containing the (*S*)-BINOL motif for fluorescent chiral discrimination (Figure 35C).[95] In this proof-of-concept study, the [3]rotaxane bound biologically-relevant dicarboxylates via 1:1 stoichiometric host-guest sandwich complexes in the space between both macrocycles. This binding conformation elicited augmented fluorescence responses over binding of smaller anions such as chloride, which occurred in each individual interlocked cavity. Notable discrimination of chiral dicarboxylate anions (*N*Boc-*S*/*R*-glutamate) and *E*/*Z* geometric isomers (fumarate/ maleate) were observed, with selectivities of 5.7 and 4.4 for the (*S*)-glutamate enantiomer and maleate respectively. MD simulations showed that the strength and directionality of XB interactions were crucial for anchoring both anionic ends of the dicarboxylates within the [3]rotaxane host framework, allowing enantio- and geometric isomer discrimination through a combination of host-guest complementarity, solvent effects and synergistic HB interactions with the macrocycle units.

Other than the *extent* of selectivity, guest enantiomer *preference* is another important facet of chiral recognition. This is very difficult to predict *a priori*, as the preferred guest enantiomer/ geometric isomer forms the energetically most stable host-guest complex resulting from numerous attractive and repulsive host-guest interactions and solvent effects. Nonetheless, there are some indications which suggest that the geometric properties of XB interactions compared to HB can influence and change the guest preferences. For instance, although free XB macrocycle **84a** and its HB analogue **84b** generally exhibit identical guest preferences, contrasting enantioselectivity was seen for (*R*/*S*)-BINOL-PO_4^-.[94] Opposite selectivity was also seen for XB receptor **80a** and its HB analogue **80c** towards NBoc-(*S*/*R*)-tryptophan, although it should be noted that the *R*-enantiomer preference by **80c** is modest (Table 5).[93] Even amongst structurally-related host molecules, dramatic contrasts in guest enantiomer selectivity have been observed. As exemplified by XB [2]rotaxane **82a**, its general (S)-enantiomer guest preference contrasts with that of free XB macrocycle **84**, despite the dominant influence of the macrocycle component in determining the *extent* of chiral discrimination. Furthermore, replacing the chiral axle unit of **82a** with an achiral one in **82b** resulted in the contrasting (*R*)-guest selectivity. Although the possibility of tuning guest preference by replacing HB motifs with σ-hole donors is highly-sought after from the point of view of molecular recognition, the influences of σ-hole interactions in this aspect of enantiomer preference remains unclear at this very preliminary stage of research.

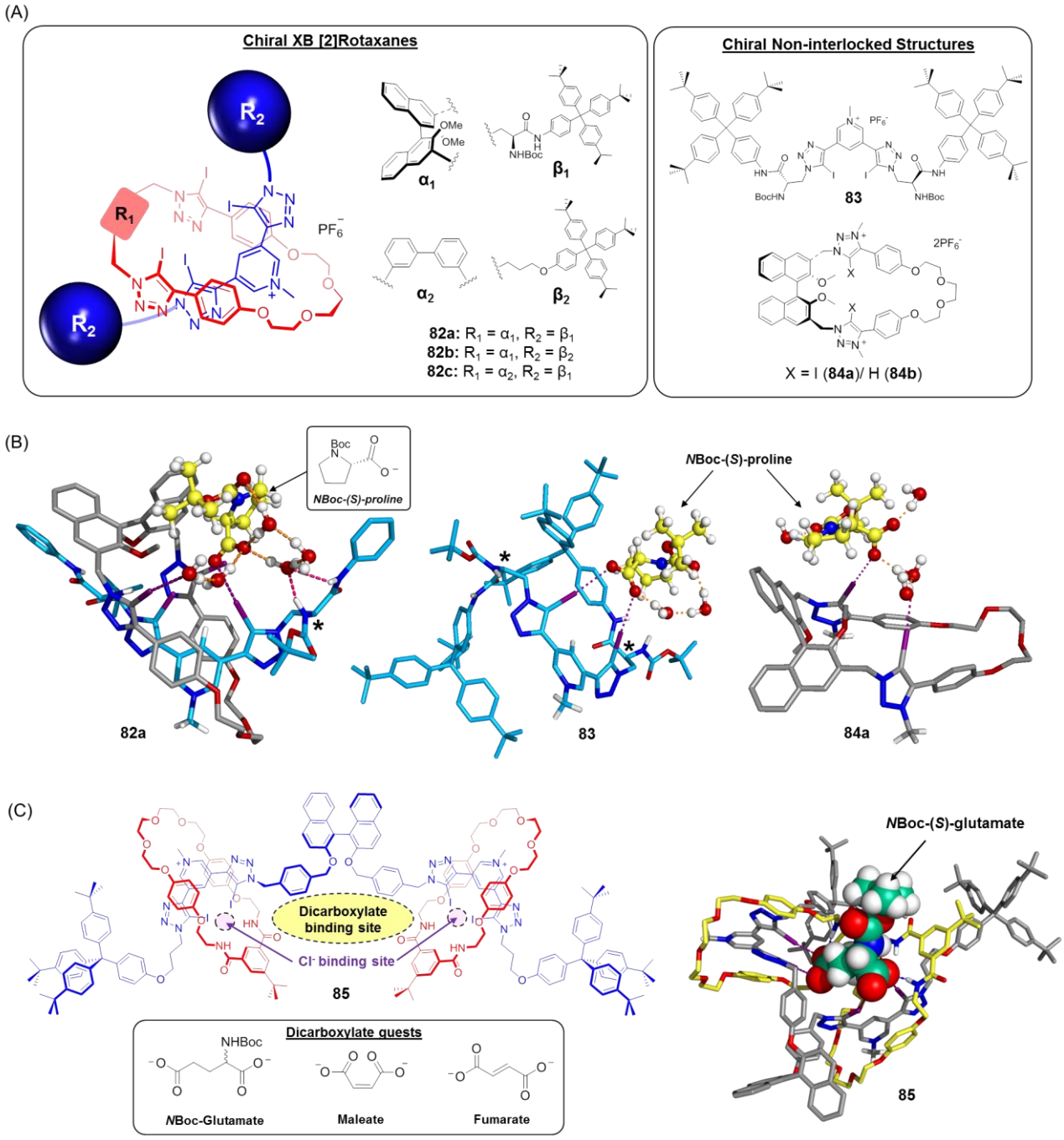

Figure 35. (A) Structures of Beer's chiral XB rotaxanes 82a-c, free non-interlocked axle 83 and macrocycles 84a/b;[94] (B) MD binding scenarios of rotaxane 82a (stopper groups removed for clarity), axle 83 and XB macrocycle 84a with *N*Boc-(*S*)-proline, showing the location of anion binding in each case. Point chiral centres are indicated by asterisks (*). Adapted with permission from reference 94. Copyright (2017) American Chemical Society; (C) Beer's chiral XB [3]rotaxane 85, dicarboxylate guests and illustrative MD binding scenario showing the host-guest 1:1 sandwich complex with *N*Boc-(*S*)-glutamate essential for its chiral discrimination.[95]

3.5 Materials Design and Nanotechnology

The various contrasting properties of σ-hole interactions in comparison to HB holds great potential for developing materials possessing novel and unexpected properties, not easily achievable with conventional HB building blocks. In particular, their stringent directionality allows easier geometric control of macroscopic supramolecular architectures, and their strength tunability and directionality (e.g. replacing XB with divalent ChB donors) enables convenient on-demand customisation of material properties. While the interested reader is referred to excellent recent reviews on the applications of XB[4,8,10] and ChB in materials science,[11] which are still in their infancy, we aim to highlight here notable recent advances and breakthroughs in materials design and nanotechnology where σ-hole-anion interactions are integral to their macroscopic properties and behaviour.

In polymer design, Schubert and Hager reported the first XB-based self-healing polymer systems comprising two components, a polycationic XB-donor copolymer and a polyanionic acceptor (Figure 36A).[96] In the former (**86a**), XB-donor iodotriazolium-containing cleft-type receptor units are copolymerised with butyl methacrylate (BMA), while the latter acceptor copolymer (**87**) contains approximately 30 % anionic carboxylate groups amidst free carboxylic acid units. Attractive interactions between both donor/acceptor copolymers were found from the exothermic ITC signature during solution-phase complexation studies, as well as FT-Raman spectroscopy, where the decrease in the wavenumber of **86a**'s C-I stretch indicated XB formation. As solid film mixtures, nano-indentation measurements also showed successful cross-linking between **86a** and **87** to form a stiff and hard material. Scratch tests at 100 °C confirmed self-healing behaviour (Figure 36B), which was a consequence of the breakage and reformation of donor-acceptor XB-carboxylate interactions at elevated temperatures. Compared to an analogous HB donor copolymer **86b**, the XB analogue **86a** required higher temperatures for complete scratch healing, reflective of its stronger association with anionic copolymer **87** from ITC studies.

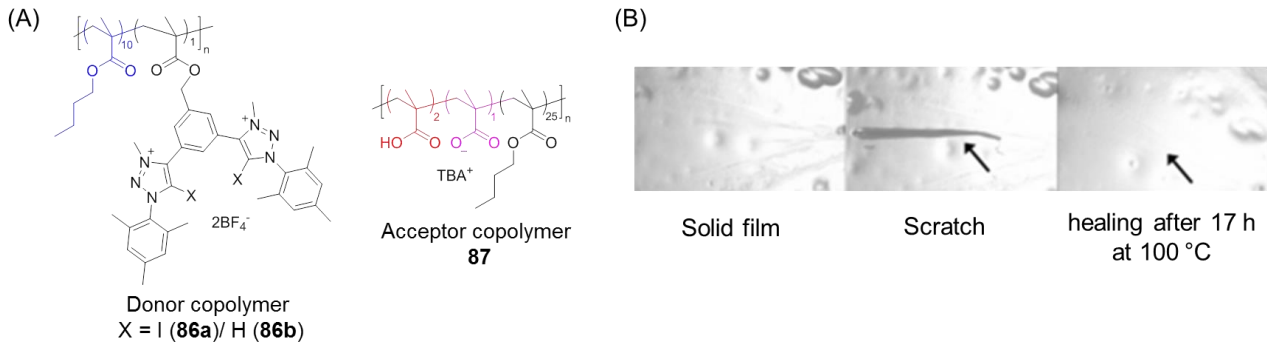

Figure 36. (A) Structures of the donor (86a,b) and acceptor (87) copolymers with BMA comprising Schubert and Hager's self-healing film network; (B) AFM images of the scratch tests showing self-healing behaviour of film 86a-87 upon heating. AFM images reproduced with permission from reference 96. Copyright (2017) John Wiley and Sons.

The applications of XB-anion interactions in the field of ionic liquid crystals (ILCs) have introduced new design principles for this class of smart materials. ILCs combine the high ionic conductivity of ionic liquids with the molecular order and fluidity of liquid crystals, allowing applications such as molecular electronics and energy storage. The strength and directionality of XB interactions with halide anions have been exploited to form large well-defined rod-like supramolecular anions such as $[C_nF_{2n+1}\text{-}I\cdots I\cdots I\text{-}C_nF_{2n+1}]^-$.[97] When coordinated in this way, the anisotropic nature of the ILC anionic component is amplified by locking the iodoperfluoroalkanes in an effectively linear geometry around the central iodide anion (Figure 37A), which act as rigid calamitic units. In combination with imidazolium cations, unconventional ILCs can result which show room temperature crystallinity. Unusually, liquid crystallinity appears to be independent of the cationic component's alkyl chain length, such that salts of 1-ethyl-3-methylimidazolium can exhibit the normally-

unachievable smectic mesophases at room temperature. This enhanced geometric control of XB-halide interactions enabled a bottom-up design approach towards engineering new properties and functionalities for ILCs. For instance, replacing the perfluoroalkyl chains with azobenzene derivatives enabled production of photo-responsive ILCs (Figure 37B).[98] Like $[C_nF_{2n+1}\text{-I}\cdots\text{I}\cdots\text{I-}\ C_nF_{2n+1}]^-$, the trans-azobenzene derivatives formed superanions held by XB interactions with a central iodide anion. When irradiated with UV light (385 nm), this resulted in trans-to-cis photoisomerism and a light-induced LC-to-isotropic phase transition was observed. This novel photoactive behaviour has the potential for applications such as light-controllable ion transporters.

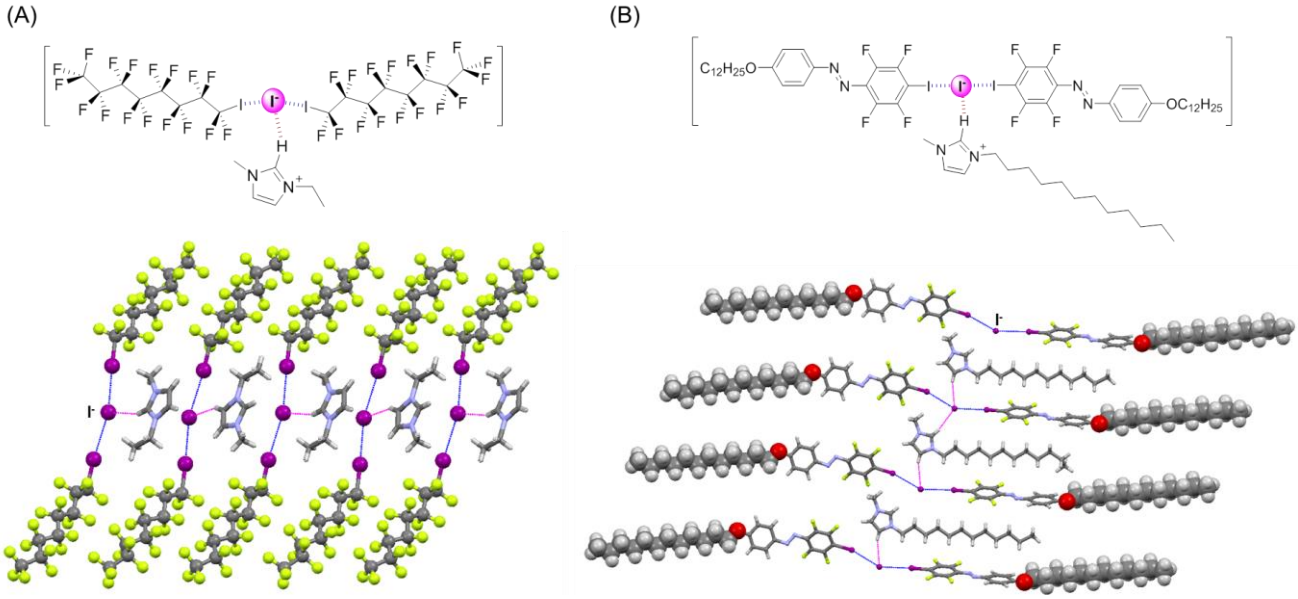

Figure 37. (A) Chemical and solid state structure of halogen-bonded $[C_8F_{17}\text{-I}\cdots\text{I}\cdots\text{I-}C_8F_{17}]^-$ supramolecular anion with 1-ethyl-3-methylimidazolium, showing the clear segregation of the perfluoroalkyl chains with the ionic salt components in the packing arrangement;[97] (B) Crystal packing of light-responsive ILC material comprised of 1-dodecyl-3-methyl imidazolium cation and azobenzene-derived halogen-bonded superanion held by a central iodide anion.[98] Halogen and hydrogen bonds are shown as blue and pink dashed lines respectively.

In nanotechnology, the dynamic mobility of mechanically-bonded components in rotaxanes and catenanes has inspired their study as molecular machines and switches. Central to exploiting them to do useful work however, is the ability to exercise precise control of these molecular movements with various forms of external stimuli. Recently, Beer and co-workers have demonstrated for the first time that the presence of an XB donor iodotriazolium unit on the axle component of a two-station [2]rotaxane **88a** can enhance the halide-induced shuttling behaviour of the macrocycle unit from the axle's adjacent NDI motif, compared with its HB rotaxane analogue (**88b**) (Figure 38A).[99] In both non-competitive ($CDCl_3$) and competitive protic solvent media ($CDCl_3$/ CD_3OD 4:1 and 1:1 *v/v*), ^{1}H NMR studies revealed that the presence of halide anions (Cl^-/ I^-) result in augmented macrocycle positional integrity of XB rotaxane **88a** (Table 6) due to strong XB-halide interactions (Figure 38B). This rare example of enhanced conformational response of an interlocked structure to external chemical stimuli highlights the exciting possibilities that exploitation of σ-hole interactions can have on nanotechnological switchable systems.

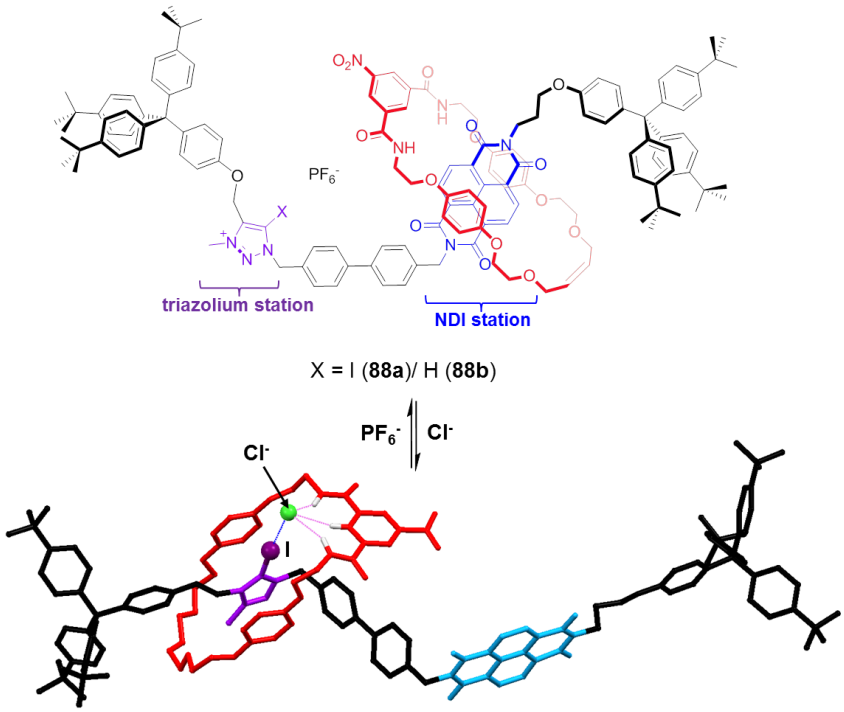

Figure 38. (A) Structures of Beer's two-station [2]rotaxanes (88a, b) containing adjacent iodo/prototriazolium and NDI units over which the macrocycle component can be positioned; (B) Crystal structure showing chloride coordination with XB interactions (in blue) from XB rotaxane 88a, driving the augmented shuttling behaviour compared with HB analogue 88b. All hydrogen atoms removed for clarity except those contributing to anion binding in the rotaxane binding site by HB interactions (dashed lines in pink).

Table 6. Percentage occupancies of the iodo/prototriazolium station of rotaxanes 88a and 88b with different anions in various solvent media.[a]

Solvent	XB rotaxane **88a**			HB rotaxane **88b**		
	PF_6^-	Cl^-	I^-	PF_6^-	Cl^-	I^-
$CDCl_3$	38	92	95	76	100	100
$CDCl_3$/ CD_3OD 4:1	52	100	92	67	87	70
$CDCl_3$/ CD_3OD 1:1	33	48	63	33	49	36

[a] Percentage occupancies determined from ^1H NMR solution-phase studies. Data reproduced with permission from reference 99- Published by The Royal Society of Chemistry.

4. CONCLUSIONS AND OUTLOOK

The field of supramolecular anion recognition, traditionally dominated by HB, has in recent years benefitted from many alternative interactions which include the family of σ-hole interactions discussed herein. In this review, we have highlighted several unique attributes of these interactions and their differences to HB pertaining to geometry, sterics, electronics and hydrophobicity, and discussed how these have been exploited to engineer host molecules with vastly contrasting anion selectivities from their HB analogues, while also often concurrently outperforming them in various applications. Compared to other non-traditional interactions receiving increasing recent attention including solvophobic and anion-π interactions, the entire family of σ-hole interactions spanning a significant fraction of the main group elements offer chemists an unprecedented degree of control over almost all important parameters of anion recognition, namely binding strength, solvent interactions, directionality and geometry. It is thus not surprising that even in this nascent phase of research, effective σ-hole-containing anion hosts have been constructed which function in a vast range of solvent polarities, from non-polar organic solvents to the 'holy grail' of anion binding in 100 % water.

A key limitation in the status quo of σ-hole anion binding research is the dearth of motifs which are stable, robust and synthetically-accessible enough to be incorporated into diverse molecular architectures, yet are capable of strong anion binding at the same time. While many XB motifs fitting these criteria are developed, and some recently-reported ChB motifs show outstanding promise, PnB and TrB-donor units are scant at best with the vast majority limited to *in-silico* studies. Nonetheless, these under-exploited σ-hole interactions show unique potential for selectively recognising anions which are traditionally highly-challenging targets for binding in competitive protic solvents, as exemplified by TrB Si/ Ge-based cages for fluoride. In addition at this stage, σ-hole anion binding research is dominated by halide recognition, with other families of anions such as oxoanions, transition metal complex anions, linear species (CN^-, N_3^-, SCN^-, OCN^-) and even super-chaotropic anions including dodecaborate clusters[100] being comparatively overlooked. Given the rich chemistry and critical importance of some of these anion families in nature, especially oxoanions, the potential of σ-hole interactions for selective recognition of these species remains unrealised.

Finally, applications of σ-hole anion binding, currently dominated overwhelmingly by XB, demonstrate how the unique properties of these interactions can give unexpected, novel, yet highly-desirable behaviour. The kinship of these sister σ-hole interactions, with predictably different properties (e.g. contrasting geometric control) offer great potential for a bottom-up design approach towards specific applications. To achieve these targets however, effective methods of incorporating σ-hole motifs into a range of structures need to be developed. This may not be as daunting as it sounds, as creative and unorthodox adaptations of well-established synthetic protocols may prove to be unexpectedly successful, with the use of AMT strategies for XB and ChB rotaxane construction being a notable case in point. We hope that this review will inspire further studies of anion recognition by the wider class of σ-hole interactions, leading to novel applications and the development of new functional sensors and materials in the near future.

AUTHOR CONTRIBUTIONS

Conceptualisation, writing and editing were done jointly by J.Y.C.L and P.D.B.

ACKNOWLEDGMENTS

J.Y.C.L gratefully acknowledges the Agency for Science, Technology and Research (A*STAR), Singapore, for postdoctoral funding.

REFERENCES AND NOTES

1. Evans, N.H., and Beer, P.D. (2014). Advances in Anion Supramolecular Chemistry: From Recognition to Chemical Applications. Angew. Chem. Int. Ed. *53*, 11716–11754.

2. Gale, P.A., Howe, E.N.W., and Wu, X. Anion Receptor Chemistry. Chem *1*, 351–422.

3. Desiraju Gautam R., Ho P. Shing, Kloo Lars, Legon Anthony C., Marquardt Roberto, Metrangolo Pierangelo, Politzer Peter, Resnati Giuseppe, and Rissanen Kari (2013). Definition of the halogen bond (IUPAC Recommendations 2013). Pure Appl. Chem. *85*, 1711.

4. Cavallo, G., Metrangolo, P., Milani, R., Pilati, T., Priimagi, A., Resnati, G., and Terraneo, G. (2016). The Halogen Bond. Chem. Rev. *116*, 2478–2601.

5. Brown, A., and Beer, P.D. (2016). Halogen bonding anion recognition. Chem Commun *52*, 8645–8658.

6. Bauzá, A., Mooibroek, T.J., and Frontera, A. (2015). The Bright Future of Unconventional σ/π-Hole Interactions. ChemPhysChem *16*, 2496–2517.

7. Legon, A.C. (2017). Tetrel, pnictogen and chalcogen bonds identified in the gas phase before they had names: a systematic look at non-covalent interactions. Phys Chem Chem Phys *19*, 14884–14896.

8. Gilday, L.C., Robinson, S.W., Barendt, T.A., Langton, M.J., Mullaney, B.R., and Beer, P.D. (2015). Halogen Bonding in Supramolecular Chemistry. Chem. Rev. *115*, 7118–7195.

9. Beale, T.M., Chudzinski, M.G., Sarwar, M.G., and Taylor, M.S. (2013). Halogen bonding in solution: thermodynamics and applications. Chem Soc Rev *42*, 1667–1680.

10. Berger, G., Soubhye, J., and Meyer, F. (2015). Halogen bonding in polymer science: from crystal engineering to functional supramolecular polymers and materials. Polym Chem *6*, 3559–3580.

11. Mahmudov, K.T., Kopylovich, M.N., Guedes da Silva, M.F.C., and Pombeiro, A.J.L. (2017). Chalcogen bonding in synthesis, catalysis and design of materials. Dalton Trans *46*, 10121–10138.

12. Scheiner, S. (2013). The Pnicogen Bond: Its Relation to Hydrogen, Halogen, and Other Noncovalent Bonds. Acc. Chem. Res. *46*, 280–288.

13. Bauzá, A., Mooibroek, T.J., and Frontera, A. (2016). Tetrel Bonding Interactions. Chem. Rec. *16*, 473–487.

14. Stenlid, J.H., and Brinck, T. (2017). Extending the σ-Hole Concept to Metals: An Electrostatic Interpretation of the Effects of Nanostructure in Gold and Platinum Catalysis. J. Am. Chem. Soc. *139*, 11012–11015.

15. Bauzá, A., and Frontera, A. (2015). Aerogen Bonding Interaction: A New Supramolecular Force? Angew. Chem. Int. Ed. *54*, 7340–7343.

16. Clark, T., Hennemann, M., Murray, J.S., and Politzer, P. (2007). Halogen bonding: the σ-hole. J. Mol. Model. *13*, 291–296.

17. Politzer, P., and Murray, S.J. (2017). σ-Hole Interactions: Perspectives and Misconceptions. Crystals *7*.

18. Bauza, A., Quinonero, D., Deya, P.M., and Frontera, A. (2013). Halogen bonding versus chalcogen and pnicogen bonding: a combined Cambridge structural database and theoretical study. CrystEngComm *15*, 3137–3144.

19. Guo, X., An, X., and Li, Q. (2015). Se···N Chalcogen Bond and Se···X Halogen Bond Involving F2C═Se: Influence of Hybridization, Substitution, and Cooperativity. J. Phys. Chem. A *119*, 3518–3527.

20. Kolář, M.H., and Hobza, P. (2016). Computer Modeling of Halogen Bonds and Other σ-Hole Interactions. Chem. Rev. *116*, 5155–5187.

21. Politzer, P., Murray, J.S., and Clark, T. (2015). σ-Hole Bonding: A Physical Interpretation. In Halogen Bonding I: Impact on Materials Chemistry and Life Sciences, P. Metrangolo and G. Resnati, eds. (Cham: Springer International Publishing), pp. 19–42. Available at: https://doi.org/10.1007/128_2014_568.

22. Řezáč, J., Riley, K.E., and Hobza, P. (2012). Benchmark Calculations of Noncovalent Interactions of Halogenated Molecules. J. Chem. Theory Comput. *8*, 4285–4292.

23. Robinson, S.W., Mustoe, C.L., White, N.G., Brown, A., Thompson, A.L., Kennepohl, P., and Beer, P.D. (2015). Evidence for Halogen Bond Covalency in Acyclic and Interlocked Halogen-Bonding Receptor Anion Recognition. J. Am. Chem. Soc. *137*, 499–507.

24. Pascoe, D.J., Ling, K.B., and Cockroft, S.L. (2017). The Origin of Chalcogen-Bonding Interactions. J. Am. Chem. Soc. *139*, 15160–15167.

25. Shahi, A., and Arunan, E. (2014). Hydrogen bonding, halogen bonding and lithium bonding: an atoms in molecules and natural bond orbital perspective towards conservation of total bond order, inter- and intra-molecular bonding. Phys Chem Chem Phys *16*, 22935–22952.

26. Murray, J.S., Resnati, G., and Politzer, P. (2017). Close contacts and noncovalent interactions in crystals. Faraday Discuss *203*, 113–130.

27. Scheiner, S. (2016). Highly Selective Halide Receptors Based on Chalcogen, Pnicogen, and Tetrel Bonds. Chem. – Eur. J. *22*, 18850–18858.

28. Scheiner, S. (2017). Comparison of halide receptors based on H, halogen, chalcogen, pnicogen, and tetrel bonds. Faraday Discuss.

29. Scheiner, S. (2017). Assembly of Effective Halide Receptors from Components. Comparing Hydrogen, Halogen, and Tetrel Bonds. J. Phys. Chem. A *121*, 3606–3615.

30. Sarwar, M.G., Dragisic, B., Sagoo, S., and Taylor, M.S. (2010). A Tridentate Halogen-Bonding Receptor for Tight Binding of Halide Anions. Angew. Chem. Int. Ed. *49*, 1674–1677.

31. Borissov, A., Lim, J.Y.C., Brown, A., Christensen, K.E., Thompson, A.L., Smith, M.D., and Beer, P.D. (2017). Neutral iodotriazole foldamers as tetradentate halogen bonding anion receptors. Chem Commun *53*, 2483–2486.

32. Tepper, R., Schulze, B., Bellstedt, P., Heidler, J., Gorls, H., Jager, M., and Schubert, U.S. (2017). Halogen-bond-based cooperative ion-pair recognition by a crown-ether-embedded 5-iodo-1,2,3-triazole. Chem Commun *53*, 2260–2263.

33. Tepper, R., Schulze, B., Jäger, M., Friebe, C., Scharf, D.H., Görls, H., and Schubert, U.S. (2015). Anion Receptors Based on Halogen Bonding with Halo-1,2,3-triazoliums. J. Org. Chem. *80*, 3139–3150.

34. Walter, S.M., Kniep, F., Herdtweck, E., and Huber, S.M. (2011). Halogen-Bond-Induced Activation of a Carbon–Heteroatom Bond. Angew. Chem. Int. Ed. *50*, 7187–7191.

35. Jungbauer, S.H., and Huber, S.M. (2015). Cationic Multidentate Halogen-Bond Donors in Halide Abstraction Organocatalysis: Catalyst Optimization by Preorganization. J. Am. Chem. Soc. *137*, 12110–12120.

36. Schulz, N., Sokkar, P., Engelage, E., Schindler, S., Erdelyi, M., Sanchez-Garcia, E., and Huber, S.M. XB, or not XB, that is the question: The Interaction Modes of Haloimidazolium Salts in Solution. Chem. – Eur. J., n/a–n/a.

37. Massena, C.J., Wageling, N.B., Decato, D.A., Martin Rodriguez, E., Rose, A.M., and Berryman, O.B. (2016). A Halogen-Bond-Induced Triple Helicate Encapsulates Iodide. Angew. Chem. Int. Ed. *55*, 12398–12402.

38. Cametti, M., Raatikainen, K., Metrangolo, P., Pilati, T., Terraneo, G., and Resnati, G. (2012). 2-Iodo-imidazolium receptor binds oxoanionsvia charge-assisted halogen bonding. Org Biomol Chem *10*, 1329–1333.

39. Tepper, R., Schulze, B., Görls, H., Bellstedt, P., Jäger, M., and Schubert, U.S. (2015). Preorganization in a Cleft-Type Anion Receptor Featuring Iodo-1,2,3-Triazoles As Halogen Bond Donors. Org. Lett. *17*, 5740–5743.

40. Mole, T.K., Arter, W.E., Marques, I., Félix, V., and Beer, P.D. (2015). Neutral bimetallic rhenium(I)-containing halogen and hydrogen bonding acyclic receptors for anion recognition. Concepts Struct. Bond. Organomet. Compd. *792*, 206–210.

41. Mungalpara, D., Stegmuller, S., and Kubik, S. (2017). A neutral halogen bonding macrocyclic anion receptor based on a pseudocyclopeptide with three 5-iodo-1,2,3-triazole subunits. Chem Commun *53*, 5095–5098.

42. Caballero, A., Zapata, F., and Beer, P.D. (2013). Interlocked host molecules for anion recognition and sensing. Coord. Chem. Rev. *257*, 2434–2455.

43. Caballero, A., Zapata, F., White, N.G., Costa, P.J., Félix, V., and Beer, P.D. (2012). A Halogen-Bonding Catenane for Anion Recognition and Sensing. Angew. Chem. *124*, 1912–1916.

44. Mullaney, B.R., Thompson, A.L., and Beer, P.D. (2014). An All-Halogen Bonding Rotaxane for Selective Sensing of Halides in Aqueous Media. Angew. Chem. Int. Ed. *53*, 11458–11462.

45. Langton, M.J., Robinson, S.W., Marques, I., Félix, V., and Beer, P.D. (2014). Halogen bonding in water results in enhanced anion recognition in acyclic and rotaxane hosts. Nat Chem *6*, 1039–1043.

46. Denis, M., and Goldup, S.M. (2017). The active template approach to interlocked molecules. Nat. Rev. Chem. *1*, 0061.

47. Langton, M.J., Xiong, Y., and Beer, P.D. (2015). Active-Metal Template Synthesis of a Halogen-Bonding Rotaxane for Anion Recognition. Chem. – Eur. J. *21*, 18910–18914.

48. Lim, J.Y.C., Bunchuay, T., and Beer, P.D. (2017). Strong and Selective Halide Anion Binding by Neutral Halogen-Bonding [2]Rotaxanes in Wet Organic Solvents. Chem. – Eur. J. *23*, 4700–4707.

49. Walter, S.M., Kniep, F., Rout, L., Schmidtchen, F.P., Herdtweck, E., and Huber, S.M. (2012). Isothermal Calorimetric Titrations on Charge-Assisted Halogen Bonds: Role of Entropy, Counterions, Solvent, and Temperature. J. Am. Chem. Soc. *134*, 8507–8512.

50. Cornes, S.P., Davies, C.H., Blyghton, D., Sambrook, M.R., and Beer, P.D. (2015). Contrasting anion recognition behaviour exhibited by halogen and hydrogen bonding rotaxane hosts. Org Biomol Chem *13*, 2582–2587.

51. Bianchi, A., and García-Espa˜na, E. (2011). Thermodynamic Aspects of Anion Coordination. In Anion Coordination Chemistry (Wiley-VCH Verlag GmbH & Co. KGaA), pp. 75–140. Available at: http://dx.doi.org/10.1002/9783527639502.ch2.

52. Lim, J.Y.C., and Beer, P.D. (2015). Superior perrhenate anion recognition in water by a halogen bonding acyclic receptor. Chem. Commun. *51*, 3686–3688.

53. Cornes, S.P., Sambrook, M.R., and Beer, P.D. (2017). Selective perrhenate recognition in pure water by halogen bonding and hydrogen bonding alpha-cyclodextrin based receptors. Chem Commun *53*, 3866–3869.

54. Chivers, T., and Laitinen, R.S. (2015). Tellurium: a maverick among the chalcogens. Chem Soc Rev *44*, 1725–1739.

55. Lee, L.M., Corless, V.B., Tran, M., Jenkins, H., Britten, J.F., and Vargas-Baca, I. (2016). Synthetic, structural, and computational investigations of N-alkyl benzo-2,1,3-selenadiazolium iodides and their supramolecular aggregates. Dalton Trans *45*, 3285–3293.

56. Semenov, N.A., Pushkarevsky, N.A., Beckmann, J., Finke, P., Lork, E., Mews, R., Bagryanskaya, I.Y., Gatilov, Y.V., Konchenko, S.N., Vasiliev, V.G., *et al.* (2012). Tellurium–Nitrogen π-Heterocyclic Chemistry – Synthesis, Structure, and Reactivity Toward Halides and Pyridine of 3,4-Dicyano-1,2,5-telluradiazole. Eur. J. Inorg. Chem. *2012*, 3693–3703.

57. Garrett, G.E., Gibson, G.L., Straus, R.N., Seferos, D.S., and Taylor, M.S. (2015). Chalcogen Bonding in Solution: Interactions of Benzotelluradiazoles with Anionic and Uncharged Lewis Bases. J. Am. Chem. Soc. *137*, 4126–4133.

58. Dutton, J.L., Martin, C.D., Sgro, M.J., Jones, N.D., and Ragogna, P.J. (2009). Synthesis of N,C Bound Sulfur, Selenium, and Tellurium Heterocycles via the Reaction of Chalcogen Halides with −CH3 Substituted Diazabutadiene Ligands. Inorg. Chem. *48*, 3239–3247.

59. Garrett, G.E., Carrera, E.I., Seferos, D.S., and Taylor, M.S. (2016). Anion recognition by a bidentate chalcogen bond donor. Chem Commun *52*, 9881–9884.

60. Benz, S., Macchione, M., Verolet, Q., Mareda, J., Sakai, N., and Matile, S. (2016). Anion Transport with Chalcogen Bonds. J. Am. Chem. Soc. *138*, 9093–9096.

61. Chandrasekhar, V., and Thirumoorthi, R. (2009). Halide-Capped Tellurium-Containing Macrocycles. Inorg. Chem. *48*, 10330–10337.

62. Citeau, H., Kirschbaum, K., Conrad, O., and Giolando, D.M. (2001). A novel cage organotellurate() macrocyclic host encapsulating a bromide anion guest: [Li(THF)][(PrTe)OB rLi(THF)BrBr][middle dot]2THF. Chem Commun, 2006–2007.

63. Zhao, H., and Gabbaï, F.P. (2010). A bidentate Lewis acid with a telluronium ion as an anion-binding site. Nat Chem *2*, 984–990.

64. Wonner, P., Vogel, L., Düser, M., Gomes, L., Kniep, F., Mallick, B., Werz, D.B., and Huber, S.M. (2017). Carbon–Halogen Bond Activation by Selenium-Based Chalcogen Bonding. Angew. Chem. Int. Ed. *56*, 12009–12012.

65. Lim, J.Y.C., Marques, I., Thompson, A.L., Christensen, K.E., Félix, V., and Beer, P.D. (2017). Chalcogen Bonding Macrocycles and [2]Rotaxanes for Anion Recognition. J. Am. Chem. Soc. *139*, 3122–3133.

66. Jones, J.S., and Gabbaï, F.P. (2016). Coordination- and Redox-Noninnocent Behavior of Ambiphilic Ligands Containing Antimony. Acc. Chem. Res. *49*, 857–867.

67. Müller, G., Brand, J., and Jetter, S.E. (2001). Donor-acceptor Complexes between Organoamines and Phosphorus Tribromide. Naturforsch B *56*, 1163–1171.

68. Chen, Y., Yao, L., and Lin, X. (2014). Theoretical study of (FH2X)n·Y (X=P and As, n=1–4, Y=F−, Cl−, Br−, I−, NO3− and SO42−): The possibility of anion recognition based on pnicogen bonding. Comput. Theor. Chem. *1036*, 44–50.

69. Hirai, M., Cho, J., and Gabbaï, F.P. (2016). Promoting the Hydrosilylation of Benzaldehyde by Using a Dicationic Antimony-Based Lewis Acid: Evidence for the Double Electrophilic Activation of the Carbonyl Substrate. Chem. – Eur. J. *22*, 6537–6541.

70. Qiu, J., Unruh, D.K., and Cozzolino, A.F. (2016). Design, Synthesis, and Structural Characterization of a Bisantimony(III) Compound for Anion Binding and the Density Functional Theory Evaluation of Halide Binding through Antimony Secondary Bonding Interactions. J. Phys. Chem. A *120*, 9257–9269.

71. Villaescusa, L.A., Lightfoot, P., and Morris, R.E. (2002). Synthesis and structure of fluoride-containing GeO2 analogues of zeolite double four-ring building units. Chem Commun, 2220–2221.

72. Taylor, P.G., Bassindale, A.R., El Aziz, Y., Pourny, M., Stevenson, R., Hursthouse, M.B., and Coles, S.J. (2012). Further studies of fluoride ion entrapment in octasilsesquioxane cages; X-ray crystal structure studies and factors that affect their formation. Dalton Trans *41*, 2048–2059.

73. Dai, X., Choi, S.-B., Braun, C.W., Vaidya, P., Kilina, S., Ugrinov, A., Schulz, D.L., and Boudjouk, P. (2011). Halide Coordination of Perhalocyclohexasilane Si6X12 (X = Cl or Br). Inorg. Chem. *50*, 4047–4053.

74. Muhammad, S., Bassindale, A.R., Taylor, P.G., Male, L., Coles, S.J., and Hursthouse, M.B. (2011). Study of Binuclear Silicon Complexes of Diketopiperazine at SN2 Reaction Profile. Organometallics *30*, 564–571.

75. Kalikhman, I., Girshberg, O., Lameyer, L., Stalke, D., and Kost, D. (2001). Tautomeric Equilibrium between Penta- and Hexacoordinate Silicon Chelates. A Chloride Bridge between Two Pentacoordinate Silicons. J. Am. Chem. Soc. *123*, 4709–4716.

76. Bauzá, A., Ramis, R., and Frontera, A. (2014). Computational study of anion recognition based on tetrel and hydrogen bonding interaction by calix[4]pyrrole derivatives. Comput. Theor. Chem. *1038*, 67–70.

77. Mahmoudi, G., Safin, D.A., Mitoraj, M.P., Amini, M., Kubicki, M., Doert, T., Locherer, F., and Fleck, M. (2017). Anion-driven tetrel bond-induced engineering of lead(ii) architectures with N[prime or minute]-(1-(2-pyridyl)ethylidene)nicotinohydrazide: experimental and theoretical findings. Inorg Chem Front *4*, 171–182.

78. Southern, S.A., Errulat, D., Frost, J.M., Gabidullin, B., and Bryce, D.L. (2017). Prospects for 207Pb solid-state NMR studies of lead tetrel bonds. Faraday Discuss.

79. Chowdhury, B., Sinha, S., and Ghosh, P. (2016). Selective Sensing of Phosphates by a New Bis-heteroleptic RuII Complex through Halogen Bonding: A Superior Sensor over Its Hydrogen-Bonding Analogue. Chem. – Eur. J. *22*, 18051–18059.

80. Zapata, F., Caballero, A., Molina, P., Alkorta, I., and Elguero, J. (2014). Open Bis(triazolium) Structural Motifs as a Benchmark To Study Combined Hydrogen- and Halogen-Bonding Interactions in Oxoanion Recognition Processes. J. Org. Chem. *79*, 6959–6969.

81. Barendt, T.A., Docker, A., Marques, I., Félix, V., and Beer, P.D. (2016). Selective Nitrate Recognition by a Halogen-Bonding Four-Station [3]Rotaxane Molecular Shuttle. Angew. Chem. Int. Ed. *55*, 11069–11076.

82. Lim, J.Y.C., Cunningham, M.J., Davis, J.J., and Beer, P.D. Halogen bonding-enhanced electrochemical halide anion sensing by redox-active ferrocene receptors. Chem Commun *51*, 14640–14643.

83. Lim, J.Y.C., and Beer, P.D. (2017). A Halogen Bonding 1,3-Disubstituted Ferrocene Receptor for Recognition and Redox Sensing of Azide. Eur. J. Inorg. Chem. *2017*, 220–224.

84. Oliveira, R., Groni, S., Fave, C., Branca, M., Mavre, F., Lorcy, D., Fourmigue, M., and Schollhorn, B. (2016). Electrochemical activation of a tetrathiafulvalene halogen bond donor in solution. Phys Chem Chem Phys *18*, 15867–15873.

85. Mullaney, B.R., Cunningham, M.J., Davis, J.J., and Beer, P.D. (2016). Acyclic halogen and hydrogen bonding diquat-containing receptors for the electrochemical sensing of anions. Polyhedron *116*, 20–25.

86. Liu, Z.-X., Sun, Y., Feng, Y., Chen, H., He, Y.-M., and Fan, Q.-H. (2016). Halogen-bonding for visual chloride ion sensing: a case study using supramolecular poly(aryl ether) dendritic organogel systems. Chem Commun *52*, 2269–2272.

87. Bulfield, D., and Huber, S.M. (2016). Halogen Bonding in Organic Synthesis and Organocatalysis. Chem. – Eur. J. *22*, 14434–14450.

88. Takagi, K., Yamauchi, K., and Murakata, H. (2017). Halogen-Bonding-Mediated and Controlled Cationic Polymerization of Isobutyl Vinyl Ether: Expanding the Catalytic Scope of 2-Iodoimidazolium Salts. Chem. – Eur. J. *23*, 9495–9500.

89. Benz, S., Mareda, J., Besnard, C., Sakai, N., and Matile, S. (2017). Catalysis with chalcogen bonds: neutral benzodiselenazole scaffolds with high-precision selenium donors of variable strength. Chem Sci.

90. Schmauck, J., and Breugst, M. (2017). The potential of pnicogen bonding for catalysis - a computational study. Org Biomol Chem *15*, 8037–8045.

91. Jentzsch, A.V., Emery, D., Mareda, J., Nayak, S.K., Metrangolo, P., Resnati, G., Sakai, N., and Matile, S. (2012). Transmembrane anion transport mediated by halogen-bond donors. Nat Commun *3*, 905.

92. Vargas Jentzsch, A., and Matile, S. (2013). Transmembrane Halogen-Bonding Cascades. J. Am. Chem. Soc. *135*, 5302–5303.

93. Lim, J.Y.C., Marques, I., Ferreira, L., Felix, V., and Beer, P.D. (2016). Enhancing the enantioselective recognition and sensing of chiral anions by halogen bonding. Chem Commun *52*, 5527–5530.

94. Lim, J.Y.C., Marques, I., Félix, V., and Beer, P.D. (2017). Enantioselective Anion Recognition by Chiral Halogen-Bonding [2]Rotaxanes. J. Am. Chem. Soc. *139*, 12228–12239.

95. Lim, J.Y.C., Marques, I., Félix, V., and Beer, P.D. A Chiral Halogen Bonding [3]Rotaxane for Recognition and Sensing of Biologically-relevant Dicarboxylate Anions. Angew. Chem. Int. Ed., n/a–n/a.

96. Tepper, R., Bode, S., Geitner, R., Jäger, M., Görls, H., Vitz, J., Dietzek, B., Schmitt, M., Popp, J., Hager, M.D., *et al.* (2017). Polymeric Halogen-Bond-Based Donor Systems Showing Self-Healing Behavior in Thin Films. Angew. Chem. Int. Ed. *56*, 4047–4051.

97. Cavallo, G., Terraneo, G., Monfredini, A., Saccone, M., Priimagi, A., Pilati, T., Resnati, G., Metrangolo, P., and Bruce, D.W. (2016). Superfluorinated Ionic Liquid Crystals Based on Supramolecular, Halogen-Bonded Anions. Angew. Chem. Int. Ed. *55*, 6300–6304.

98. Saccone, M., Palacio, F.F., Cavallo, G., Dichiarante, V., Virkki, M., Terraneo, G., Priimagi, A., and Metrangolo, P. (2017). Photoresponsive ionic liquid crystals assembled via halogen bond: en route towards light-controllable ion transporters. Faraday Discuss *203*, 407–422.

99. Barendt, T.A., Robinson, S.W., and Beer, P.D. (2016). Superior anion induced shuttling behaviour exhibited by a halogen bonding two station rotaxane. Chem Sci *7*, 5171–5180.

100. Assaf, K.I., Ural, M.S., Pan, F., Georgiev, T., Simova, S., Rissanen, K., Gabel, D., and Nau, W.M. (2015). Water Structure Recovery in Chaotropic Anion Recognition: High-Affinity Binding of Dodecaborate Clusters to γ-Cyclodextrin. Angew. Chem. *127*, 6956–6960.